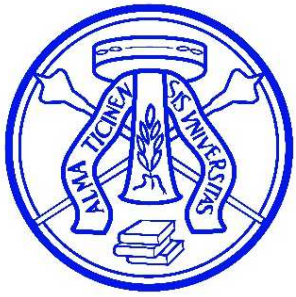

UNIVERSITÀ DEGLI STUDI DI PAVIA

DOTTORATO IN SCIENZE CHIMICHE E FARMACEUTICHE E INNOVAZIONE INDUSTRIALE

(XXXIII Ciclo)

Coordinatore: Chiar.mo Prof. Giorgio Colombo

DEVELOPMENT OF NEW GLYCOSAMINOGLYCAN-BASED STERILE FORMULATIONS

Tutor
Chiar.ma Prof.ssa Franca Ferrari

Co-tutor
Chiar.ma Prof.ssa Silvia Rossi

Tutor aziendale
Dott. Andrea Maria Giori

Tesi di Dottorato di

Marta Cicognani

A.A. 2019/2020

Table of Contents

PREMISE

Glycosaminoglycans (GAGs) are polysaccharides consisting of long chains of disaccharides in which at least one of the two units is an aminosugar. Hyaluronic acid (HA) is the most abundant GAG in human body, being located both in the dermis, where it is responsible for skin hydration and plasticity [1], and in the synovial fluid, where it promotes joint lubrication and shock absorption [2]. Other functions played by HA within the body include wound repair, cell migration and cell signaling.

Due to its versatility, the polymer has recently gained a prominent role in biomedical research and has been used in several fields such as tissue engineering and cancer treatment through a multitude of different forms (e.g. viscoelastic solutions, scaffolds, nanoparticles) [3].

Besides these applications hyaluronic acid has been fruitfully employed in the formulation of several medical devices present on the market either as sterile solution in prefilled syringe intended for intra-articular (viscosupplementation) administration or as artificial tears for the treatment of Dry Eye Syndrome due to its protective and lubricating action on the cornea.

However, all medical devices based on HA and administered for these two purposes, present some drawbacks.

The main problem of products intended for intra-articular administration is to successfully simulate the healthy synovial fluid, which is characterized by low viscosity and cross over point at low frequencies. This goal is difficult to be achieved using low concentrations (2.5-4 mg/mL) of high molecular weight (5-6 $x10^6$ Da) hyaluronic HA [4].

In the case of commercial artificial tears based on HA the issue is to best mimic the rheological and lubrication properties of tear films [5].

The understanding of these problems and the need to improve the efficacy of the medical devices already exiting on the market, usually based on a single HA grade, prompted the research for new HA-based formulations for viscosupplementation or to be used as artificial tears.

The key factor for both kind of formulations was the employment of a mixture of different HA grades, namely the addition of a low MW HA to a high MW HA, with the aim to ascertain the possible synergy of the two grades in the improvement of the functional properties (in particular rheological and lubrication properties) of the finished product.

In **Chapter 1** the formulation development of a novel HA-based formulation intended for viscosupplementation is described. This chapter has been object of the paper "DoE-Assisted development of a novel glycosaminoglycan-based injectable formulation for viscosupplementation. *Pharmaceutics* **2020,** *12*, 681-695".

Chapter 2 deals with the development of a novel medical device (artificial tears) based on binary mixtures of HA.

The more promising prototype developed on lab scale and selected on the basis of rheological and tribology measures was scaled up. The results obtained on the pilot batch proved the biocompatibility and stability of the product. The further passage on industrial scale didn't point out any critical aspect. The product gained the CE mark and is now on the market as Class II medical device.

The studies performed in Chapter 1 and 2 pointed out the need for an analytical method suitable not only as a routine test for the release of HA-based medical devices but also as a stability indicating tool capable of detecting the presence of hyaluronic acid-like structure contaminants present in low concentrations and of degradation products.

To this purpose the feasibility of NMR analysis as stability indicating method, coupled with gel permeation (GPC)/ size exclusion (SEC) chromatography was investigated as described in **Chapter 3**.

References

1. Papakonstantinou, E.; Roth, M.; Karakiulakis G. Hyaluronic acid: A key molecule in skin aging. *Dermato-Endocrinology*, **2012**, *4*, 253-258.
2. Fam, H.; Bryant, J.T.; Kontopoulou, M. Rheological properties of synovial fluids. *Biorheology* **2007**, *44*, 59–74.
3. Dovedytis, M.; Liu, Z.J.; Barlett, S. Hyaluronic acid and its biomedical applications: A review. *Eng. Reg.* **2020**, *1*, 102-113.
4. Mathieu, Pierre; Conrozier, T.; Vignon, E.; Rozand, Y; Rinaudo, M. Rheologic behavior of osteoarthritic synovial fluid after addition of hyaluronic acid - A pilot study. *Clin. Orthop. Relat. Res*. **2009**, *467*, 3002–3009.
5. Muller-Lierheim, W.G.K. Tear substitutes. *Current Contactology*, **2015**, *11*, 17-19.

Introduction

1. Glycosaminoglycans

Glycosaminoglycans (GAGs) are unbranched single-chain polymers made of disaccharide units containing N-acetylhexosamine and hexose. The second sugar is a hexuronic acid in all GAGs except than in keratan sulphate, which contains galactose instead of glucose [1-3]. GAGs are expressed on cell surface and in the extracellular matrix (ECM).
GAGs can be divided into two classes: sulphated and not sulphated (Table 1).

Table 1. Sulphated and not sulphated glycosaminoglycans (mod. from ref. 1).

Name	Constituent sugars	Sulphate	Proteoglycans	Approx. MW
Hyaluronan	Glucuronic acid Glucosamine	-	-	10^5-10^7
Chondroitin 4-(-6) sulphates	Glucuronic acid Galactosamine	+	+	10-50.10^3
Dermatan sulphate	Iduronic acid Galactosamine	+	+	10-50.10^3
Keratan sulphate	Galactose Glucosamine	+	+	5-15.10^3
Heparan sulphate	Glucuronic and iduronic acid Glucosamine	+	+	10-50.10^3
Heparin	Glucuronic and iduronic acid Glucosamine	+	+	5-20.10^3

Sulphated GAGs are synthesized by specific enzymes of cell Golgi apparatus, whereas hyaluronan (HA) is produced by transmembrane proteins called HA synthases. Whereas HA is not linked to a protein and it is synthesized starting from its reducing end (-OH), the sulphated GAGs are built up from the non-reducing end and synthesized as side chains attached to a protein that forms the so called proteoglycans (PGs) [4].

The degradation of PGs usually takes place in the ECM, whereas the final breakdown of GAGs takes place inside cell lysosomes in the reverse sequence of their synthesis [5]. The latter breakdown of GAGs is catalysed either by hydrolases (e.g. heparin hydrolase, different exoglycosidases), responsible for hydrolytic cleavage, or by lyases (e.g. heparinases, chondroitinases, hyaluronidases) that catalyse the cleavage of glycosidic bonds [6].

Each class of GAGs is characterized by a unique structure (Figure 1) from which their activity depends [7].

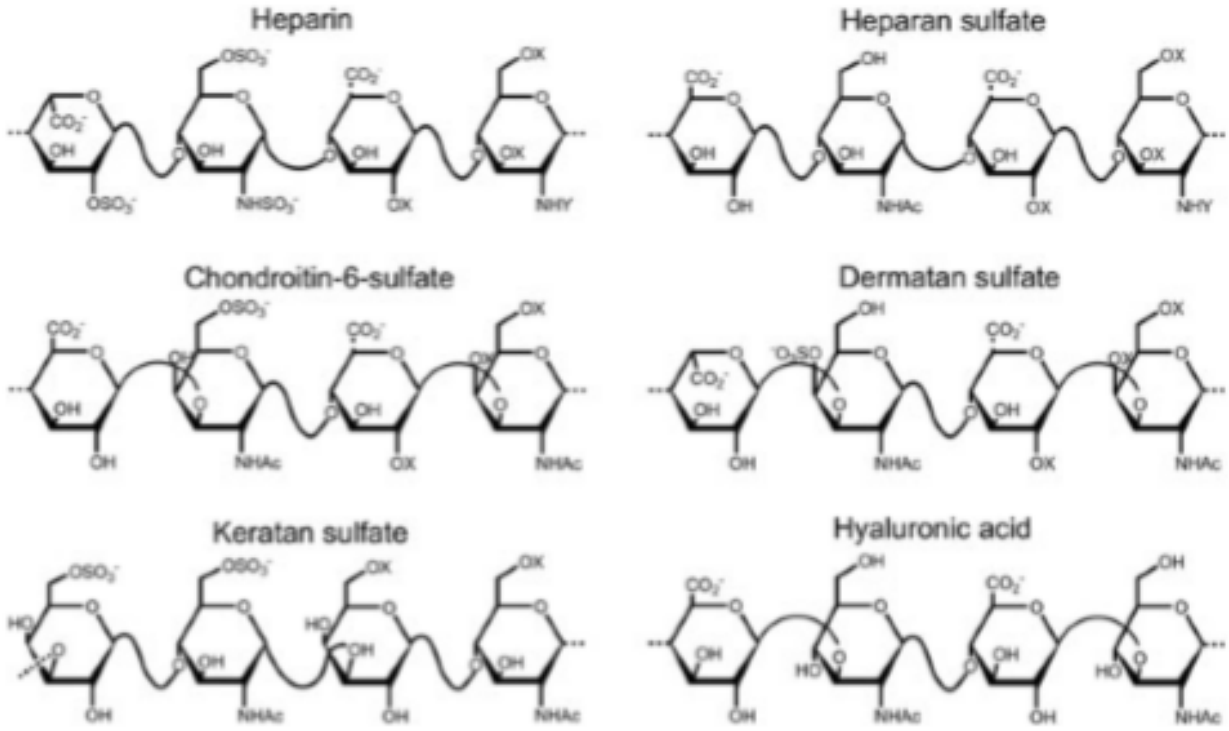

Figure 1. Major disaccharide repeating unit of glycosaminoglycans.
(X = -OH or –OSO_3-; Y = - Ac or -OSO_3-)

Heparin (Hep) and Heparan sulphate (HS)

Hep and HS are composed of alternating saccharide units of N-acetylated or N-sulphated D-glucosamine that are α(1-4) or β(1-4) linked to uronic acids (L-iduronic or D-glucuronic acid). Hep and HS are synthesized as PGs, with Hep being processed only in connective-tissue-type mast cells or basophils, while HSPGs are produced in almost all mammalian cells [8].

Hep is characterized by marked anticoagulant and antithrombotic activities [9], whereas HS is capable of activating or inhibiting cytokines such as interleukins and tumour necrosis factor α (TNF-α) [10].

Keratansulphate (KS)

KS is composed by β(1-4) GlcNAc and β(1-3) galactose disaccharides, which can be sulphated at C6. Therefore, KS is the only GAG without carboxyl groups. The main source of KS is the cornea, where the highest concentration is found. Unlike other sulphated GAGs, KS is synthesized as differently assembled saccharide chains connected to its core proteins [11].

Chondroitin sulphate (CS) and Dermatan sulphate (DS)

Chondroitin is synthesized like other galactosaminoglycans containing N-acetylgalactosamine alternating with glucuronic acid [12].

CS is constituted by alternating β(1-4) GlcA and β(1-3) N-acetylgalactosamine (GalNAc) units that can be sulphated at carbon 4 (CS-A) and/or at carbon 6 (CS-C) of the galactosamine unit and, in addition, at carbon 2 and/or at carbon 3 of the GlcA unit [13].

DS, also known as CS-B, is composed by alternating D-GlcAor L-IdoA units (partially sulphated at carbon 2) and GalNAc units, that can be sulphated at carbon 4 or at carbon 6 [14].

CS and DS are essential elements of various PGs. In cartilage, CS-containing PGs work as shock absorber by resisting compressive forces via water uptake or influence the skin tissue elasticity [1,15].

DS is similar to Hep, being characterized by anticoagulant and antithrombotic activities [9].

Non-sulfated Chondroitin (NSC)

NSC is an exogenous molecule for humans, which increases collagen type II expression.

NSC chains have been found only in squid skin, in Caenorhabditis elegans (a transparent nematode living in temperate soil environments, in the dried saliva of Collocalia swiftlets (edible bird's-nest) [16], and in the capsules of some pathogenic bacteria, where NSC acts as molecular camouflage protecting the microbe and enhancing infection.

NSC is a precursor of chondroitin sulfate (CS) but sulfation not always occurs, and some NSC is also present in ECM of several tissues and organs (e.g. prostate), even if in lower quantity when compared to CS and other sulfated GAGs.

NSC can be produced by fermentation using an integrated strategy based on the optimization of a three-phase fermentation process (batch-fed, batch-in and microfiltration regimen) and by genetically modified bacteria [17].

1.1. Hyaluronan (Hyaluronic acid, HA)

1.1.1. History

In 1934, Karl Meyer and John Palmer described a new polysaccharide isolated from bovine vitreous humour. They found that the substance contained an uronic acid and an aminosugar and named the polysaccharide "hyaluronic acid" from hyaloid (vitreous) plus uronic acid [18]. The term "hyaluronan" was introduced in 1986 to conform to polysaccharide nomenclature.

The original development of HA as a product used in medicine was entirely due to Balazs, who developed the first non-inflammatory, highly purified high molecular weight HA from the umbilical cord and rooster combs [19]. In the early 1980s, HA was used to prepare plastic intraocular lenses for implantation and it became a major material in ophthalmic surgery.

1.1.2. Physical-chemical and structural properties

The uronic acid and aminosugar in the disaccharide are D-glucuronic acid and d-N-acetylglucosamine and are linked together through alternating β(1-4) and β(1-3) glycosidic bonds. Both sugars are spatially related to glucose which, in the beta configuration, allows all of its bulky groups (the hydroxyls, the carboxylate moiety and the anomeric carbon on the adjacent sugar) to be in sterically favourable equatorial positions, whereas all of the small hydrogen atoms occupy the less sterically favourable axial positions. Thus, the structure of the disaccharide is energetically very stable [20,21].

HA represents the only non-sulphated GAG and is not linked to a protein core. In contrast to sulphated GAGs, HA is synthesized by integral membrane proteins (HA-synthases) from its reducing end and it is released to the extracellular space [21,22].

The highest HA concentrations in humans are found in umbilical cord, skin, the vitreous body of the eye [1,23] and in synovial fluid where the viscoelastic properties of HA solutions are the basis of the viscous and elastic properties of the synovial fluid [24].

HA has distinct biological properties, depending on its molecular weight (distribution). High molecular weight (HMW) HA has anti-angiogenic, immunosuppressive and anti-inflammatory properties, whereas low molecular weight (LMW) HA is highly angiogenic, immune-stimulant and it exhibits pro-inflammatory properties [25]. In humans, the MW of HA is correlated to age and to pathology, especially in the case of cartilage. For instance, a decrease of the mean MW of HA in synovial fluid due to reactive oxygen species (ROS), that are generated during inflammation processes, is found in osteoarthritis (OA) patients [26].

1.1.3. Primary and secondary structure of hyaluronate in solution

The physical-chemical properties of aqueous solutions of HA derive from its unique macromolecular structure. In aqueous salt solutions, the molecule can be characterized as a random-coil polyelectrolyte with some stiffness. One cause of stiffening may be an array of hydrogen bonds linking adjacent sugar residues.

The four hydrogen bonds possible for each disaccharide unit belong to two general types: (i) a hydrogen bond between the ring oxygen of each sugar residue and an hydroxyl group on the adjacent sugar residue, and (ii) hydrogen bonds involving the amide group of the 2-acetamido-2-deoxy-/3-D-glucopyranose (GlcNAc) residue [27,28].

The employment of NMR technique for the analysis of HA solutions can be very informative about hydrogen bond position, polymer configuration, secondary structure and intra – and inter chain interactions that may be responsible for gel formation [29].

For instance, NMR spin-spin relaxation times of ^{1}H proton in the methyl group of the acetamido deoxyglucose residues, enable to demonstrate that aqueous solutions of HA consist of two distinct domains [30]: one domain is characterized by the mobility expected for freely flexible linear polysaccharide chain, whereas the other regions are stiff and indicative of strong inter-chain interactions.

1.1.4. The pathways of hyaluronan cleavage

The mechanisms of HA cleavage include both enzymatic and non-enzymatic reactions [31-34].

Enzymatic catabolism of hyaluronan

Enzymatic degradation of HA is mainly due to hyaluronidases (Hyals). Meyer [35] identified the three principal types of hyaluronidases: two classes of eukaryotic endoglycosidase hydrolases and a prokaryotic lyase-type of glycosidase.

Hyaluronidases do not have absolute substrate specificity, but are capable of utilizing chondroitin and chondroitin sulfate as substrates. The only difference is that these two GAGs are not effective substrates and the reactions proceed slowly [36].

A further limitation for hyaluronidase activity is the presence of hyaluronidase inhibitors [37] such as vitamin C [38], heparin and dextran sulphate [39].

Non-enzymatic catabolism of hyaluronan

There are a lot of non-enzymatic reactions that degrade HA, such as acidic and alkaline hydrolysis, ultrasonic degradation, degradation by oxidants and thermal degradation [40].

Similarly to other polysaccharides, HA can be degraded by acid or alkaline hydrolysis. Chemical hydrolysis proceeds in a random way and determines the formation of a statistical mixture of oligo- and mono-saccharides that can hardly be used for any specific purpose.

Similarly to other polysaccharides containing 4-substituted or non-reducing glycuronic acids, HA degrades in alkaline conditions, with the formation of unsaturated glucuronic acid units — 4-deoxy-hex-4-enoglucuronate [41]. Similarly, the N-acetylglucosamine unit of HA is degraded with alkaline treatment (Figure 2), giving rise to furan containing species [42].

It has been demonstrated that HA solutions undergo random degradation or racemization in acid media [43], therefore the products of acidic hydrolysis also contain moieties different from those present in native HA (Figure 3).

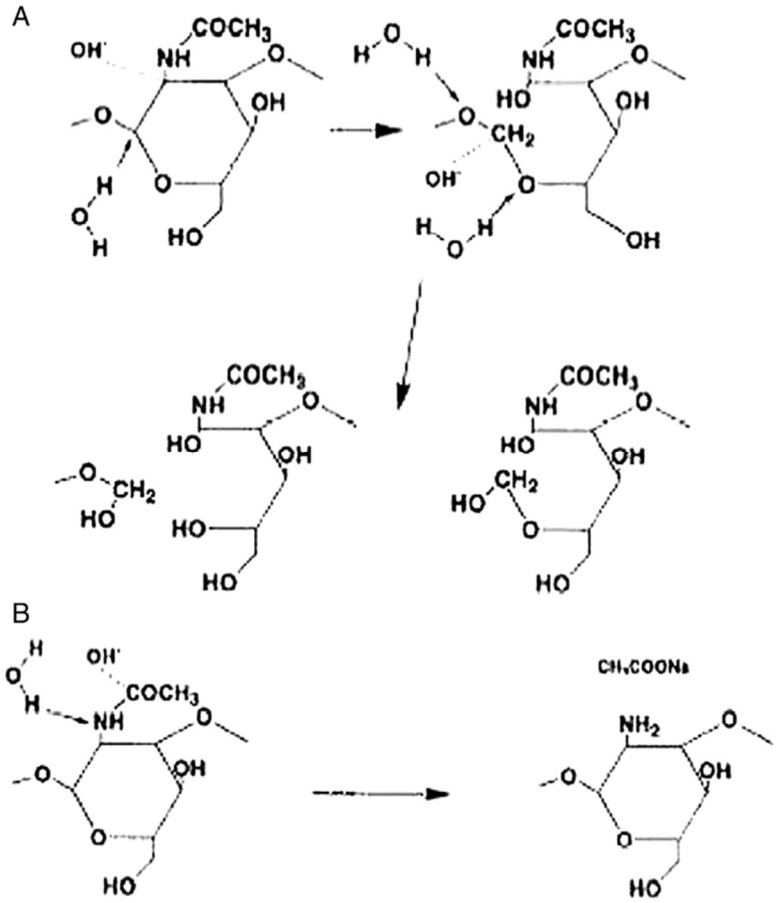

Figure 2. Two-step pathway mechanism of the hydrolysis of HA in alkaline conditions.

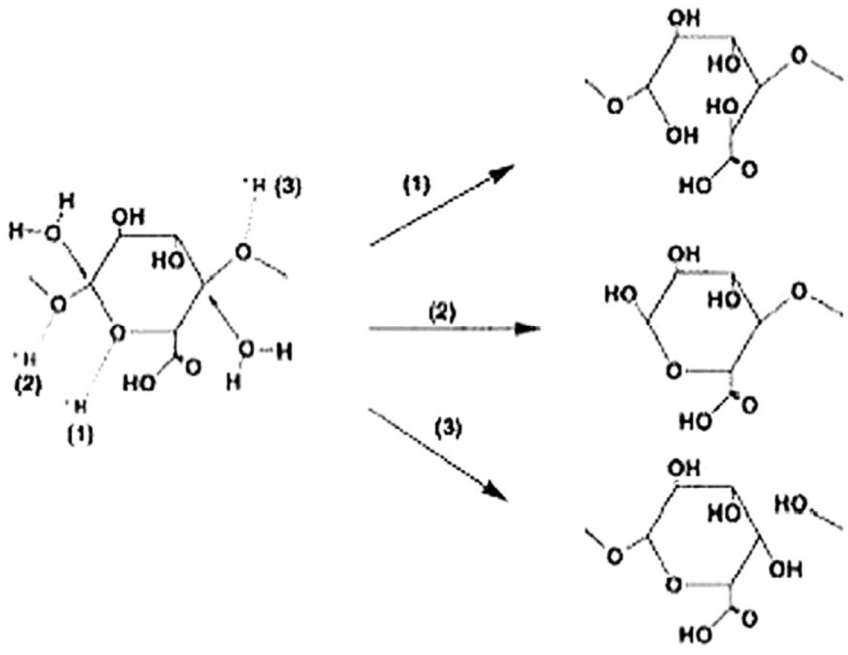

Figure 3. Mechanism of the hydrolysis of HA in acidic conditions. Three possible sites of proton attack on the glucuronic acid unit and the corresponding degradation pathways are marked with numbers (1)–(3).

Several human diseases are associated with harmful action of reactive oxygen species (ROS) [44]. For example, in rheumatoid arthritis (RA) a progressive degradation of hydrophilic polymers, including HA, occurs in synovial fluid (SF). In the acute phases of the disease, a large number of neutrophils accumulated in patient's SF and their products, especially ROS, can contribute to the destruction of joint structures. Due to chronic inflammation, the ROS alter or destroy the joint structure to such an extent that it is no longer functional. The altered tissue is recognized as "foreign", and subsequently autoimmune reactions promote the disease and make RA a systemic ailment affecting the entire body [31].

1.1.5. Rheology of HA aqueous solutions

HA in the surface layers of articular cartilage and of synovial tissue absorbs mechanical stress thereby protecting the cells and collagen network from mechanical shock and deformation. In other words, this polysaccharide serves in these tissue layers as a shock absorber [45,46].

The protective action of HA aqueous solutions depends on their rheological properties: HA solutions, in fact, are reversible gels with a temporary network structure [47]. In particular, HA solutions are non-Newtonian fluids with a shear rate dependent viscosity [48,49]. The viscoelastic properties of HA solutions are characterized by dynamic shear moduli at various strain frequencies: the dynamic loss module (G'') or viscous module, that represents the energy dissipated when the molecule is submitted to a strain, and the dynamic storage module (G') or elastic module that represents the energy stored when the molecule is submitted to a strain. The elasticity, also called entropy elasticity, depends on the states of order or disorder in the arrangement of the molecular chains of HA [45]. For high MW HA solutions, G' exceeds G'' at high frequencies, whereas the opposite occurs at low frequencies [50], the dynamic moduli G' and G'', therefore exhibit a cross over point in the two moduli *vs* frequency profiles.

In addition to MW, the presence of ions such as Na^+, Ca^{++} and K^+ and small molecules such as urea and glucose could also affect the rheology of HA solutions.

1.1.6. HA production

Traditionally HA has been extracted from rooster combs, whereas nowadays it is mainly produced via microbial fermentation, which enables lower production costs and minor environmental pollution [51-53].

Gram- positive Streptococcus sp. are the main producers of HA on industrial scale. In fact, as HA does not initiate an immune response, bacteria such as *Streptococcus zooepidemicus* synthesises HA as a means to encapsulate its cells and exhibit molecular mimicry to escape detection from the host's immune system [54].

The first commercially fermented HA was produced from *Streptococcus zooepidemicus* by Shiseido in the 1980s. Nevertheless, the production of HA from Streptococcus sp. presents two limits: the presence of bacterial endotoxins and the problem that streptococci are pathogenic [55].

For this reason HTL, the largest producer of HA in Europe, has selected HA produced by *Streptococcus equithatis*, since it is a non-pathogen microorganism for humans. According to HTL certificates of analysis the endotoxin amount largely complies with the limits reported in the HA monograph of Ph. Eur. 10th Ed. (less than 0.5 IU/mg for intra-articular preparations).

Molecular weight is an important quality parameter for a commercial HA product and during the HA production from Streptococcus sp. there are some key factors that influence HA molecular weight, such as: the balance between the synthesis rate of HA and the providing rate of precursor sugars [56], the balance between glycolytic rate and HA synthesis rate [57], a right combination of high dissolved oxygen level, that favours a high molecular weight, and mild shear stress [58]. These process parameters have been able to generate HA products with molecular weights above 1MDa, suitable for biomedical and cosmetic uses [59]. Since 2018 HTL has also commercialized a very high molecular weight HA, about 3.5 MDa.

Recombinant HA production has emerged as an attractive alternative to bacterial synthesis. According to this approach both Gram-positive and Gram-negative bacteria are used as hosts, including Bacillus sp. [55], *Lactococcus lactis* [60], Agrobacterium sp. [61] and *Escherichia coli* [62].

1.1.7. HA applications

Due to its peculiar properties, HA is employed for many purposes:

- Orthopaedic application: HA plays a vital role in the development of cartilage, in the maintenance of the synovial fluid and the regeneration of tendons [63]. Thanks to its viscoelastic nature and ability to form highly hydrated matrices, HA acts in the joint as a lubricant and shock absorber and for this reason it is used for viscosupplementation [64].
- ophthalmology: intraocular injection of HA during surgery is used to maintain the shape of the eye anterior chamber. Furthermore, HA solutions also serve as a viscosity-enhancing component of eye drops and as an adjuvant to eye tissue repair [21,65].
- dermatology and wound-healing applications: HA is useful to support dermal regeneration and augmentation. Moreover, as a result of its ability to form hydrated, expanded matrices, HA has also been successfully used in cosmetic applications such as soft tissue augmentation [66,23].
- cardiovascular application: HA is effective for increasing blood compatibility of cardiovascular implants such as vascular grafts and stents [21,67,68].

Thank to all these applications, the global hyaluronic acid market has been valued equal to 6500 million US$ in 2018 and will reach 13400 million US$ by the end of 2025, growing at a rate of 9.5% in the period 2019-2025 [33].

2. Synovial fluid (SF) and SF related diseases

2.1. Chemical composition of synovial fluid

All human joints are lined with a tissue called synovium. Synovium produces synovia, also called synovial fluid (SF) because of its resemblance to egg white [69]. The synovial fluid of joints normally functions as a biological lubricant, providing low-friction and low-wear properties to articulating cartilage surfaces [70].

Molecules postulated to play a key role, alone or in combination, in lubrication are proteoglycan 4 (PRG4), HA and surface-active phospholipids (SAPLs).

The PRG4s are present in SF at a concentration of 0.05-0.35 mg/ml [71]. HA is a major component of SF found in healthy joints at a concentration of 1-4 mg/mL and molecular weight of 1.6-10.9x10^6 Da.

SAPLs are small amphiphilic molecules that are present in synovial joints at a relatively high concentration, 0.1−0.2 mg/mL [72]. There are two types of SAPLs in synovial fluid: phosphatidylcholines (PCs), with diacyl tails and a phosphatidylcholine head group, and non-phosphatidylcholines (e.g. phosphatidylglycerol) which are present in smaller quantities. There are saturated PCs (SPCs) and unsaturated species (USPCs) (determined by the presence of double bonds in their fatty acid chains). Saturated PCs are the dominant class of PC and, among these, dipalmitoyl phosphatidylcholine (DPPC) is the most surface-active moiety of articular cartilage [73]. In fact, phospholipids readily self-assemble to form bilayer structures. The polar regions of phospholipids favourably interact with water, making them highly hydrated. The repulsion between two zwitterionic phospholipid bilayers is high, but effective only at short distance, due to a combination of hydration and entropic protrusion forces [74]. This repulsion maintains the fluid water layer that facilitates sliding with little energy dissipation, i.e., the friction force is low. This has been observed for adsorbed phospholipid bilayers in the synovial joint and for articular cartilage sliding against a steel surface [75].

The protein content of SF depends on whether the joint is in healthy or diseased ; the protein content in normal fluid is substantially lower than that of plasma. However, in inflammatory and degenerative synovial fluid, the protein content increases becoming similar to plasma [76,77].

Cytokines, collagen, enzymes, proteoglycans and fibronectin are present in low amounts in normal SF and present an increased concentration in degenerative and inflammatory arthritis [78]. It has been reported that lipid concentration in normal SF is considerably lower than that of plasma, whereas in rheumatoid arthritis (RA) SF is as high as 40-60% of plasma concentration [77,79].

The composition of SF in normal, osteoarthritis (OA) and rheumatoid arthritis (RA) fluids is reported in Table 2 [50].

Clinically, SF can be aspirated to diagnose joint disease and typical examination tests include: colour, clarity, viscosity, clot formation and cytology [80,81].

Table 2. Composition of SF in normal,OA and RA fluids (mod. from ref. 50).

	Normal	OA	RA
HA MW (MDa)	6.3-7.6	1.06-3.48	3.2-6.8
HA (mg/mL)	2.50-3.65	1.07-2.60	0.39-2.19
Protein (mg/mL)	10.4-15.8	17.0-56.8	31.6-66.2
Phospholipid (mg/mL)	0.13-0.15	0.29-0.98	0.40-1.40
Total Cholesterol (mg/mL)	0.07-0.08	0.04-1.69	0.76-1.30
Triglycerides (mg/mL)	0	0.12-0.59	0.17-1.00

2.2. Viscoelastic properties of normal and pathological synovial fluid

Healthy SF is a non-Newtonian fluid with shear rate dependent viscosity [48,82,83]. On the contrary, the viscosity of RA synovial fluid can be closer to a Newtonian fluid.

The viscosity range of healthy, degenerative (OA) and inflammatory (RA) SF are 1-40 (Pa.s), 0.1-1 (Pa.s) and 0.004-0.07 (Pa.s), respectively, as shown in Figure 4 [84].

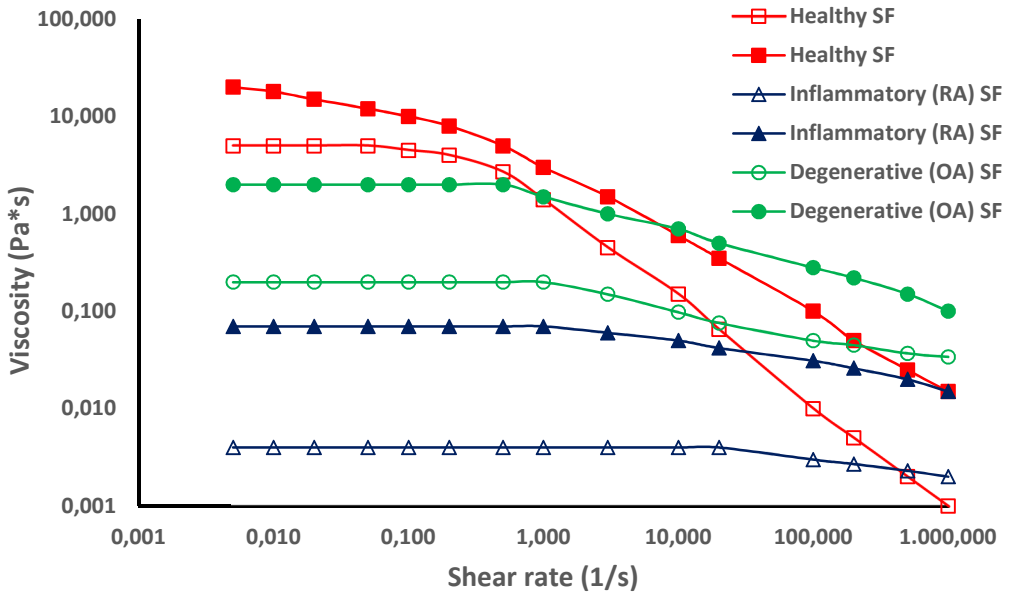

Figure 4. Viscosity profiles of healthy, degenerative and inflammatory synovial fluid.
Open symbols: lower viscosity values; filled symbols: upper viscosity values (mod. from ref. 84).

Synovial fluid is characterized by elastic properties. At low frequencies of oscillation, characteristic of slow joint motion, SF behaves as a viscous fluid, whereas at high frequencies, characteristic of rapid joint motion, it shows an elastic-like response.

As shown in Table 3 [45], the healthy SF of a young normal individual shows higher G'' than G' values at very low frequencies and the cross over point between the two moduli occurs at a relatively low frequency value (0.2-0.3 Hz). At high frequencies, the fluid exhibits an elastic-like behaviour, conceivably because it does not have enough time to dissipate energy [85]. For an old

normal individual, SF frequency at cross over lays between walking and running frequency (0.5-1.5 Hz) and is higher (0.9-1.0 Hz) than that found for a young subject. Pathological SF behaves generally as viscous fluids: its storage modulus G′ is lower than that of healthy SF and G′ doesn't intersect G′′; therefore SF of OA patients has virtually no elasticity.

Table 3. The dynamic moduli of SF from young and old normal individuals and of osteoarthritis patient.

	Frequency range applied (Hz)	**G′′ at the frequency range limits (Pa)**	**G′ values at the frequency range limits (Pa)**	**G′′, G′ value at cross over point (Pa)**	**Frequency at cross over point (Hz)**
Normal young individual	0.01-5	1.5 - 1.3	0.5 - 25	6	0.2-0.3
Normal old individual	0.01-5	0.35 – 4.0	0.1 - 15	3.5	0.9-10
OA patient	0.1 -2.5 0.4- 2.5	0.1 – 2.0	0.1 - 1.8	-	-

The rheological properties of pathological SFs are altered due to the presence of HA at both low concentration and low molecular weight [86,87], which determines not only modified viscoelastic properties, but also a viscosity reduction.

2.3. Viscosupplementation for osteoarthritis treatment

Osteoarthritis (OA) is the most frequent form of arthritis and it represents the most common cause of human disease and disability. In the United States, OA is second only to ischemic heart disease as a cause of work disability in men older than 50 years [88,89] and is expected to affect 59.4 million (18.2%) people in the United States by 2020 [89].

The primary goals for clinical management of OA localized at the knee are to minimize pain, to maintain or improve joint mobility and to minimize functional impairment [90]. The American College of Rheumatology suggests an initial non operative, non invasive treatment consisting of physical therapy, weight loss, bracing and/or assistive devices followed by pharmacologic intervention. Pharmacologic intervention may include topical and oral analgesics, non steroidal anti-inflammatory drugs (NSAIDs), COX-2 inhibitors, opioids, and steroids. When non operative treatment is ineffective, patients are often subjected to viscosupplementation (VS) with hyaluronic acid [88,91].

Intra-articular injection of HA is carried out under sterile conditions. It is usually preceded by an aspiration to remove any liquid effusion that may be present, with the aim of decreasing the concentration of in situ inflammatory mediators and limiting the dilution effect on the injected material [92]. Clinical studies have demonstrated that HA viscosupplementation is generally well tolerated [93]. Although significant complications are rare, mild adverse effects have been reported in 3% to 20% of patients. The most common complication associated with intra-articular HA injection is an inflammatory reaction at the injection site, characterized by localized injection site pain and a knee effusion. These injection site reactions are usually mild and self-limited, and

resolve without intervention within 1 to 3 days [94]. Other mild adverse effects that have been reported include post injection itching, headaches and calf pain.

Viscosupplementation was firstly proposed by Balazs in 1982 [45], who suggested that intra-articular injection of highly purified (protein content <0.3%) concentrated (10 to 20 mg/mL) HA solutions, containing fairly large molecules (MW 1 - 3 million Da), can influence the healing and regeneration of the cartilage and soft tissues of the joint. In fact, in a normal adult knee, there are approximately 2 mL of SF with a HA concentration of 2.5 to 4.0 mg/mL. This endogenous HA, which is produced by type B synoviocytes and fibroblasts of the synovial membrane, has a molecular weight of 5 to 7 $\times 10^6$Da [95].

It has been demonstrated that during the progression of osteoarthritis, the concentration and molecular weight of HA within the synovial fluid are reduced thanks to the dilution consequent to inflammatory effusion, abnormal synoviocyte production, and molecular fragmentation [96]. This alteration in HA structure and concentration during the degenerative process decreases the material ability to effectively lubricate the joint surface and compensate the stresses associated with weight bearing. Additionally, fragmented low-molecular weight HA has been shown to possess a pro-inflammatory effect [97].

Injection of HA into the joint space of an osteoarthritic knee has been demonstrated to improve the quantitative and qualitative properties of endogenous HA, by increasing joint lubrication in the short term [98]. Additionally, exogenous HA supplementation may provide significant anti-inflammatory effects within the joint space, by affecting leukocyte function and by reducing the concentration of inflammatory mediators, such as prostaglandins and fibronectin [99].

Viscosupplementation of knee joint (Figure 5) has entered the clinical practice in various countries from many years ago: Japan and Italy in 1987, Canada in 1992, Europe in 1995, and in the United States in 1997.

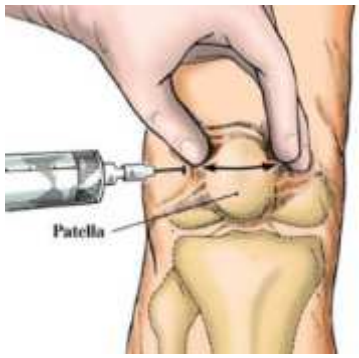

Figure 5. Intra-articular injection of HA into the keen joint.

Several trials have shown that HA therapy may have utility in treating OA pain in other joints such as ankle, shoulder, hand and hip [100].

3. Tear fluid and tear fluid deficiency related diseases

3.1. Tear fluid composition

Natural tears possess three major functions: they preserve the metabolism of the ocular surface, enable the maintenance of a smooth surface that allows regular light refraction, and lubricate the ocular surface to facilitate blinking [101,102].

Natural tears consist of an aqueous solution (water being the major component ≅98 %) having complex compositions: in fact, they contain salts, hydrocarbons, proteins and lipids.

The structural components of tears are responsible for the three-layered architecture of the tear film. The innermost mucus layer is produced by the cells of the conjunctiva. The mucus helps the overlying watery layer to spread evenly over the eye.

The middle or aqueous layer is the largest and thickest layer produced by the glands of the upper lids and the accessory tear glands and it contains essentially a very dilute salt water solution [103]. This layer keeps the eye moist and helps in the removal of any dust, debris, or foreign particle.

The uppermost layer of tear film is a very thin layer of lipids. This layer helps to decrease water evaporation from the watery layer beneath it.

The tear fluid also consists of a complex mixture of proteins, immunoglobulins, mucins, electrolytes, cytokines, lysozymes, lactoferrin, with an antibacterial effect, and moreover contains growth factors [104].

Tears are characterized by osmolarity of 309 mOsm/L and average pH of 7.25 [105].

Insufficient tear production causes damage to the eyelid ocular surface and determines pain and discomfort [106].

3.2. Dry eye disease

Dry eye disease is recognized as a consequence of the loss of lachrymal fluid functionality associated with changes in tear fluid composition and tear film stability [107], which determine inflammation of the ocular surface.

The two main types of dry eye syndrome (DES), as identified by the International Dry Eye workshop report (2007), are Aqueous Deficient Dry Eye (ADDE), characterized by a failure of lacrimal secretion, and evaporative dry eye (EDE), that is characterized by an excessive water loss from the exposed ocular surface in the presence of normal tear secretive function [108].

The International Dry Eye Workshop (2007) defined DES a multifactorial disease of the tears and ocular surface that determines discomfort, visual disturbance and tear film instability with potential damage to the ocular surface. DES is accompanied by increased osmolality of the tear film and inflammation of the ocular surface [109]. DES is associated with decreased ability to perform certain activities which require visual attention such as reading, driving and computer related work [110].

The prevalence of dry eye syndrome increases with age, especially in people older than 50 years [111]. In particular in women, after menopause, an imbalance between oestrogen and androgen hormones excites inflammation of lacrimal gland. Up to 20% people with rheumatoid arthritis are also affected by DES [112]. Other individuals, that are likely to be affected, include patients with *Helicobacter pylori*, computer users and long term contact lens wearers [113]. A special case of DES is known as "Sjogren's syndrome", which is characterized by the combination of tear deficiency and dry mouth (xerostomia) [114].

The diagnosis of DES is made by combining the information obtained from the visual inspection of the eye and by performing diagnostic tests. For example, the time required for the tear film to break up following a blink is investigated through a test called "Tear Film Breakup Time" (TBUT), i.e. a quantitative test that measures tear film stability.

A simple and easy way to recognize the severity of the dryness is the staining method: special dyes such as Rose Bengal, lissamine green, and fluorescein are used [115] to determine abnormalities of eye surface, quality of tear film and severity of dryness.

The Schirmer test quantitatively measures the tear production by the lacrimal gland during fixed time period [116,117].

DES is treated in various ways. The goals of treatment are to relieve the symptoms, to improve patient's comfort, to return the eye surface and tear film to the physiologic state, and, whenever possible, to prevent corneal damage. Treatments encompass environmental or dietary modifications, use of artificial tear substitutes, uptake of anti-inflammatory or immune-modulatory drugs (such as Cyclosporine A) via topical or systemic administration up to occlusion surgery, which consists of inserting punctal plugs (silicone or collagen) into the tear drainage area to keep the tears in the eyes for a longer time [106].

The healthcare burden of DES is continually increasing. Surveys have estimated the prevalence of DES, varying between 5% and 30% in various age groups across different countries and worldwide [118,119]. The estimated number of people affected by DES ranges from 25 to 30 million people all over the world.

3.3. Artificial tears

3.3.1. Artificial tears composition and function

Artificial tears, consisting of aqueous eye drops with lubricant properties, are currently the mainstay of DES therapy and they should mimic as closely as possible the desirable properties of natural tears.

For this reason artificial tears should have a composition which is compatible with the maintenance of a normal eye surface epithelium. When damage exists, the artificial tear solution should provide an environment in which the epithelium can recover the normal structure and function [120].

Artificial tears are currently the mainstay of DES therapy. They account for at least $540 million in annual sales globally and are the preferred first-line therapy due to their non invasive nature and low side effect profile.

Lubricant tears represent the first line of treatment. Mild disease conditions require the application of lubricant drops four times a day while severe cases need greater frequency of administration (10–12 times a day). In case of moderate to severe forms of DES, artificial tears can be associated with drugs such as cyclosporine, corticosteroids, and tetracycline, to reduce signs and symptoms [106].

FDA classifies artificial tears in two classes: demulcents and emollients.

Demulcents are substances that soothe the mucous membranes and, in the case of artificial tears, provide lubrication in the form of a mucoprotective film. They can alleviate discomfort, aid in water retention and decrease friction on the eye surface.

The FDA has established six categories of ophthalmic demulcents that must fall within a specified concentration range: cellulose derivatives, dextran 70, gelatin, liquid polyols, polyvinyl alcohol and povidone. These products can be used alone or in combinations of up to three substances.

One of the most commonly used demulcent is carboxymethylcellulose (CMC) that increases tear viscosity and possesses mucoadhesive properties, enabling its permanence on the ocular surface for long time periods. The concentration of commercially available CMC artificial tear products ranges from 0.2% to 1%. Cellulose derivatives are found in products like Refresh Tears (Allergan), GenTeal Tears (Alcon) and TheraTears (Akorn) [121].

Emollients, such as fats or oils, increase the lipid layer thickness of the tear film, stabilize the tear film and reduce evaporation. Emollients typically use a combination of mineral oil, light mineral oil and white petrolatum. Artificial tears that contain lipids must be formulated as an emulsion. Current lipid-based artificial tears include Systane Balance and Systane Complete (mineral oil) by Alcon , Refresh Optive Advanced (castor oil) and Refresh Optive Mega-3 (castor oil and flaxseed oil) by Allergan, Soothe XP (mineral oil and light mineral oil) by Bausch&Lomb and Retaine MGD (mineral oil and light mineral oil, OCuSoft) [121].

Artificial tears have been classified in order to facilitate their knowledge in view of clinical use [101,122]. These classifications are based mainly on biological effects and chemical composition of the products. Classification by biophysical and biochemical properties includes (1) osmotic pressure, (2) surface tension, (3) lubricity/viscosity and (4) evaporation. Classification by chemical composition includes (1) water, (2) saline solutions, (3) glycerol, monosaccharides, disaccharides, (4) polysaccharides that include mucilages (gums), dextrans and glycosaminoglicans such as chondroitin sulphate and sodium hyaluronate, (5) synthetic derivatives such as vinyl polymers or polyethylene glycol, (6) gelatins, (7) biological fluids and (8) lipids.

Many studies in the literature have demonstrated that tear substitutes containing hyaluronic acid are able to improve tear film stability and to delay water evaporation from the tear film thanks to their mucomimetic, viscoelastic and water-retention properties [122,123].

In particular, the administration of tear substitutes based on HA determined a DES symptoms reduction greater not only than the one of saline [120], but also than that of tear substitutes based

on other hydrophilic polymers such as carboxymethylcellulose [124] or hydroxypropyl-methylcellulose [125] both characterized by viscoelastic properties similar to HA.

The successful use of a 0.1% solution of high MW hyaluronan solution for the treatment of severe dry eye cases has been described since the early 1980s [126].

In 1995, the product Hyalein®, developed by the Japanese ophthalmic manufacturer Santen, was approved by the Japanese drug regulatory agency. In 1998, the first hyaluronan eye drops arrived also on the German market. Since then, specialists and patients have had the possibility to choose between a large number of hyaluronan-based tear substitutes that are expected to be successful products also in the future [123].

Preservatives are often added to multidose containers of artificial tears to reduce the risk of bacterial contamination and to prolong the shelf life.

The most common preservative used in ocular solutions are benzalkonium chloride (BAK), chlorobutanol, sodium perborate, thiomersal, disodium edentate and oxychloro complex (SOC).

When dealing with artificial tear formulation, it must be taken into account, however, that preservatives can cause toxic epithelial effects and hypersensitivity reactions, ranging from mild irritation to severe corneal and conjunctival scarring [127,122].

Preservative-free eye drops prevent these effects and they are indicated in case of severe dry eye syndrome or when high doses of lubricants are required .

3.3.2. Rheological properties of artificial tears

Artificial tears should mimic as closely as possible the desirable properties of normal tears.

Tears also have a low surface tension with a mean value of 43-44 mN/m in normal subjects in comparison with ≅ 72 mN/m, typical of water. The standard belief for many years has been that both these properties depend on the presence of goblet-cell secreted mucins, dissolved in the aqueous tears, which are in equilibrium with the gel layer of mucus coating the conjunctival and corneal surfaces [128].

The rheological properties of tear fluid and tear fluid substitutes must accomplish the shearing forces generated by eye or lid movements, and the shear rates determined by their application. Two distinct rheological regimes can be recognised in the eye.

One is a low-shear static condition, typical of the open eye between two consecutive blinks. In this condition, a tear substitute must resists the drainage of the precorneal film, which would lead to film thinning and break-up. A high viscosity of the product will aid its maintenance on eye surface in static (open eye) condition.

During blinking, another situation, accompanied by a high-shear regimen, occurs. In fact, the combination of a high lid speed with a small film thickness results in a high velocity gradient and in shear rate values up to 20000 sec^{-1} [129]. This condition impairs the usefulness of a high viscosity film, since it will cause unacceptable dragging forces on the epithelial surfaces [130], and, on the contrary, prompts for a low viscosity of the tear film.

Although many polymers currently used in commercial artificial tears are Newtonian, these formulations show an uneasy compromise between a viscosity high enough to resist draining in the open eye, but low enough to avoid drag sensations and surface damage during blinking.

The combination of optimal rheological behaviour of tear substitutes (i.e. high viscosity at rest, open eye, and low viscosity during blinking) would be best achieved by the use of a pseudoplastic fluid (i.e. a non-Newtonian fluid exhibiting shear-thinning), whose viscosity is high at low shear rates and low at high shear rates, rather than by a Newtonian fluid, whose viscosity is independent on shear rate.

It is known that human tears, possess this property thanks to their content of soluble muco-glycoprotein [131]. In fact, tear fluid viscosity is about 65 mPa·s when the eyes are open, and decreases to 10 mPa·s during blinking [128].

Therefore the formulation development of new tear substitutes, namely containing HA, would aim at attaining a non-Newtonian behaviour, similar to natural tears. In this perspective, it must be taken in mind that the higher the molar mass of hyaluronic acids, the more the viscosity of hyaluronic acid solutions depends on shear forces [132].

Moreover the formulation development of HA artificial tears must be founded on the rheological characterization of its aqueous solution, in particular on the evaluation of a zero shear viscosity (η_0), to mimic the conditions of open eyelid, and a high shear viscosity (η_{1000}, i.e. viscosity measured at 1000 s^{-1} shear rate) to mimic the situation when the rim of the lids glides over the corneal epithelium during blinking.

The literature [133,134] reports variable-shear viscosity results of tears, obtained from rotational rheometry, which measures total torque as a function of rotational speed. The results can be interpreted in terms of an entangled meshwork of linear polymer molecules which tend to be pulled apart by shearing, but which can re-entangle at low shear rates (resulting in high viscosity). At high shear rates, instead, the speed of separation of molecules prevents re-entanglement (resulting in low viscosity). During viscous flow, energy is applied to the system to cause motion of the molecules, but it is entirely taken up in overcoming frictional forces and it is dissipated as heat. This dissipation rapidly reduces the flow of polymer molecules as the shearing force is removed; therefore viscosity is determined by the rate of shear. In fact, the entangled meshwork of polymer molecules possesses elasticity as well as viscosity, since energy input can be absorbed by distorting the meshwork in a recoverable manner as well as by causing some relative movement of the molecules or viscous flow [128].

HA tear substitute solutions have been recently classified in five categories on the basis of their viscoelastic properties [135], as shown in Table 4.

Table 4. Classification of HA artificial tears according to [135].

Type	Viscoelastic properties	Uses
1	$\eta 0 < 6$ mPa·s : close to Newtonian flow properties	Treatment of light DES, indicated also for patients wearing contact lenses
2	6 mPa·s < $\eta 0$ < 16 mPa·s: low effectiveness and no "prolonged effect"	
3	16 mPa·s < $\eta 0$ <32 mPa·s : good effectiveness	Universal application
4	$\eta 0$>32 mPa·s and $\eta 1000$ < 12 mPa·s: **best simulation of tear fluidity**	**Universal application, even with patients with recurrent corneal erosions**
5	$\eta 0$ >32 mPa·s and $\eta 1000$ > 12 mPa·s: high zero shear viscosity, but exerting high shear forces on the corneal epithelium during blinking	Caution should be taken when using eye gels especially in patients with sensitive corneal epithelium, in patients wearing contact lenses and when there are chronic inflammatory conditions in case of moderate to severe dry eye

On the basis of Table 4 the best functional properties will characterize artificial tears belonging to type 4.

4. References

1. Fraser, J.; Laurent, T.C.; Laurent, U.B. Hyaluronan:its nature, distribution, functions and turnover. *J. intern. Med*. **1997**, *242*, 27-33.
2. Gandhi, N.S.; Mancera, R.L. The Structure of glycosaminoglycans and their interactions with proteins. *Chem. Biol. Drug Des*. **2008**, *72*, 455-482.
3. Blanco, A; Blanco, G. Carbohydrates. In: Medical Biochemistry, Academic Press, 2017; Chapter 4, pp. 88-89.
4. Gabius, H. Proteoglycans. In:*The sugar code: fundamentals of glycosciences.* Wiley-Blackwell, Chichester, UK 2009; pp. 199-215.
5. Harvey, R.; Ferrier, D. Glycosaminoglycans, proteoglycans and glycoproteins. In: *Biochemistry 5thed.;* Wolters Kluwer Health/Lippincott Williams & Wilkins, Philadelphia, USA 2011; pp.157-171.
6. Linhardt, R.; Avci, F.Y.; Toida, T.; Kim, Y.S.; Cygler, M. CS lyases: structure, activity, and applications in analysis and the treatment of disease. *Adv. Pharmacol.* **2006,** *53*, 187-215.
7. Kowitsch, A.; Zhou, G.; Groth, T. Medical application of glycosaminoglycans a review. *J. Tissue Eng. Regen. Med*. **2018**, *12*, e23-e41.
8. Rabenstein, D. Heparin and heparan sulphate: structure and function. *Nat. Prod. Rep.* **2002,** *19*, 312-331.
9. Pavao, M. Structure and anticoagulant properties of sulphated glycosaminoglycans from primitive Chordates. *An. Acad. Bras. Ciec.* **2002**, *74*, 105-112.
10. Whitelock, J.; Iozzo, R. Heparan sulphate a complex polymer charged with biological activity. *Chem. Rev*. **2005**, *105*, 2745-2764.
11. Funderburgh, J. Keratan sulfate biosynthesis. *IUBMB life* **2002**, *54*, 187-194.
12. Silibert, J.; Sugumaran, G. Biosynthesis of chondroitin/dermatan sulphate. *IUBMB life* **2002**, *54*, 177-186.
13. Lauder, R. M. Chondroitin sulphate: a complex molecule with potential impacts on a wide range of biological systems. *Complement. Ther. Med.* **2009**, *17*, 56-62.

14. Trowbridge, J.; Gallo, R. Dermatan sulphate: new functions from an old glycosaminoglycan. *Glycobiology* **2002**, *12*, 117R-125R.
15. Willard, V.P.; Kalpakci, K.N.; Reimer, A.J.; Athanasiou, K.A. The Regional contribution of glycosaminoglycans to temporomandibular joint disc compressive properties. *J. Biomech. Eng*. **2012**, *134*, 011011-1 – 011011-8.
16. Nakagawa, H.; Hama Y.; Sumi, T.; Li, C.; Maskos, K.; Kalayanamitra, K.; Mizumoto, S.; Sugahara, K.; Li, T. Occurrence of a nonsulphated chondroitin proteoglycan in the dried saliva of Collocalia swiftlets(edible bird's-nest). *Glycobiology* **2007**, *17*, 157-164.
17. De Rosa, M.; Schiraldi, C.; Cimini, D. Biotechnological production of chondroitin.*Patent No. WO 2010/136435 A1* **2010**.
18. Meyer, K.; Palmer, J. The polysaccharide of the vitreous humor. *J. Biol. Chem.* **1934**, *107*, 629-634.
19. Balazs, E.; Sweeney, D. The molecular biology of the vitreous. In: *New and controversial aspects of retinal detachment;* Hoeber Medical Division, Harper & Row, New York, USA, 1968; pp. 3-15.
20. Haxaire, K.; Braccini, I.; Milas, M.; Rinaudo, M.; Perez, S. Conformational behaviour of hyaluronan in relation to its physical properties as probed by molecular modeling. *Glycobiology* **2000**, *10*, 587-594.
21. Necas, J.; Bartosikova, L.; Brauner, P.; Kolar, J. Hyaluronic acid (hyaluronan): a review. *Veterinarni Medicina* **2008**, *53*, 397-411.
22. Weigel, P.; Deangelis, P. Hyaluronan synthases: a decade-plus of novel glycosyltransferases. *J. Biol. Chem.* **2007**, *282*, 36777–36781.
23. Dovedytis, M.; Liu, Z.J.; Barlett, S. Hyaluronic acid and its biomedical applications: A review. *Eng. Reg.* **2020**, *1*, 102-113.
24. Fung, Y. Bioviscoelastic fluids. In: *Biomechanics: Mechanical Properties of Living Tissues;* Springer Science & Business Media, New York, USA, 1981; pp. 220-241.
25. Stern, R.; Asari, A.A.; Sugahara, K.N. Hyaluronan fragments: an informaion-rich system. *Eur. J. Cell. Biol.* **2006**, *85*, 699-715.
26. Band, P.; Heeter, J.; Wisniewski, H.G.; Liublinska, V.; Pattanayak, C.W.; Karia, R.J.; Stabler, T.; Balazs, E.A.; Kraus, V.B. Hyaluronan molecular weight distribution is associated with the risk of knee osteoarthritis progression. *Osteoarthr. Cartil.* **2015**, *23*, 70-76.
27. Scott, J.; Heatley, F.; Hull, W.E. Secondary strucure of hyaluronate in solution. A ^{1}H-n.m.r. investigation at 300 and 500 MHz in [$^{2}H_{6}$]dimethyl sulphoxide solution.*Biochem. J.*, **1984**, *220*, 197-205.
28. Dong, Q.; Guo, X.; Li, L.; Yu, C.; Nie, L.; Tian, W.; Zhang, H.; Huang, S.; Zang, H. Understanding hyaluronic acid induced variation of water structure by near-infrared spectroscopy.*Nature* **2020**, *10*, 1387-1394.
29. Ghosh, P.; Hutadilok, N.; Adam, N.; Lentini, A. Interactions of hyaluronan (hyaluronic acid) with phospholipids ad determined by gel permeation chromatography, multi-angle laser-light-scattering photometry and ^{1}H-NMR spectroscopy. *Int. J. Biol. Macromol.* **1994**, *16*, 237-244.
30. Darke, A.; Finer, E.G.; Moorhouse, R.; Rees, D.A. Studies of hyaluronate solutions by nuclear magnetic relaxation measurements. Detection of covalently-defined, stiff segments within the flexible chains. *J. Mol. Biol.* **1975**, *3*, 477-486.
31. Stern, R.; Kogan, G.; Jedrzejas, M.; Soltes, L. The many ways to cleave hyaluronan. *Biotechnology Advances*, **2007**, *25*, 537-557.
32. Reed, M.; Damodarasamy, M.; Chan, C.K.; Johnson, M.; Wight, T.N.; Vernon, R.B. Clavage of Hyaluronan is imparied in aged dermal wounds *Matrix Biol*. **2013**, *32*, 45-51.
33. Monslow, J.; Govindaraju, P.; Purè, E. Hyaluronan – a functional and structural sweet spot in the tissue microenvironment. *Frontiers in Immunology* **2015**, *6*, 231-249.
34. Cowman, M.K. Hyaluronan and hyaluronan fragments. In: *Advances in Carbohydrate Chemistry and Biochemistry* Elsevier, 2017; 74, Chapter One, pp. 1-59.
35. Meyer, K. Hyaluronidases. In *The enzymes;* Academic Press, New York, USA, 1971; pp. 307-320.
36. Ridgen, D.; Jedzejas, M. Structures of *Streptococcus pneumoniae* hyaluronate lyase in complex with chondroitin and chondroitin sulphate disaccharides. Insights into specificity and mechanism of action. *J Biol Chem*, **2003**, *278*, 50969-50606.
37. Mio, K.; Stern, R. Inhibitors of the hyaluronidases. *Matrix Biol*, **2002**, *21*, 31-37.

38. Spickenreither, M.; Braun, S.; Bernhardt, G.; Dove, S.; Buschauer, A. Novel 6-O-acylated vitamin C derivatives as hyaluronidase inhibitors with selectivity for bacterial lyases. *Bioorg. Med. Chem. Lett.* **2006**, *16*, 5313-5316.
39. Lishanti, U.A. Inhibition of hyaluronan degradation by dextran sulphate facilitates characterization of hyaluronan synthesis: an in vitro and in vivo study. *Glycoconj J.* **2004**, *20*, 461-471.
40. Lowry, K.; Beavers, E. Thermal stability of sodium hyaluronate in aqueous solution. *J. Biomed. Mater Res.*, **1994**, *28*, 1239-1244.
41. Yang, B.; Montgomery, R. Beta-elimination of glucosyluronic residues during methylation of an acidic polysaccharide from Erwinia chrysantemi CU 643. *Carbohydr. Res.* **2001**, *332*, 317-323.
42. Tokita, Y.; Okamoto, A. Hydrolytic degradation of hyaluronic acid. *Polym. Degrad. Stab.* **1995**, *48*, 269-273.
43. Lapcik, L.Jr.; Lapcik, L.; De Smedt, S.; Demeester, J.; Chabrecek, P. Hyaluronan: preparation, strucure, propertiers, and applications. *Chem. Rev.* **1998**, *98*, 2663-2684.
44. Sies, H.; Jones, D.P. Reactive oxygen species (ROS) as pleiotropic physiological signalling agents *Mol. Cell. Biol.* **2020**, *21*, 363-383.
45. Balazs, E.A. The physical properties of the synovial fluid and the special role of hyaluronic acid. In: *Disorders of the knee*; Lippincott, Philadelphia, USA, 1982; pp. 63-75.
46. Simorano C.M.; D'Angelo, M.; He, X.; Eliyahu, E.; Shtraizent, N.; Haskins, M.; Schuchman, H. Mechanism of glycosaminoglycan-mediated bone and joint disease. *Am. J. Pathol.* **2008**, *172*, 112-122.
47. Krause, W.; Bellomo, E.G.; Colby, R.H. Rheology of sodium hyaluronate under physiological conditions. *Biomacromolecules*, **2001**, *2*, 65-69.
48. Barnett, C. Measurement and interpretation of synovial fluid viscosities. *Ann. Rheum. Dis.* **1958**, 17, 229-233.
49. Ambrosio, L.; Borzacchiello, A.; Netti, P.A.; Nicolais, L. Rheological study on hyaluronic acid and its derivative solutions. *J. Macromol. Sci.* **2007**, *36*, 991-1000.
50. Fam, H.; Brayant, J.T.; Kontopoulou, M. Rheological properties of synovial fluids. *Biorheology* **2007**, 44, 59-74.
51. Chong, F.; Nielsen, L. Amplifying the cellular reduction potential of *Streptococcus zooepidemicus*. *J. Biotechnol.* **2003**, *100*, 33-41.
52. Boeriu, C.G.; Springer, J.; Kooy, F.K.; Van Den Broek, L.; Eggink, G. Production methods for Hyaluronan. *Int. J. Carbohydr. Chem*. **2013**, article 624967, 1-14.
53. Kaur, M.; Jayaraman, G. Hyaluronan production and molecular weight is enhanced in pathway-engineered strains of lactate dehydrogenase-deficient *Lactococcus lactis Metabolic Eng. Comm*. **2016**, *3*, 15-23.
54. Boyce, C.; Chung, Y.; Alder, B. Pasteurella multocida capsule: composition, function and genetics. *J. Biotechnol.* **2000**, *83*, 153-160.
55. Widner, B.; Behr, R.; Von Dollen, S.; Tang, M.; Heu, T.; Sloma, A.; Sternberg, D.; De Angelis, P.; Weigel, P.; Brown, S. Hyaluronic acid production in *Bacillus subtilis*. *Appl. Environ. Microbiol.* **2005**, *71*, 3747-3752.
56. Sheng, J.; Ling, P.X.; Zhu, X.Q.; Guo, X.P.; Zhang, T.M., He, Y.L., Wang, F.S. Use of induction promoters to regulate hyaluronan synthase and UDP-glucose-6-dehydrogenase of *Streptococcus zooepidemicus* expression in *Lactococcus lactis*: a case study of the regulation mechanism of hyaluronic acid polymer. *J. Appl. Microbiol.* **2009**, *107*, 136-144.
57. Jagannath, S.; Ramachandran, K. Influence of competing metabolic processes on the molecular weight of hyaluronic acid synthesized by *Streptococcus zooepidemicus*. *Biochem. Eng. J.* **2010**, *48*, 148-15.
58. Duan, X.; Yang, L.; Zhang, X.; Tan, W. Effect of oxygen and shear stress on molecular weight of hyaluronic acid produced by *Streptococcus zooepidemicus*. *J. Microbiol. Biotechnol.* **2008**, *18*, 718-724.
59. Liu, L.; Liu, Y.; Li, J.; Du, G.; Chen, J. Microbial production of hyaluronic acid: current state, challenges, and perspectives. *Microb. Cell. Fact.* **2011**, *10*, 10-99.
60. Chien, L.; Lee, C. Hyaluronic acid production by recombinant *Lactococcus lactis*. *Appl. Microbiol. Biotechnol.* **2007**, 77, 339-346.
61. Mao, Z.; Chen, R. Recombinant synthesis of hyaluronan by Agrobacterium sp. *Biotechnol. Prog.* **2007**, *23*, 1038-1042.

62. Yu, H.; Stephanopoulos, G. Metabolic engineering of *Escherichia coli* for biosynthesis of hyaluronic acid. *Metabolic. Eng.* **2008**, *10*, 24-32.
63. Toole, B. Hyaluronan in morphogenesis. *Cell. and Developmental Biology* **2001**, *12*, 79-87.
64. Wen, D. Intra-articular hyaluronic acid injections for kneee osteoarthritis *Am Fam Physician* **2000**, *62*, 565-570.
65. Kojima, T. Contact lens-associated dry eye disease: recent advances worldwide and in Japan.*IOVS*, **2018**, *59*, DES102-DES108.
66. Dechert, T.; Ducale, A.E.; Ward, S.; Yager, D.R. Hyaluronan in human acute and chronic dermal wounds. *Wound Repair and Regeneration* **2006**, *14*, 252-258.
67. Papanastasopoulou, C.; Papastamataki, M.; Karampatsis, P.; Anagnostopoulou, E.; Papassotiriou, I.; Sitaras, N. Cardiovascular Risk and Serum Hyaluronic Acid: A preliminary study in a healthy population of low/intermediate risk. *J. Clin. Lab. Anal.* **2017**, *31*, e22010.
68. Yu, Y.; Zhu, S.; Hou, Y.; Li, J.; Guan, S. Sulfur contents in sulfonated hyaluronic acid direct the cardiovascular cell fate. *ACS Appl. Mater. Interfaces* **2020**, *12*, 46827-46836.
69. Gatter, R.A.; Schumacher, H.R. Joint Aspiration: indications and technique. In: *A Practical Handbook of Joint Fluid Analysis,* 2nd ed.; Lea & Febiger, Philadelphia, PA,USA, 1991; pp. 7–14.
70. Blewis, M; Nugent-Derfus, G.E.; Schmidt, T.A.; Schumacher, B.L.; Sah, R.L. A model of synovial fluid lubricant composition in normal and injured joints. *Eur. Cell Mater.* **2007**, *13*, 26-39.
71. Schmid, T.A.; Gastelum, N.S.; Nguyen, Q.T.; Schumacher, B.L.; Sah, R.L. Boundary lubrication of articular cartilage: Role of synovial fluid constituents. *Arthritis Rheum.***2007**, *56*, 882–891.
72. Wang, M.; Liu, C.; Thormann, E.; Dedinaite, A. Hyaluronan and phospholipid association in biolubrication. *Biomacromolecules* **2013**, *14*, 4198-4206.
73. Hills, B. Oligolamellar lubrication of joints by surface active phospholipid. *J. Rheumatol.* **1989**, 16, 82-91.
74. Istaelachvili, J.; Wennerstrom, H. Role of hydration and water structure in biological and colloidal interactions. *Nature* **1996**, *379*, 219-225.
75. Ozturk, H.; Stoffel, K.K.; Jones, C.F.; Stachowiak, G.W. The effect of surface-active phospholipids on the lubrication of osteoarthritic sheep knee joints: Friction. *Tribol. Lett.* **2004**, *16*, 283-289.
76. Binette, J.; Schmid, K. The proteins of synovial fluid. *Arthritis Rheum.* **1965**, *8*, 14-28.
77. Wiegand, N.; Bucs, G.; Dande, A.; Lorinczy, D. Investigation of protein content of synovial fluid with DSC in different arthritides. *J. Therm. Anal. Cal.* **2019**, *138*, 4497-4503.
78. Oxford, J.T.; Reeck, J.C.; Hardy, M.J. Extracellular matrix in development and disease. *Int. J. Mol. Sci.* **2019**, *20*, 205-210.
79. Bole, G. (1962). Synovial fluid lipids in normal individuals and patients with rheumatoid arthritis. *Arthritis Rheum.* **1962**, *5*, 589-601.
80. Platt, P. The role of the laoratory in rheumatology. Examination of synovial fluid. *Clin. Rheum. Dis.* **1983**, *9*, 51-67.
81. Seidman AJ, Limaiem F. Synovial Fluid Analysis. 2020 Oct 27. In: StatPearls [Internet]. Treasure Island (FL): StatPearls Publishing; 2020 Jan–. PMID: 30725799.
82. Al-Shakarchi, I.; Coakley, G. Synovial fluid tests. *Ass. Rheum. Patient* **2014**, 202-204.
83. Fu, J.; Ni, M.; Chai, W.; Li, X.; Hao, L.; Chen, J. Synovial fluid viscosity test is promising for the diagnosis of periprosthetic joint infection.*J. Arthroplasty* **2019**, *34*, 1197-1200.
84. Schurz, J.; Ribitsch, V. (1987). Rheology of synovial fluid. *Biorheology* **1987**, *24*, 385-399.
85. Safari, M.; Bjelle, A.; Gudmundsson, M.; Hogfors, C.; Granhed, H. Clinical assessment of rheumatic diseases using viscoelastic parametres for synovial fluid.*Biorheology*, **1990**, *27*, 659-674.
86. Stafford, C.; Niedermeier, W.; Holley, H.L.; Pigman, W. Studies on the concentration and intrinsic viscosity of hyaluronic acid in synovial fluid of patients with rheumatic diseases. *Ann. Rheum. Dis.* **1964**, *23*, 152-157.
87. Zeidier, H.; Altmann, S. New methods in synovial fluid rheology and macromolecular network structure. *Biorheology* **1981**, *18*, 122-127.
88. Divine, J.; Zazulak, B.; Hewett, T. Viscosupplementation for knee osteoarthritis. *Clin. Orthop. Relat. Res.* **2007**, *455*, 113-122.

89. Hosny, S.; McCtatchie, W.; Sofat, N.; Hing, C. Knee pain in adults & adolescents, diagnosis and treatmen. *Intech.* **2012,** *Chapter 8*, 187-218.
90. Reid, M. Viscosupplementation for osteoarthritis: a primer for primary care physicians *Adv. Ther.* **2013,** *30*, 967-986.
91. Billesberger, L.; Fisher, K.; Qadri, Y.; Boortz-Marx, R. Procedural treatments for knee osteoarthritis: a review of current injectable therapies. *Pain Res. Manag.* **2020**, ID 3873098.
92. Tanaka, N.; Sakahashi, H.; Sato, E.; Hirose, K.; Ishima, T.; Ishii, S. Intraarticular injection of high molecular weight hyaluronan after arthrocentesis as treatment for rheumatoid knees with joint effusion. *Rheumatol. Int.* **2002,** 22, 151-154.
93. Altman, R.D.Intra-articular sodium hyaluronate in osteoarthritis of the knee. *Semin. Arthritis Rheum*. **2000**, *30*, 11-18.
94. Goldberg, V.; Coutts, R. Pseudoseptic reactions to hylan viscosupplementation: diagnosis and treatment. *Clin. Orthop. Relat. Res.* **2004**, *419*, 130-137.
95. Brockmeier, S.; Shaffer, B. (2006). Viscosupplementation therapy for osteoarthritis. *Sports Med. Arthrosc.* **2006**, *14*, 155-162.
96. Tytherleigh-Strong, G.; Hurting, M.; Miniaci, A. Intra-articular hyaluronan following autogenous osteochondral grafting of the knee. *Arthroscopy* **2005**, 21, 999-1005.
97. Moreland, L.W. Drugs that block tumour necrosis factor: Experience in patients with rheumatoid arthritis. *Pharmacoeconomics* **2004**, *22*, 39–53.
98. Hempfling, H. Intra-articular hyaluronic acid after knee arthroscopy: a two-year study. *Knee Surg. Sports Traumatol. Arthrosc.* **2007**, *15*, 537-546.
99. Ghosh, P. The role of hyaluronic acid (hyaluronan) in health and disease: interactions with cells, cartilage and components of synovial fluid. *Clin. Exp. Rheumatol.* **1994**, *12*, 75-82.
100. Strauss, E.; Hart, J.; Miller, M.; Altman, R.; Rosen, J. Hyaluronic acid viscosupplememntation and osteoarthritis. *Am. J. Sports Med.* **2009**, *8*, 1636-1644.
101. Murube, J.; Paterson, A.; Murube, E. *Classification of artificial tears*. In: Lacrimal Gland, Tear Film, and Dry Eye Syndromes 2, D.A. Sullivan ed; Plenum Press, New York, USA, 1998; Chapter 99, pp. 693-704.
102. Ngai, V.; Medley, J.B.; Jones, L.; Forrest, J.; Teiehroerb, J. Friction of contact lenses: silicone hydrogel versus conventional hydrogel *Tribology and Interface Eng. Series*, **2005**, *48*, 371-379.
103. Prabha, J. Tear secretion-a short review. *J Pharn. Sci. Res.* **2014,** *6*, 155-157.
104. Tiffany, J. Tears in health and disease. *Eye* **2003**, *17*, 923-926.
105. Mengi, S.A.; Deshpande, S.G. *Ocular Drug Delivery*. In: Controlled and Novel Drug Delivery. N. K. Jain, ed.; CBS Publishers and Distributors, New Delhi, India, 1997; pp. 82-90.
106. Phadatare, S.; Momin, M.; Nighojkar, P.; Askarkar, S.; Singh, K. A Comprehensive review on dry eye disease: diagnosis, medical management, recent developments, and future challenges. *Adv.Pharm*. **2015**, article 704946, 1-12.
107. Stern, M.; Pflugfelder, S. Inflammation in dry eye. *Ocul. Surface* **2004**, *2*, 124-130.
108. Liu, H.; Yiu, C. Dry eye disease: A review of diagnostic approaches and treatments. *J. Ophhtalmol.* **2014**, *28*, 173-181.
109. Lemp, M. The definition and classification of dry eye disease: report of the definition and classification subcommittee of the international Dry Eye Workshop. *Ocular Surf.* **2007**, *2*, 75-92.
110. Grubbs, J.; Tolleson-Rinehart, S.; Huynh, K.; Davis, R. A review of quality of life measures in dry eye questionnaires. *Cornea* **2014**, 2, 215-218.
111. Schaumberg, D.A.; Dana, R.; Buring, J.; Sullivan, D. Prevalence of dry eye disease among US men: estimates from the physicians' health studies. *Arch. Ophthalmol.* **2009**, *127*, 763-768.
112. Fujiita, M.; Igarashi, T.; Kurai, T.; Sakane, M.; Yoshino, S.; Takahashi, H. Correlation between dry eye and rheumatoid arthritis activity. *Am. J. Ophtalmol.* **2005**, *140*, 808-813.
113. Blehm, C.; Vishnu, S.; Khattak, A.; Mitra, S.; Yee, R. Computer vision syndrome: a review. *Survey Ophhtalmol.* **2005**, *50*, 253-262.
114. Delaleu, N.; Jonsson, R.; Koller, M.M. Sjogren's syndrome. *Eur. J. Oral Sci.*, **2005**, *113*, 101-113.
115. Bron, A.; Evans, V.; Smith, J.A. Grading of corneal and conjunctival staining in the context of other dry eye tests. *Cornea* **2003,** 22, 640-650.

116. Pflugfelder, S.; Solomon, A.; Stern, M.E. (2000). The diagnosis and management of dry eye: a twenty-five-year review. *Cornea* **2000**, *19*, 644-649.
117. Kastelan, S.; Tomic, M.; Salopek-Rabatic, J.; Novak, B. Diagnostic procedures and management of dry eye. *Biomed. Res. Int.* **2013,** article 309723, 1-6.
118. Smith, A.; Albenz, J.; Begley, C.; Caffery, B.; Nicholos, K.; Schaumberg, D.; Schein, O. The epidemiology of dry eye disease: report of the epidemiology subcommittee of the international Dry Eye Work Shop (2007). *Ocul. Surf.* **2007**, *5*, 93-107.
119. Hashemi, H.; Khabazkhoob, M.; Kheirkhah, A.; Emamian, M.H.; Mehravaran, S.; Shariati, M.; Fotouhi, A. Prevalence of dry eye syndrome in an adult population. *Clin. Exp. Ophthalmol.* **2014**, *42*, 242-248.
120. Aragona, P.; Papa, V.; Micali, A.; Santocono, M.; Milazzo, G. Long term treatment with sodium hyaluronate-containing artificial tears reduces ocular surface damage in patients with dry eye. *Br. J. Ophhtalmol*. **2002**, *86*, 181-184.
121. Horton, M. Master the maze of artificial tears. *Review of Optometry* **2018**, *20*, 1-8.
122. Moshirfar, M.; Pierson, K.; Hanamaikai, K.; Caban, L.; Muthappan, V.; Passi, S. Artificial tears potpourri: a literature review *Clin. Ophtalmol.* **2014**, *8*, 1419-1433.
123. Muller-Lierheim, W.G.K. Tear substitutes. *Current Contactology* **2015**, *11*, 17-19.
124. Brignole, F.; Pisella, P.; Dupas, B.; Baeyens, V.; Baudouin, C. Efficacy and safety of 0.18% sodium hyaluronate in patients with moderate dry eye syndrome and superficial keratitis. *Graefes Arch. Clin. Exp.Ophhtalmol.* **2005**, *243*, 531-538.
125. Prabhasawat, P.; Tesakibul, N.; Kasetsuwan, N. Performance profile of sodium hyaluronate in patients with lipid tear deficiency randomised, double-blind, controlled, exploratory study. *Br. J. Ophhtalmol*. **2007**, *91*, 47-50.
126. Polack, F.; McNiece, M.T. The treatment of dry eyes with Na hyaluronate (Healon) - a preliminary report. *Cornea* **1982,***1,* 133-136.
127. Smith, G.; Lee, S.; Taylor, H. Open evaluation of a new non-preserved artificial tear. *Aust. Ophthalmol.* **1993**, *21,* 105-109.
128. Tiffany, J.M. *Viscoelastic properties of human tears and polymer solutions.* In: Lacrimal gland, tear film, and dry eye syndromes, D.A. Sullivan ed.; Plenum Press, New York, 1998; Chapter 33, pp. 267-270.
129. Dudinski, O.; Finnin, B.C.; Reed, B.L. Acceptability of thickened eye drops to human subjects. *Curr. Therap. Res.* **1983**, *33*, 322-337.
130. Hammer, M.; Burch, T. Viscous corneal protection by sodium hyaluronate, chondroitin sulphate, and methylcellulose. *Invest. Ophthamol. Vis. Sci.* **1984**, *25*, 1329-1332.
131. Kaura, R.; Tiffany, J. The role of mucous glycoproteins in the tear film. In: *The preocular tear film: in health, disease, and contact lens wear.* Holly, F.J., Lamberts, D.W., Mac Keen, D.L. eds.; Dry Eye Institute, Texas, USA, 1986; pp. 728-732.
132. Bothner, H.; Wik, O. Rheology of hyaluronate. *Acta Otoralingol. Suppl.* **1987**, *442*, 25-30.
133. Hamano, H.; Mitsunaga, S. Viscosity of rabbit tears. *Jap. J.Opthalmol.* **1973**, 17, 290-299.
134. Tiffany, J. The viscosity of human tears. *Intl. Ophthalmol.* **1991**, *16*, 371-376.
135. Muller-Lierheim, W.G.K. Hyaluronic acid eye drops. *Current Contactology* **2015**, *11*, 1-3.

Chapter 1

DoE-assisted development of a novel glycosaminoglycan-based injectable formulation for viscosupplementation

1. Introduction

All human joints are lined with a tissue called synovium, which is surrounded by synovial fluid [1]. This is a viscous, non-Newtonian fluid, whose main role is to reduce frictions between the articular cartilages during movements. Synovial fluid contains glucose, uric acid, proteins (lubricin), proteoglycan, polysaccharides (in particular glycosaminoglycans), and phospholipids [2].

Hyaluronic acid (HA), also known as hyaluronan, is the major component of synovial fluid and its concentration in healthy joints is 1.45–3.12g/L [3].

HA is a high-molecular-weight linear (MW) natural glycosaminoglycan, consisting of D-glucuronic acid and D-N-acetyl glucosamine disaccharides bound with β-glycosidic linkages [4]. It is an essential component of the extracellular matrix (ECM) that is present at high concentration in human umbilical cord, synovial fluids, connective tissue, skin, and vitreous body [5]. Since carboxyl groups (COO -) are completely ionized at physiological pH, it possesses hydrophilic and water-retaining properties, forming a viscous gel that is characterized by peculiar rheological properties. In particular, HA solutions are characterized by a gel-like behaviour at high frequencies and a liquid-like behaviour at low frequencies. In physiological fluids, the ions shield the negative charges of polymer backbone, and HA chains behave as random coils. The entanglement concentration decreases on increasing MW, meaning that the longer chains overlap each other at lower concentration. An increase in MW and/or concentration corresponds to high values of viscoelastic moduli and a marked shear-thinning behaviour [6]. These properties are relevant for the structural function of HA in connective tissue as well as for the lubricating and cushioning activities in the ophthalmic aqueous humour and synovial fluid [4].

Chemically, hyaluronan is a linear high MW polysaccharide consisting of repeating units of D-glucuronic acid and N-acetyl-glucosamine, with an average molecular weight of 7×10^6 g/mol in healthy synovial fluid [5].

Phospholipids (i.e., phosphatidylcholine) are small amphiphilic molecules that are present in synovial joints at a relatively high concentration, 0.1–0.2 mg/mL [7].

The synovial fluid of joints normally functions as a biological lubricant, providing low-friction and low-wear properties to articulating cartilage surfaces through the putative contributions of HA and surface active phospholipids [2].

In order to perform this function, the synovial fluid has a viscoelastic, non-Newtonian, behavior because its viscosity varies with the variation of the applied force. In the absence of movement, or with slow movements, the viscous behavior prevails (measured by the viscous modulus G'') and therefore the lubrication capacity increases as well.

When joints are in movement (for example during rapid walking or running), elastic behavior prevails (measured by the elastic modulus G'), which is essential to protect joints during loading.

In the synovial fluid of a healthy individual, the inversion between the two modules occurs at low frequencies, generally lower than 1–2 Hz. This frequency, called the cross over frequency, corresponds for example to the transition from slow walking to running.

However, in older people, in arthritis, injury, and artificial joint failure, there is an increased friction between the joint surfaces and concomitant erosion of the load-bearing elements [8].

In these cases, the cross over frequency is characterized by the disappearance of the cross over point. In fact, the synovial fluid never shows a predominance of elastic behavior, and G' is always lower than G''. This change in the rheological properties of the fluid depends on a change in the composition. There is a reduction both in the average MW and concentration of HA.

As a further consequence, the dynamic viscosity drops, passing from an average value of some tens of Pa.s to values close to or lower than 1Pa.s. Similarly, the value of G' at the frequency of 2.5 Hz drops from about 120 Pa to values below 10 Pa [9,10].

A variety of treatments have been proposed to restore the physiological joint environment in case of injury and arthritis. Some biological drugs proved capable of reducing pain and inflammation [11,12]. Therapeutic joint lavage has been used, as such or in combination with anti-inflammatory steroids [13,14] to cleanse the joint from cartilage degradation products, pro-inflammatory cells, and destructive enzymes associated with arthritis [15].

Injections of HA in the joint cavity (called viscosupplementation) have been reported to restore the viscosity and protective functions of the synovial fluid [16,17].

HA, usually sodium hyaluronate, is frequently used in aqueous solution for viscosupplementation. HA can be used in its native form, thus being characterized by linear molecules, or it can be chemically cross-linked to modify its aqueous solubility.

The rheological properties of HA solutions are directly influenced by the MW, concentration, and cross-linking. The higher the MW, the better the viscoelastic behavior of the solution. Unfortunately, MWs similar to the physiological ones (6–7 $\times 10^6$Da) are not achieved with usual production methods; as a consequence, the hyaluronate used in viscosupplementation has an average molecular weight of 1–4$\times 10^6$ Da.

To overcome this limit, one solution could be the increase of HA concentration, but this determines a viscosity increase that, in turn, can make administration difficult.

Given these premises, the aim of the present work was the development of a viscoelastic glycosaminoglycan (GAG)-based formulation in a pre-filled sterile syringe that is capable of best mimicking the functional (rheological and lubricating) properties of healthy synovial fluid when administered into the impaired joint.

The research project was divided in two steps: the first one was addressed to the DoE (Design of Experiment)-assisted optimization of a sterile injectable formulation based on two HA grades, having different MWs. Such an approach is helpful in pharmaceutical development, since it can predict the optimal composition satisfying all the formulator's demands on the basis of few experiments and statistical analysis of the results. Therefore, thanks to this approach, the best formulation can be found on a sound mathematical and statistical basis, saving time and effort in comparison to a conventional trial and error approach [18].

The rationale for this formulation choice is based on the knowledge that, so far, no commercial products intended for viscosupplementation and based on a single HA grade or even on binary HA mixture possesses optimal properties in comparison with healthy synovial fluid.

The HA grades were a very high MW (VHMW) produced by fermentation, which was chosen since it represents the highest HA MW currently available, and a low MW (LMW) that was expected to reduce the dynamic viscosity at low shear rates.

HA concentrations were set in the range 1–3% w/v in order to avoid the attainment of a too-viscous system that is not comparable with the healthy synovial fluid and not compatible with industrial plants (namely syringe-filling machine due to the too high pressure required).

The influence of HA MW and concentration on formulation rheological properties was investigated. A full factorial design was employed to identify the optimal formulation in terms of concentration and relative fraction of two HA MWs, i.e., the one characterized by the best functional (viscous and viscoelastic) properties in comparison with those of healthy synovial fluid. In the second step of the work, an endogenous amphiphilic molecule (phosphatidylcholine, PC) was added to the HA-based formulation optimized in the first step in order to improve lubricant properties as well as to obtain a composition as similar as possible to that of synovial fluid, in which phospholipids represent the second major component after HA. The development was focused on the study of PC incorporation mode into the aqueous HA product, i.e., on the more suited manufacturing process. The lubricating properties of both optimized HA formulation and optimized HA+PC formulation were assessed by means of tribology measures and compared with those of a commercial product (containing HA at concentration higher than 3% w/v) and of physiologic solution (0.9% w/w NaCl aqueous solution), used as control.

Tribology allows investigating the frictions of cartilages under defined conditions, both in oscillatory or rotational motion over a broad range of sliding velocities and normal pressures. Thanks to tribology measures, it is therefore possible to investigate the lubricating properties of a formulation.

The final HA+PC product, packaged in pre-filled sterile syringes, was subjected to a preliminary stability test (6 months) in ICH (International Council for Harmonisation) long-term and accelerated conditions: at each time point frequency at cross over, dynamic viscosity at 0.01 s^{-1} shear rate, pH and osmolality were compared on a statistical basis with those measured at time zero.

2. Materials and Methods

2.1. Materials

The following materials were used: injectable grade sodium hyaluronate very high MW (VHMW HA): 3.5 ×10^6 Da (HTL Sas, Javene, France); injectable grade sodium hyaluronate low MW (LMW HA): 100.000 Da (HTL Sas, Javene, France); sodium chloride (Merck & Co., Frankfurt, Germany); dibasic sodium phosphate anhydrous (Chemische Fabrik Budenheim KG, Budenheim, Germany); monobasic sodium phosphate dehydrate (Chemische Fabrik Budenheim KG, Budenheim, Germany); water for injections (WFI) (Ph. Eur. 10th Ed., Monograph 0169); injectable grade fat-free soybean phospholipid rich in phosphatidylcholine (Lipoid GmbH, Ludwigshafen, Germany).

2.2. Sample Preparation

Polymer solutions with total HA concentration equal to 1%, 2%, or 3% w/v were prepared by hydrating for 12 h at 50°C the two HA grades in pH 7.0 buffered aqueous solution, obtained by adding a fixed NaCl amount (0.75% w/w) to a pH 7.4 phosphate buffer solution (0.05% dibasic sodium phosphate anhydrous, monobasic sodium phosphate dihydrate in 100 mL of distilled water). Then, the bulk solutions were divided into syringes formed by a luer lock syringe barrel 2.25 mL (BD Hypack™ SCF™, Becton Dickinson, Le Point de Claix, France) and a plunger (West Pharmaceutical Services Inc., Exton, *Penn*, USA).

Pre-filled syringes were steam sterilized in autoclave (mod. FOB2-TS, Fedegari, Pavia, Italy) at 121°C for 15 min and formulations were characterized as described in Section 2.4. The sterilization process produces a marked decrease in sample viscosity ranging from 80% to 25%, depending on the shear rate considered (greater at low shear rates).

2.3. DoE approach: full factorial design

A full factorial design, considering all the possible combinations between the factors and their levels, was chosen [19–21].

Namely, two factors (corresponding to the polymer concentration (factor A) and relative fraction of the two HA grades (factor B)) at three levels were considered; therefore, experimental trials were carried out on 3^2 (9) possible mixtures of the two components.

For each factor, the upper level was indicated as +1 and the lower level was as indicated as –1. In particular, for the factor "polymer concentration", the three levels were: 1% w/v (–1), 2% w/v (0), 3% w/v (+1); for the factor "relative fraction" of the two HA grades, the three levels were: VHMW:LMW HA weight ratio 1:9 (–1), VHMW:LMW HA weight ratio 5:5 (0), VHMW:LMW HA weight ratio 9:1 (+1). Therefore, each formulation was characterized by two values (Table 1): the first one (on the left) relevant to the VHMW:LMW HA weight ratio, and the second one (on the right) relevant to the HA % w/v concentration.

Table 1. Experimental points of the full factorial design. HA: hyaluronic acid, LMW: low molecular weight, VHMW: very high molecular weight.

Factor		HA concentration (% w/v)		
		1	2	3
VHMW: LMW HA ratio	**1:9**	–1; –1	–1; 0	–1 ; +1
	5:5	0; –1	0; 0	0; +1
	9:1	+1; –1	+1; 0	+1; +1

In Table 2, the % (w/v) compositions of the 9 formulations of the full factorial design are reported.

Table 2. % (w/v) composition of the formulations of the full factorial design.

Formulation	HA VHMW	HA LMW	NaCl	Phosphate buffer pH 7.4
1	0.1	0.9	0.75	up to 100
2	0.5	0.5	0.75	up to 100
3	0.9	0.1	0.75	up to 100
4	0.2	1.8	0.75	up to 100
5	1.0	1.0	0.75	up to 100
6	1.8	0.2	0.75	up to 100
7	0.3	2.7	0.75	up to 100
8	1.5	1.5	0.75	up to 100
9	2.7	0.3	0.75	up to 100

2.4. Characterization of formulations of the full factorial design

The formulations, corresponding to the different experimental points of the full factorial design, were characterized for pH (pH meter Seven Compact S220 (Mettler Toledo, Columbus, OH, USA), osmolality (Cryoscopic osmometer Osmomat O30, Gonotec, Berlin, Germany), and rheological properties (frequency and viscosity at cross over point, tan δ and dynamic viscosity), as described hereafter.

Rheological properties were evaluated at 25°C by means of a rotational rheometer (Modular Compact Rheometer MCR302, Anton Paar GmbH, Graz, Austria), equipped with a cone plate (C50/1: Ø 50 mm; angle = 1°) combination as measuring system.

Two kinds of rheological measures were carried out to compare formulations: oscillatory and viscosity tests.

Oscillatory tests (strain sweep and oscillation test) were carried out. At first, a strain sweep test enabled finding the linear viscoelastic region; subsequently, a stress chosen in the linear viscoelastic region was applied at frequencies in the range of 0.1–100 rad/s, corresponding to human knee joint solicitations, to measure the viscoelastic moduli (G′=elastic modulus and G′=viscous modulus) versus frequency profiles.

A viscosity test was also effected in the shear rate range 0.01–300 s^{-1}.

2.5. Optimization procedure

The following response variables were considered for each formulation: the frequency and the viscosity measured at the cross over point (i.e., when G′ =G′′), the tan δ (i.e., G′′/G′ ratio) calculated at 2.5 Hz, which was chosen as the frequency exerted on knee joints during a run and the dynamic viscosity measured at 0.01 s^{-1} shear rate, which was chosen to mimic in vivo rest conditions.

The relationship of each response variable with the two factors (polymer concentration and relative fraction of the two HA grades) was investigated. Experimental data were subjected to

multiple regression analysis, effected by means of a statistical software package (Statgraphics 5.0, Statistical Graphics, Rockville, MD, USA) [19–21].

A series of models including linear, quadratic, and special cubic was considered.

The best-fit model was chosen on the basis of statistical parameters such as F-ratio for significance of regression and adjusted correlation coefficient for the goodness of fit of the model [21–23].

The effect of each factor and of their interactions on each response variable was estimated by means of Pareto charts. Two-dimensional (2D) contour plots showing the iso-response lines of each response variable as a function of the levels of two factors were obtained.

2.6. Preparation and characterization of optimized HA formulation

The formulation of optimized composition, chosen on the basis of the results of the experimental design, was prepared as described in Section 2.3 and subjected to the same characterization carried out on the nine formulations of the full factorial design.

In addition, syringeability measures were carried out by a dynamometer (Mod. 5942 - INSTRON®, Norwood, MA, USA) equipped with a syringe text fixture able to accommodate a wide variety of syringe sizes. The syringe test fixture complies with the ISO 7886-1 Annex G (Test method for forces required to operate plunger). During the test, a compression rod, mounted at the crosshead, moves down at constant velocity and pushes the plunger, ejecting the product through a 27 G needle (0.4×40 mm) (Terumo, Leuven, Belgium).

A run speed of 10 mm/min was set to simulate the injection rate during product administration. Force versus time data were recorded, and the maximum force required was retained as extrusion force.

2.7. PC emulsion preparation

Injectable grade fat-free soybean phospholipid rich in PC is not soluble, but it is dispersible in water to form an oil/water emulsion. Preliminary studies proved that the maximum PC concentration suitable for stable o/w emulsion was 0.05% w/v (data not shown); this concentration is half that of PC in healthy synovial fluid (≅0.1% w/v).

The PC o/w emulsion was prepared in two steps: at first, PC was dispersed in water under magnetic stirring (C-MAG HS 7, IKA®-Werke GmbH & Co. KG, Staufen, Germany) at 1000 rpm for 10 minutes; then, the dispersion was homogenized with a state rotor system (Ultraturrax T10, IKA®-Werke GmbH & Co. KG, Staufen, Germany) at 30,000 rpm for 5 minutes. The mean particle size of PC droplets was 219.9 nm and the PDI was 0.397 (Zetasizer Nano ZS, Malvern Instruments Ltd., Worcestershire, UK).

2.8. Preparation of the optimized HA+PC formulation

The two liquid phases were separately prepared. The first phase, prepared according to the procedure described in Section 2.3, consisted in the HA optimized formulation 10% more concentrated than that expected in the final product: namely, the total HA concentration was equal to 1.65% w/v, corresponding to 0.96% w/v of VHMW HA grade and 0.69% w/v of LMW HA grade.

The second phase consisted of a 0.5% w/v PC o/w emulsion, which was prepared according to Section 2.7. The second phase was added to the first one in a 1:9 volume ratio. The two phases were mixed for 1 hour at 300 rpm by means of mechanical stirring with a paddle (Eurostar 20, IKA®-Werke GmbH & Co. KG, Staufen, Germany) to obtain a new and homogeneous liquid phase that represented the desired HA+PC formulation.

In order to exclude foreign particles, the emulsion was filtered under pressure through a polypropylene filter with 5 μm pores (Sartopore PP2 Midi Cap, Sartorius Stedim Biotech GmbH, Gottingen, Germany). The filtrate was left to rest overnight to eliminate air bubbles. The day after, the bulk solution was divided into pre-filled syringes that were steam sterilized in autoclave (FOB2-TS, Fedegari, Pavia, Italy) at 121°C for 15 min.

2.9. Characterization of the optimized HA+PC formulation

An optimized HA+PC formulation was characterized for pH, osmolality, rheological properties, as described for HA-based formulation, and tribology measures.

2.9.1. Tribology measures

Tribology measures were performed using a rotational rheometer (Modular Compact Rheometer MCR302, Anton Paar GmbH, Graz, Austria) equipped with the tribology measuring cell T-PTD 200.

To best simulate in vivo conditions, a biological substrate (pig femur) was used.

The formulation under test (0.5 g) was loaded on the cartilage placed on a steel disc and a probe, containing a cylinder of bone plus cartilage, was lowered to contact the sample, exerting a force equal to 1 Newton. To minimize sample evaporation, measures were effected at 20°C. Thermosetting was assured by a Peltier heating plane.

The lubrication properties of the optimized HA+PC formulation were compared with those of the optimized HA formulation and of a commercial product intended for viscosupplementation (Synovial), containing HA in a 3.2 % w/v concentration. Physiologic solution was also subjected to tribology measure as control.

2.9.2. Stability studies

A preliminary stability study was carried out in ICH long-term (25°C/60% RH) and accelerated (40°C/75% RH) conditions on the optimized HA+PC formulation, which was packaged in pre-filled syringes. The parameters taken into account at each and every checkpoint (1, 2, 3, and 6 months) and compared with those measured at time zero were frequency at cross over, dynamic viscosity in rest condition (0.01 s^{-1}), pH, and osmolality.

2.9.3. Statistical analysis

Whenever appropriate, experimental values of the various types of measures were subjected to statistical analysis. In particular, one-way Anova, followed by post hoc Sheffè test or Mann–Whitney U-test were employed (Statgraphics 5.0, Statistical Graphics Corporation, Rockvillle, MD, USA) [24].

3. Results and Discussion

3.1. Properties of the formulations of the Full Factorial Design

All formulations of the experimental design were characterized by pH value in the range 6.5–7.0 and osmolality was in the range 250–400 mOsm/kg, which is in the range of an intra-articular environment in physiologic conditions. Dynamic viscosity measures demonstrated that all formulations considered in the experimental design are characterized by pseudoplastic behavior, which is functional to easy syringeability. As an example, the flow curves and G′ and G′′ profiles of some formulations (2, 3, 5, 6) are reported in Figures 1 and 2, respectively.

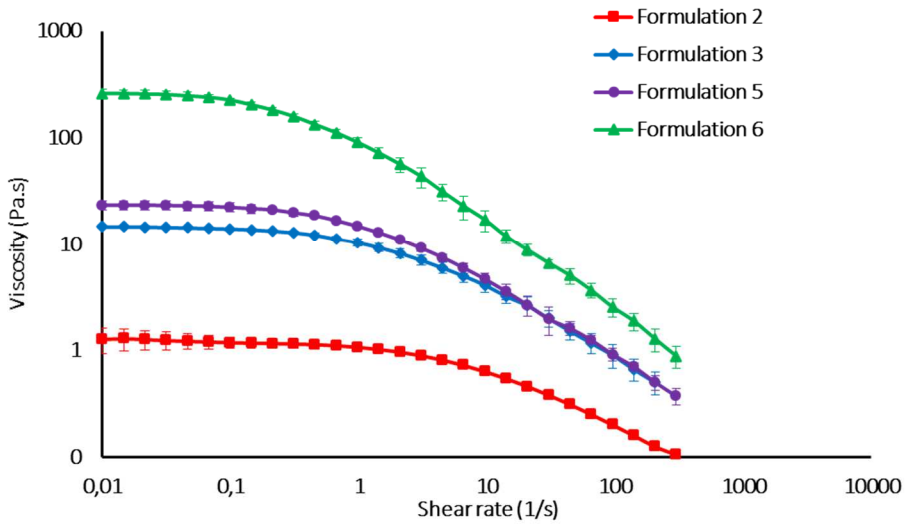

Figure 1. Flow curves of some HA formulations of the experimental design (mean values ± s.d., *n*=3).

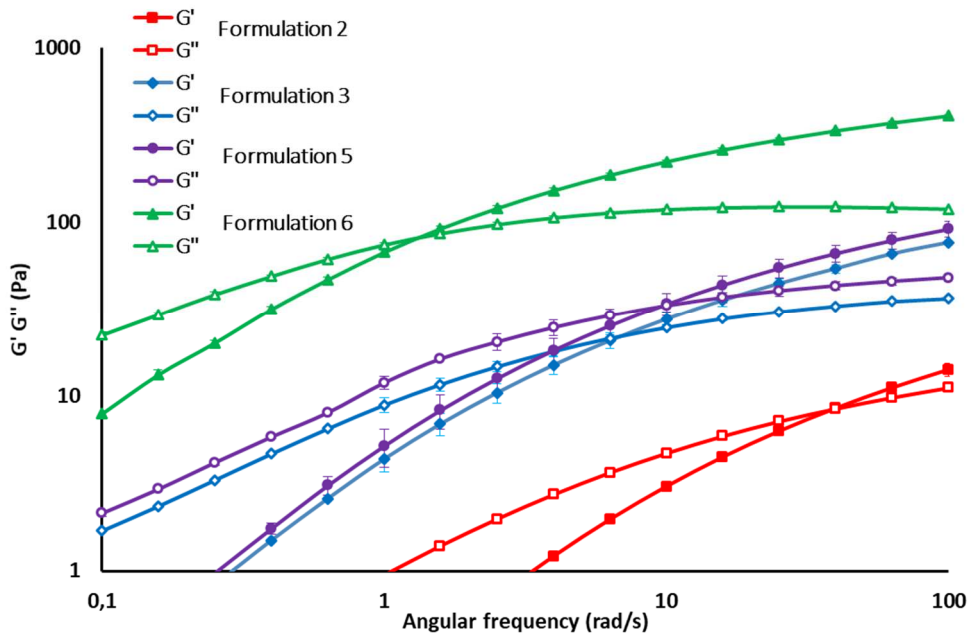

Figure 2. G′ and G′′ profiles of some HA formulations of the experimental design (mean values ± s.d., n=3).

The mean values of all the response variables for the experimental design are reported in Table 3 together with those of the healthy synovial fluid [10], which was taken as a reference.

Table 3. Response variables of the formulations of the full factorial design (mean values ± s.d.; n = 3).

Formulation	Frequency at cross over (rad/s)	Viscosity at cross over (Pa.s)	Tan δ at 2.5 Hz	Dynamic viscosity at 0.01 s^{-1} (Pa.s)
1	87.3 (±10.06)	0.5 (±0.2)	1.357 (±0.237)	0.72 (±0.06)
2	39.1 (±1.01)	8.45 (±0.11)	1.318 (±0.012)	1.27 (±0.34)
3	7.16 (±1.14)	22.39 (±0.15)	0.785 (±0.038)	14.66 (±0.40)
4	55.0 (±5.0)	1.26 (±0.49)	3.157 (±0.819)	1.77 (±0.12)
5	6.00 (±0.97)	28.52 (±1.24)	0.746 (±0.035)	23.24 (±2.38)
6	1.33 (±0.05)	82.14 (±1.30)	0.468 (±0.004)	259.41 (±24.14)
7	31.83 (±12.04)	2.43 (±0.47)	8.049 (±2.472)	3.00 (±0.11)
8	1.84 (±0.04)	66.88 (±2.37)	0.523 (±0.004)	139.07 (±9.75)
9	0.62 (±0.01)	212.90 (±4.87)	0.369 (±0.005)	1184.93 (±129.09)
Healthy synovial fluid	1-10	20-80	0.39	1-40

It can be observed that formulations 1, 4, and 7, containing a high fraction of LMW HA, are characterized by poor viscoelastic properties with a prevalence of viscous over elastic behaviour, as demonstrated by the tan δ values, which are much higher than those of synovial fluid in physiologic conditions. Formulation 9 is not suitable, as well, for intra-articular administration, since the high fraction (9:1) and concentration (2.7% w/v) of VHMW HA determine the high rigidity of the system, as demonstrated by the high viscosity at cross over and high viscosity at 0.01 s^{-1} shear rate. All the other formulations, with the exception of formulation 2, are characterized by frequency and viscosity values at cross over in the range of those reported for healthy synovial fluid.

A low VHMW HA fraction always determines an increase in tan δ values, as demonstrated in the case of formulations 1, 4, and 7 for which the high/low MW ratio is 1:9 and for formulation 2, for which the concentration of VHMW HA is only 0.5% w/v.

As for dynamic viscosity at a 0.01 s^{-1} shear rate, the majority of formulations are characterized by values similar to that of the healthy synovial fluid, with the exception of formulations 6, 8, and 9 containing the highest concentrations of VHMW HA, which are equal to 1.8%, 1.5%, and 2.7% w/v, respectively.

3.2. Multiple regression analysis

The best-fit model for all the response variables (frequency and viscosity at cross over point (G'=G''), tan δ at 2.5 Hz, and dynamic viscosity at 0.01 s^{-1} of the nine formulations considered in the experimental design was found to be the quadratic one:

$$Y_1=\beta_0 + \beta_1X_1 + \beta_2X_2 + \beta_3X_1X_2 + \beta_4X_1^2 + \beta 5X_2^2$$

where:

Y_1 = response variable; X_1= polymer concentration (factor A); X_2= relative fraction of the two HA grades (factor B); β_0, β_1, β_2, β_3, β_4, and β_5 = estimated coefficients of the model.

The equation represents the quantitative effect of factors (X_1, X_2) upon each of the responses.

The effect of each factor and that of their interactions on each response variable was estimated by means of Pareto charts (Figure 3). These graphical representations are useful to determine which factors and relevant interactions have a significant effect, negative or positive, on each response variable of the experimental design [19, 20].

In Figure 3 a,c, Pareto charts show that both factors exert a negative effect on frequency at cross over and tan δ at 2.5 Hz: in fact, these parameters decrease on increasing polymer concentration and VHMW:LMW HA weight ratio. In particular, tan δ decreases on increasing the VHMW HA, indicating that a higher fraction of the high MW polymer grade determines an increase in the elastic over viscous behavior of the formulation.

The Pareto charts reported in Figure 3b and 3d demonstrate that both factors have a positive effect on viscosity at cross over and dynamic viscosity in rest condition (shear rate 0.01 s^{-1}): in fact, the higher values of both response variables are encountered on increasing the polymer concentration and VHMW:LMW HA weight ratio.

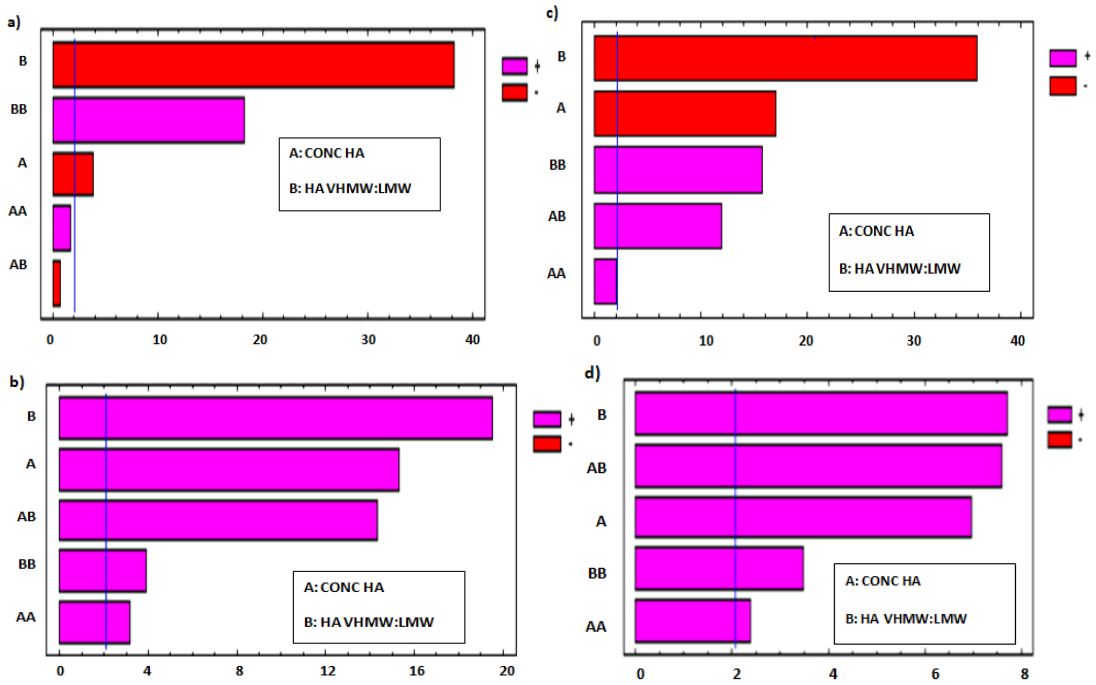

Figure 3. Standardized Pareto chart of the effect of each factor and that of their interactions on each response variable of the full factorial design: (**a**) frequency at cross over, (**b**) viscosity at cross over, **c)** tan δ at 2.5 Hz, **d)** dynamic viscosity in rest condition (0.01 s^{-1} shear rate). A= HA concentration; B= VHMW:LMW HA ratio; AA, BB, AB: interaction terms [25].

For all response variables, 2D contour plots were drawn according to the best-fit model, as illustrated in Figure 4a–d. The lines in each plot represent the formulation compositions for which a same response value is predicted by the model.

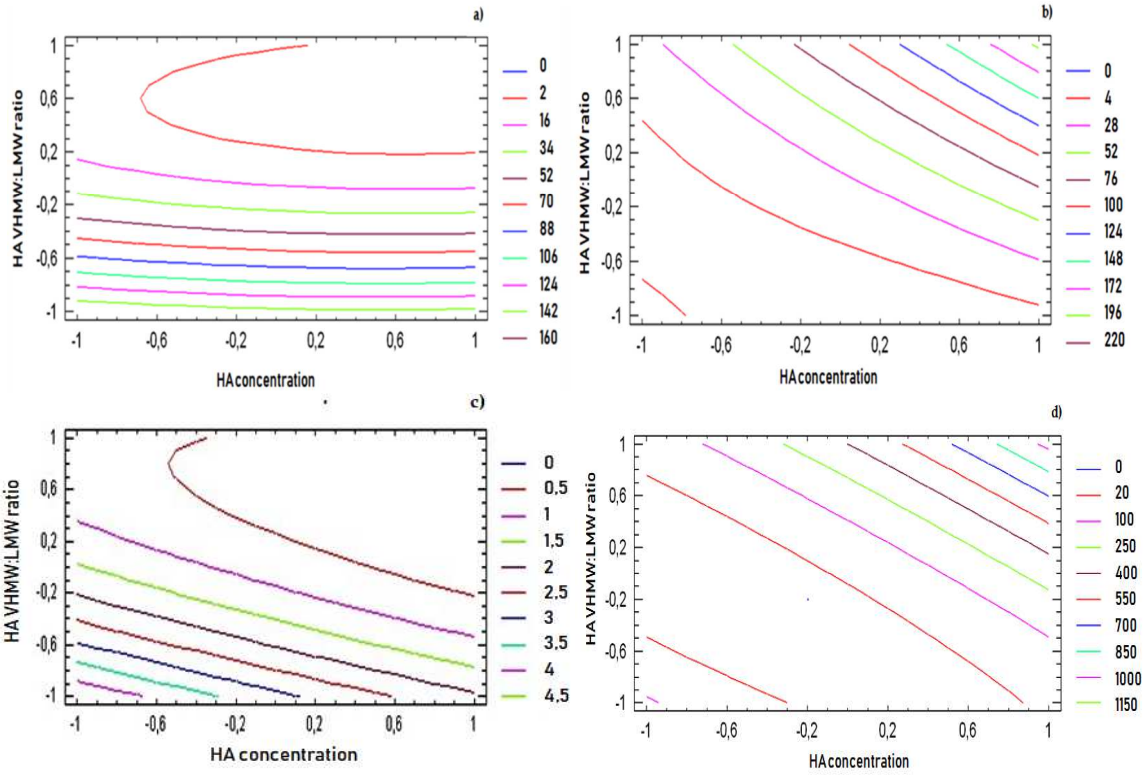

Figure 4. Two-dimensional (2D) contour plots drawn according to the best-fit model for each response variable: **a)** frequency at cross over, **b)** viscosity at cross over, **c)** tan δ at 2.5 Hz, **d)** dynamic viscosity in rest condition (0.01 s^{-1} shear rate).

The individual contour plots were subsequently superimposed (Figure 5) to identify the region of the experimental domain (shaded area) that fulfills all the constraints decided to optimize the formulation: frequency at cross over lower than 20 (rad/s), viscosity at cross over in the range 20-80 (Pa.s), tan δ at 2.5 Hz lower than 0.7, dynamic viscosity at 0.01 s^{-1} lower than 100 (Pa.s).

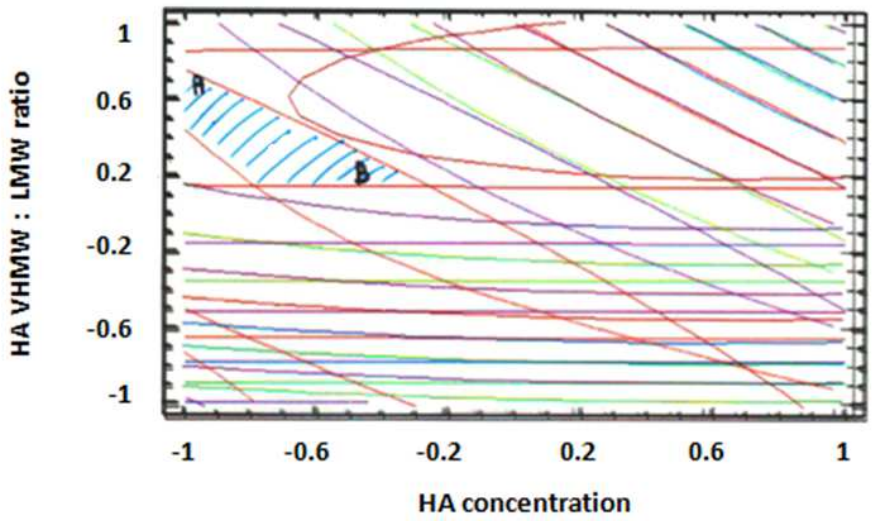

Figure 5. Combined contour plot showing the region of the experimental domain (shaded area) that satisfies all the constraints of the response variables.

Two optimized formulations were chosen inside the region of the experimental domain satisfying all the constraints. The two formulations (A and B) were selected at the extreme of the optimized area, in order to challenge the model and test its predictive power.

Formulation A contained 1.1% (w/v) of HA with a VHMW:LMW HA ratio equal to 78:22, whereas formulation B contained 1.5% (w/v) of HA with a VHMW:LMW HA ratio equal to 58:42. The % (w/v) composition of the optimized formulations are reported in Table 4.

Table 4. % (w/v) composition of the two optimized formulations.

Formulation	VHMW HA	LMW HA	NaCl	Phosphate buffer pH 7.4
A	0.86	0.24	0.75	up to 100
B	0.87	0.63	0.75	up to 100

The results obtained from the characterization of the two optimized formulations are reported in Table 5.

Table 5. Experimental parameters of the optimized formulations (mean values ± s.d.; n=4).

Formulation	Frequency at cross over (rad/s)	Viscosity at cross over (Pa.s)	Tan δ at 2.5 Hz	Dynamic viscosity at 0.01 s^{-1} (Pa.s)	pH	Osmolality (mOsm/Kg)	Extrusion force (N)
Formulation A	8.32 (±0.32)	20.6 (±0.30)	0.815 (±0.016)	10.98 (±0.44)	6.85 (±0.02)	345 (±2)	10.89 (±0.11)
Formulation B	9.09 (±0.27)	22.9 (±0.30)	0.848 (±0.006)	12.07 (±0.46)	6.83 (±0.02)	351 (±2)	11.25 (±0.08)

As for rheological properties, the experimental results of the 4 parameters considered fell inside the confidence interval of the values predicted by the model at p<0.05 to indicate its predictive power. pH and osmolality values of both formulations fell inside the acceptance range, and extrusion force was compatible with an easy syringeability. It must be underlined that no statistical difference was observed between homogeneous parameters of the two formulations (Mann–Whitney U-test, N.S.).

On the basis of these results, formulation B was chosen as the optimized HA formulation, since it contains the higher HA concentration (1.5% w/v) and was considered for further steps of pharmaceutical development.

3.3. Properties of the optimized HA+PC formulation

In Table 6, the aspect, pH, and osmolality values of the optimized HA formulation and of the HA+PC formulation as well as their functional properties (rheological parameters) are compared with those of synovial fluid. It can be observed that the addition of PC does not affect the viscous and viscoelastic properties of the formulation, as confirmed by the statistical analysis (Mann–Whitney test, N.S.), which are comparable to those of the optimized HA formulation. Only the

aspect is different: the presence of the water-insoluble PC produces a whitish and opalescent aspect.

Table 6. Aspect and functional parameters of the optimized HA formulation with and without phosphatidylcholine (PC) (mean values ± s.d.; *n*=4).

Sample	Aspect	Frequency at cross over (rad/s)	Viscosity at cross over (Pa.s)	Tan δ at 2.5 Hz	Dynamic viscosity at 0.01 s^{-1} (Pa.s)	pH	Osmolality (mOsm/Kg)
HA 1.5% (w/v)	colorless and transparent	9.09 (±0.27)	22.90 (±0.30)	0.848 (±0.006)	12.07 (±0.46)	6.83 (±0.02)	351 (±2)
HA 1.5% + PC 0.05% (w/v)	whitish, slightly opalescent	9.49 (±0.28)	21.65 (±0.37)	0.862 (±0.007)	11.74 (±0.51)	6.64 (±0.07)	345 (±1)
Healthy synovial fluid	*N/A*	*1-10*	*20-80*	*0.39*	*1-40*	*N/A*	*N/A*

In Figure 6 the tribology profiles of the optimized 1.5% w/v HA formulation (formulation B) and the optimized HA formulation containing 0.05% w/v PC are compared with those of a commercial product (Synovial containing 3.2% w/v HA) and those of physiological solution (taken as control).

In the first portion of the curve, corresponding to low torque values, friction forces between cartilage and formulation prevail over the torque applied: the sample undergoes deformation, but it does not move. At the breakaway point, the slope of the curve dramatically changes: the sample begins to move, since the torque applied prevails over frictional forces.

The smaller the deflection angle at the breakaway point, the greater the lubrication properties of the formulation [26].

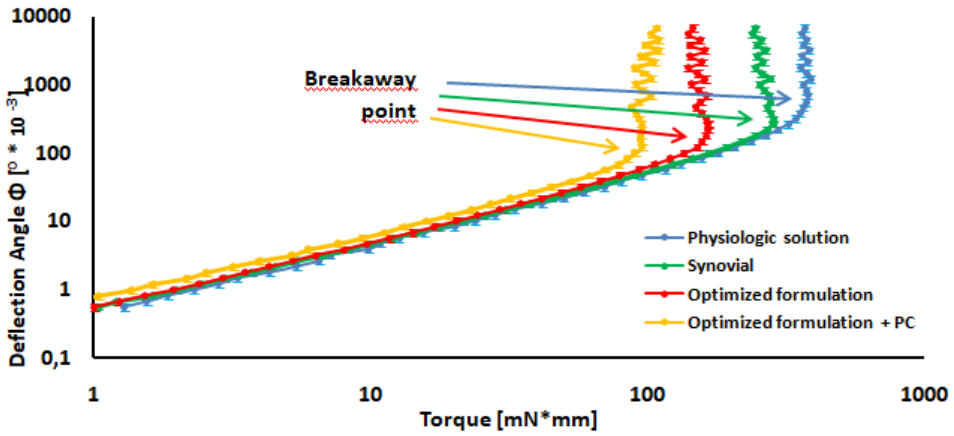

Figure 6. Comparison of tribology profiles (mean values ± s.d., *n* = 3).

It is noteworthy that the optimized HA formulation is characterized by sensibly better lubrication properties that the commercial product, besides containing more than a half HA concentration (1.5 *vs* 3.2 % w/v). This result points out that an optimized mixture of two HA

grades, characterized by quite different MWs, can be better suited for viscosupplementation, although at low HA concentration than products based on higher HA concentrations.

The lubrication properties of the optimized HA formulation are further improved by the addition of PC, even at low concentration (0.05% w/v), corresponding to half the physiological one (≅0.1% w/v).

3.3.1. Stability Studies

The results of the stability study are reported in Table 7.

Table 7. Aspect and functional parameters of the optimized HA formulation with PC subjected to stability study in ICH long-term and accelerated conditions (mean values ± s.d.; *n*=3).

Check-points	Aspect	Frequency at cross over (rad/s)		Dynamic viscosity at 0.01 s^{-1} (Pa.s)		pH		Osmolality (mOsm/kg)	
		25°C/ 60% RH	40°C/ 75% RH	25°C/ 60% RH	40°C/ 75% RH	25°C/ 60% RH	40°C/ 75% RH	25°C/ 60% RH	40°C/ 75% RH
time zero	whitish, slightly opalescent	9.49 (±0.28)		11.74 (±0.51)		6.64 (±0.07)		345 (±1.34)	
1 month	whitish, slightly opalescent	9.55 (±0.32)	10.21 (±0.58)	11.57 (±0.32)	11.03 (±0.41)	6.62 (±0.04)	6.60 (±0.05)	342 (±1.17)	343 (±1.23)
2 months	whitish, slightly opalescent	9.60 (±0.29)	10.26 (±0.69)	11.39 (±0.39)	10.75 (±0.40)	6.62 (±0.03)	6.61 (±0.04)	343 (±1.11)	344 (±1.32)
3 months	whitish, slightly opalescent	9.64 (±0.33)	10.20 (±0.39)	11.21 (±0.31)	9.95 (±0.35)	6.60 (±0.07)	6.59 (±0.05)	347 (±1.30)	344 (±1.21)
6 months	whitish, slightly opalescent	9.77 (±0.47)	10.01 (±0.42)	10.68 (±0.42)	9.77 (±0.39)	6.63 (±0.04)	6.62 (±0.06)	346 (±1.18)	340 (±1.04)

As for the aspect, no difference was observed at the various checkpoints with respect to time zero in both storage conditions. This result indicates the physical stability of PC in the oil/water emulsion.

Frequency values at the cross over point were not affected by increasing the time in both storage conditions in comparison with time zero (one-way Anova, N.S.), thus indicating the maintenance of viscoelastic properties of the formulation.

In the case of dynamic viscosity in rest conditions, no differences were observed between the results obtained in long-term conditions (one-way Anova, N.S.). On the contrary, in accelerated conditions, viscosity at 0.01 s^{-1} tends to slightly decrease over time in comparison with time zero; the statistical analysis pointed out that such a decrease is statistically significant only after 6 months (one-way Anova, $p<0.05$, post hoc Sheffè test $p<0.01$). However, it must be underlined that the viscosity measured at 0.01 s^{-1}, even in accelerated stability conditions, remains well inside the range (1–40 Pa.s) reported for healthy synovial fluid.

No statistically significant differences were found for pH and osmolality values in both storage conditions with respect to time zero (One way Anova, N.S.)

4. Conclusion

The employment of a very high MW HA in association with a low MW HA represents a winning strategy to prepare a novel HA-based sterile injectable formulation intended for intra-articular administration. The DoE approach proved successful to optimize the best polymer concentration and relative fraction of the two HA grades, saving time and experiments.

The addition of PC to the HA optimized formulation proved useful to obtain a product more similar in composition to the synovial fluid and characterized by lubrication properties markedly improved in comparison with the optimized HA formulation and with a commercial product containing a double HA concentration.

5. References

1. Gatter, R.A.; Schumacher, H.R. Joint Aspiration: Indications and Technique. In: *A Practical Handbook of Joint Fluid Analysis,* 2nded.; Lea&Febiger, Philadelphia, PA, USA, 1991; pp. 7–14.
2. Blewis, M.E.; Nugent–Derfus, G.E.; Schmidt, T.A.; Schumacher, B.,L.; Sah, R.L. A model of synovial fluid lubricant composition in normal and injured joints .*Eur. Cells Mat.* **2007**, *13*, 26–39.
3. Tamer, T.M. Hyaluronan and synovial joint: Function, distribution and healing. *Interdiscip. Toxicol.* **2013**, *6*, 111–125.
4. Laurent, T.; Fraser, J. Hyaluronan. *FASEB J.***1992**, *6*, 2397–2404.
5. Fraser, J.; Laurent, T.; Laurent , U. Hyaluronan: Its nature, distribution, functions and turnover. *J. Intern. Med.* **1997**, *242*, 27–33.
6. Dodero, A.; Williams, R.; Gagliardi, S.; Vicini, S.; Alloisio, M.; Castellano, M. A micro–rheological and rheological study of biopolymers solutions: Hyaluronic acid. *Carbohydr. Polym*. **2019**, *203*,349–355.
7. Schmidt, T.A.; Gastelum, N.S.; Nguyen, Q.T.; Schumacher, B.L.; Sah, R.L. Boundary lubrication of articular cartilage: Role of synovial fluid constituents. *Arthritis Rheum*. **2007**, *56*, 882–891.
8. Buckwalter, J.A.; Mankin,H.J. Articular cartilage. Part II: Degeneration and osteoarthrosis, repair, regeneration, and transplantation. *J. Bone Jt. Surg. Am.* **1997**, *79*, 612–632.
9. Garg, H.G.; Halas,C.A. Viscoelastic properties of hyaluronan and its therapeutic use.In: *Chemistry and Biology of Hyaluronan.* Elsevier Science, Philadelphia, PA, USA, 2004; pp. 415–455.
10. Fam, H.; Bryant, J.T.; Kontopoulou, M. Rheological properties of synovial fluids. *Biorheology* **2007**, *44*, 59–74.
11. Furst, D.E. Anakinra: Review of recombinant human interleukin–I receptor antagonist in the treatment of rheumatoid arthritis. *Clin. Ther.* **2004**, *26*,1960–1975.
12. Moreland, L.W. Drugs that block tumour necrosis factor: Experience in patients with rheumatoid arthritis. *Pharmacoeconomics* **2004**, *22*, 39–53.
13. Frias, G.; Caracuel, M.A.; Escudero, A.; Rumbao, J.; Perez Gujo, V.; del Carmen Castro, M.; Font, P.; Gonzalez, J.; Collantes, E. Assessment of the efficacy of joint lavage versus joint lavage plus corticoids in patients with osteoarthritis of the knee. *Curr. Med. Res. Opin.* **2004**, *20*, 861–867.
14. Tanaka, N.; Sakahashi, H.; Hirose, K.; Ishima, T.; Ishii, S. Volume of a wash and the other conditions for maximum therapeutic effect of arthroscopic lavage in rheumatoid knees.*Clin. Rheumatol*.**2006**, *25*,65–69.
15. Ayral,X. Arthroscopy and joint lavage. *Best Pr. Res. Clin. Rheumatol.* **2005**, *19*, 401–415.
16. Moreland, L.W. Intra–articular hyaluronan (hyaluronic acid) and hylans for the treatment of osteoarthritis: Mechanisms of action. *Arthritis Res.* **2003**, *5*, 54–67.
17. Tehranzadeh, J.; Booya, F.; Root, J. Cartilage metabolism in osteoarthritis and the influence of viscosupplementation and steroid: A review. *ActaRadiol.* **2005**, *46*,288–296.
18. Tenci, M.; Rossi, S.; Bonferoni, M.C.; Sandri, G.; Mentori, I.; Boselli, C.; Icaro Cornaglia, A.; Daglia, M.; Marchese, A.; Caramella, C.; Ferrari, F. Application of DoE approach in the development of mini–

capsules, based on biopolymers and manuka honey polar fraction, as powder formulation for the treatment of skin ulcers. *Int. J. Pharm.* **2017**, *516*, 266–277.
19. Dejagher, B.; Van der Heyden, Y. The use of experimental design in separation science. *Acta Chromatogr.* **2009**, *21*,161–201.
20. Dejagher, B.; Van der Heyden, Y. Experimental designs and their recent advances in setup, data interpretation and analytical applications. *J. Pharm. Biomed. Anal.* **2011**, *56*,141–158.
21. Draper, N.R.; Smith, H. Selecting the "best" regression equation. In: *Applied Regression Analysis*,3rded.;Wiley & Sons, New York, NY, USA, 1998; Chapter 15, pp.327–368.
22. Bolton, S.; Bon, C. Optimization techniques and screening designs. In: *Pharmaceutical Statistics–Practical and Clinical Applications,* 5th ed.; Informa Heathcare, NewYork, USA, 2010; Chapter 16, pp. 425–467.
23. Mori,M.; Rossi, S.; Ferrari, F.; Bonferoni, M.C.; Sandri, G.; Chlapanidas, T.; Torre, M.L.; Caramella,C. Sponge–like dressings based on the association of chitosan and sericin for the treatment of chronic skin ulcers. I. Design of experiments–assisted development. *J. Pharm. Sci.* **2016**, *105*, 1180–1187.
24. De Muth, J.E. One–Way Analysis of Variance (ANOVA). In *Basic Statistics and Pharmaceutical statistical Applications,* 3rded.; CRC Press, Boca Raton, FL, USA, 2014; pp. 205–231.
25. Pund, S.; Shete, Y.; Jagadale, S. Multivariate analysis of physicochemical characteristics of lipid based nanoemulsifying cilostazol—Quality by design. *Colloids Surf. B.Biointerfaces***2014**, *115*, 29–36.
26. Stachowiak, G.W. How tribology has been helping us to advance and to survive. *Friction* **2017**, *5*, 233–247.

Chapter 2

Development of a novel medical device (artificial tears) based on binary mixtures of HA

1. Introduction

Natural tears consist of an aqueous solution (water being the major component ≅98 %) having complex compositions: in fact it contains salts, hydrocarbons, proteins, and lipids. Tears are characterized by osmolarity = 309 mOsm/L and average pH = 7.25 [1].

Natural tears possess three major functions: they maintain the metabolism of the ocular surface, enable the maintenance of a smooth surface that allows regular light refraction, and lubricate the ocular surface to facilitate blinking [2], which in turn exerts a washing funtion, towards pathogens and foreign bodies.

The International Dry Eye Workshop (2007) defined Dry Eye Syndrome (DES) also known as keratoconjunctivitis sicca (KCS) as a multi factorial disease of the tears and ocular surface that determines discomfort, visual disturbance, and tear film instability with potential damage of the ocular surface. DES is accompanied by increased osmolarity of the tear film and inflammation of eye surface [3].

A special case of DES is known as "Sjogren's syndrome", which is characterized by the combination of tear deficiency and dry mouth (xerostomia) [4].

Dry eye syndrome (DES) increases with age, in particular in menopause [5]; moreover, up to 20% of people with rheumatoid arthritis present DES [6]. Other individuals that are likely to be affected include patients with Helicobacter pylori, computer users [7] and long term contact lens wearers [8].

The diagnosis is clinical; the ocular examination reveals alterations of the conjunctiva and of the tear film. The Schirmer test is the method most commonly used to evaluate aqueous tear production; the test uses blotting paper cut into strips which are hooked over the lower lid margin. The method most frequently used to assess tear film stability is to measure the tear break-up time (TBUT) [9].

DES is treated in various ways: the goals of treatments are to relieve the symptoms, to improve patient's comfort, to return the ocular surface and tear film to the normal state and, whenever possible, to prevent corneal damage. Treatments encompass environmental or dietary modifications, use of artificial tear substitutes, uptake of anti-inflammatory or immune-modulatory drugs (such as Cyclosporine A) via topical or systemic administration up to punctual occlusion surgery, which consists of inserting punctal plugs (silicone or collagen) into the tear drainage area to keep the tears in the eyes longer [9,10].

Artificial tears, consisting of aqueous eye drops with lubricant properties, are currently the mainstay of DES therapy and they should mimic as closely as possible the desirable properties of natural tears.

Ideally a tear replacement solution will be able, like natural tears, to cope with both the low-shear region and minor movements of the open eye, and the high-shear region typical of blinking. This is best achieved by a pseudoplastic fluid (i.e. a non-Newtonian fluid exhibiting shear-thinning), whose viscosity is high at low shear rates and low at high shear rates, rather than by a Newtonian fluid, whose viscosity is independent on shear rate. Natural human tears, due to their

content of soluble mucous glycoproteins, are known to possess this property [11]: in particular, natural tear viscosity is about 65 mPa·s when eyes are open, and decreases to 10 mPa·s during blinking [12].

Not all commercially available artificial tears possess pseudoplastic properties.

On the contrary, artificial tears based on HA show a non-Newtonian behaviour, similar to that of natural tears and are therefore particularly beneficial for the treatment of DES.

Many studies in the literature demonstrated that HA tear substitutes are able to improve tear film stability and to delay water evaporation from the tear film thanks to their mucomimetic, viscoelastic and water-retention properties [13,14]. In particular, tear substitutes based on HA proved able to sensibly reduce DES symptoms non only in comparison with saline [15], but also with tear substitutes based on other hydrophilic polymers such as carboxymethylcellulose [16] or hydroxypropyl-methylcellulose [17], both characterized by viscoelastic properties similar to HA.

Given these premises, the aim of this work was the development, in accordance to ISO guideline 10093, of hyaluronic acid (HA) based sterile artificial tears, classified as IIb class medical device, capable of best mimicking natural tears, to be used for DES treatment and containing a HA concentration higher than the commercial product (Octilia 0.3% w/v artificial tears) by IBSA Farmaceutici. Although an increase in HA concentration could conceivably determine problems in sterile filtration due to the concomitant increase in viscosity of the polymeric solution, the rationale for such formulation choice is to obtain a product characterized by optimal rheological and lubrication properties, as similar as possible to tear fluid.

The research was divided in two steps.

The first phase was devoted to the identification of the HA grades and concentration to be employed for lab scale preparation of artificial tear formulations, characterized by viscosity at rest (open eye) and upon blinking as similar as possible to those of human tears.

The first formulation challenge was to develop a new artificial tear formulation at HA concentration higher than 0.3% w/v.

Another formulation challenge concerns sterilization: artificial tears, in fact, must be sterile but it isn't possible heat sterilization of HA solutions in final containers because vials are made of plastic. So the only possibility to achieve sterility is filtration through 0.22 μm pore-size filters. Unfortunately, previous IBSA experience showed that with high MW HA (1.4-2.1x10^6 Da) the maximum filterable concentration is equal to 0.4% w/v.

To encompass this problem, it was decided to use HA mixtures containing both low (L) and high (H) molecular weight in accordance to the IBSA patent WO 2012032151 "Hybrid cooperative complexes of hyaluronic acid" i.e. complexes characterized by very stable interactions between molecules, due to the occurrence of weak forces, such as hydrogen bonds or hydrophobic interactions [18].

According to this patent, it is possible to prepare stable LMW/HMW HA hybrid cooperative complexes, by submitting aqueous mixtures of Low and High MW HA to a suitably configured thermal cycle.

Four parameters critically determine the formation of LMW/HMW – HA complexes in aqueous solutions and their rheological properties:

a) the simultaneous presence of two HA grades (LMW-HA and HMW-HA) in the same solution;

b) the molecular weight of the two HA grades used for the formation of the LMW/HMW HA hybrid system : according to the patent, cooperative hybrid complexes, characterized by a decrease in viscosity, are obtained when the molecular weight of the low HA grade is in the range 1 $x10^4$ - 1 $x10^6$ Da and the one of high HA grade is ≥ LMW HA/0.9.

c) the relative proportions of the two HA grades used: the decrease in viscosity consequent to formation of the complex increases on increasing the LMW/HMW HA stoichiometric ratio. Usually such a ratio falls between 0.1 and 10, preferably from 0.5 to 2.

d) the thermal cycle to which the solution is exposed: the solution is first heated to temperatures between 80 and 160°C, preferably between 100 and 120°C and then cooled rapidly to room temperature.

Three lab scale artificial tear formulations containing two HA grades in a 1:1 weight ratio and having increasing total HA concentration in the range 0.3 - 0.5 % w/v were prepared according to the method described above and subjected to rheological characterization. In particular the flow curves measured at 25°C (storage temperature) and 37°C (*in vivo* temperature) were compared. Besides flow measures, another rheological test called Rot Rot Rot was performed at 37°C to better mimic the shear conditions (and relevant viscosity) with open eyelid or during blinking.

In order to choose the best HA artificial tear candidate, the classification proposed by Muller-Lierheim for HA tear substitutes [19] was considered. The author classifies HA eye drops in five categories, according to their viscosity at low and high shear rates, to evaluate their efficacy as artificial tears.

Before proceeding to the second phase of the work, the best lab scale formulation, chosen on the basis of its optimal similarity to natural tears, was compared with the commercial product by IBSA Farmaceutici (Octilia 0.3% w/v artificial tears), containing the same HMW HA of the new formulation under development. Such a comparison had the aim to evaluate whether the new experimental formulation was better than that already available on the market.

In particular, the comparison regarded the rheological as well as the lubricating properties, evaluated on the basis of tribology measures.

In the second phase, the most promising formulation was at first scaled to pilot batch size: product stability was determined in long term and accelerated ICH conditions and biocompatibility was assessed according to the ISO guideline 10093, in order to obtain for the developed class IIb medical device the CE mark, required to reach the market. Once ascertained stability and biocompatibility, the further step envisaged to prepare a batch on industrial scale.

2. Materials and Methods

2.1. Materials

The following materials were used: injectable grade sodium hyaluronate low MW (LMW): 100000 Da (HTL Sas, Javene, France); injectable grade sodium hyaluronate high MW (HMW): 1.4-2.1 $x10^6$ Da (HTL Sas, Javene, France); water for injections (WFI) (Ph Eur. 10th Ed. Monograph 0169);

sodium chloride (Merck & Co., Frankfur, Germany); monobasic sodium phosphate monohydrate (Chemische Fabrik Budenheim KG, Budenheim, Germany); dibasic sodium phosphate dodecahydrate (Chemische Fabrik Budenheim KG, Budenheim, Germany); dihydrogen potassium phosphate ACS grade anhydrous (PanReac AppliChem ITW Reagents, Milan, Italy); potassium hydroxide solution 32% w/v ACS grade (VWR Chemicals, Milan, Italy); sodium tetraborate dodecahydrate ACS grade (VWR Chemicals, Milan, Italy); sulphuric acid concentrated 95-97% w/w ACS grade (VWR Chemicals, Milan, Italy); carbazole ACS grade (VWR Chemicals, Milan, Italy); absolute ethyl alcohol ACS grade (VWR Chemicals, Milan, Italy); glucuronic acid standard (LGC, Middlesex, UK).

2.2. Artificial tears formulations prepared on lab scale

The two HA grades (HMW e LMW) were selected in order to satisfy the formula HMW HA≥ LMW HA/0.9 and they were used in a 1:1 w:w ratio, according to the IBSA patent WO 2012032151.

Three formulations were prepared containing HA concentrations in the range 0.3-0.5 % w/v, and having the % w/v composition reported in Table 1.

The lowest HA concentration was chosen as the one used in the commercial product Octilia 0.3% w/v artificial tears.

Table 1. % (w/v) composition of the three artificial tear formulations prepared on lab scale.

Ingredient	**% w/v composition**		
	Sample A	***Sample B***	***Sample C***
HA HMW	0.15	0.2	0.25
HA LMW	0.15	0.2	0.25
Sodium chloride	0.75	0.75	0.75
Dibasic sodium phosphate dodecahydrate	0.30	0.30	0.30
Monobasic sodium phosphate monohydrate	0.066	0.066	0.066
WFI	up to 100 mL	up to 100 mL	up to 100 mL

Each sample was prepared on lab scale (100 mL) according to the thermal cycle described in the IBSA patent WO 2012032151 and hereafter reported.

90 g of WFI were weighed in a 100 mL flask. The water was heated to 85°C (±5°C) on a heating magnetic stirrer equipped with an electronic thermometer (IKA C-MAG HS 7 and ETS-D5,IKA®-Werke GmbH & Co. KG, Staufen, Germany). 0.75 g of sodium chloride, 0.3 g of dibasic sodium

phosphate dodecahydrate and 0.066 g of monobasic sodium phosphate monohydrate were added at 85°C (±5°C); the preparation was stirred for 10 min at 500 rpm to allow salt dissolution. Subsequently, the two HA grades were weighed and added to the saline solution. Each preparation was magnetically stirred at 1000 rpm for 15 min at 85°C. Then heating was turned off and, after 30 min each sample reached 25°C. Stirring was continued at 1000 rpm for 1 h to enable HA complete hydration.

The pH of each solution was determined (pH meter Seven Compact S220, Mettler Toledo, Columbus, Ohio, USA). All samples showed pH values close to neutrality: pH 7.0 for samples A and C and pH 7.1 for sample B. Additional WFI was then added to each flask up to 100 mL.

Finally each solution underwent sterile filtration. The choice of the sterilizing filter was made in collaboration with Sartorius. Filterability trials were performed at room temperature and at a constant pressure equal to 800 mBar, that represents the working pressure. The filtration equipment (Sartorius Stedim Biotech GmbH, Gottingen, Germany), shown in Figure 1, was employed. The set up of the filtration equipment to achieve filtration at constant pressure was adapted to individual test conditions.

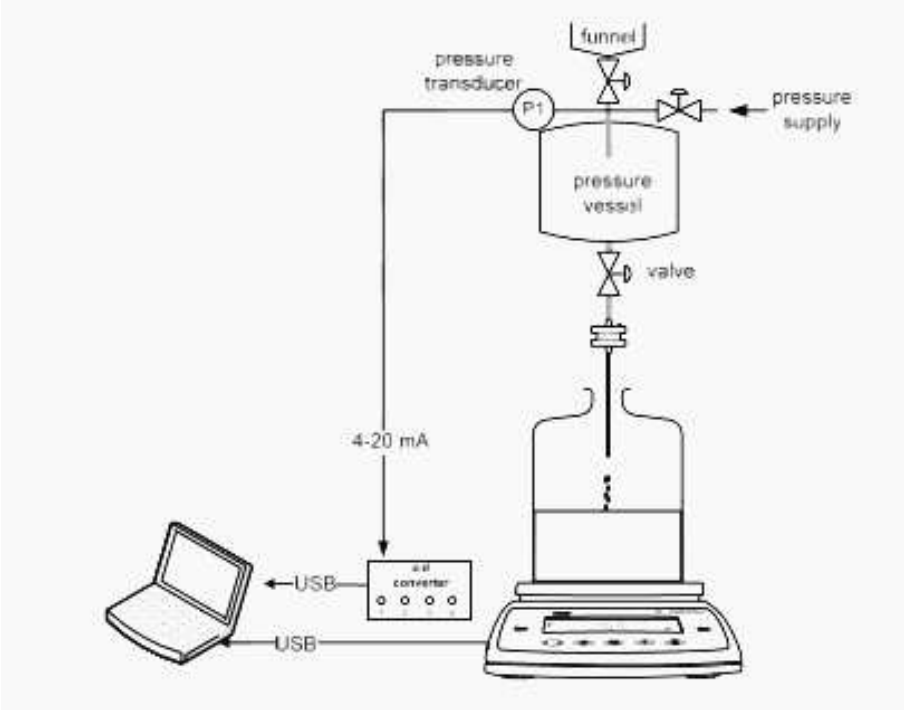

Figure 1. Scheme of the filtration equipment used for filterability trials.

The pressure and the amount of filtrate were recorded as a function of time by means of a pressure transducer and a balance. The data were collected and recorded by a PC.

Two different filters were tested: Sartopore®2 and Sartopore® Platinum.

The first trial was carried out with 47 mm diameter membranes; based on the results obtained, a second trial was arranged using the same type of filter but with a larger filter surface: Sartopore® Capsule (size 4) (Sartorius Stedim Biotech GmbH, Gottingen, Germany).

Sartopore®2 is a sterilizing grade and mycoplasma retentive pharmaceutical filter with high total throughput and chemical compatibility, characterized by flow rate performance useful for a broad range of applications.

Sartopore® Platinum is a sterilizing grade pharmaceutical filter using Twin Pleat® technology, with permanently hydrophilic membrane surface modifications for optimal total throughput, low binding and low flush volumes for secure and reliable integrity testing. The parameters (filtrate volume and flow rate) measured with the two filters for filtration of 300 mL of a 0.4 % w/v HMW HA solution are compared in Figure 2.

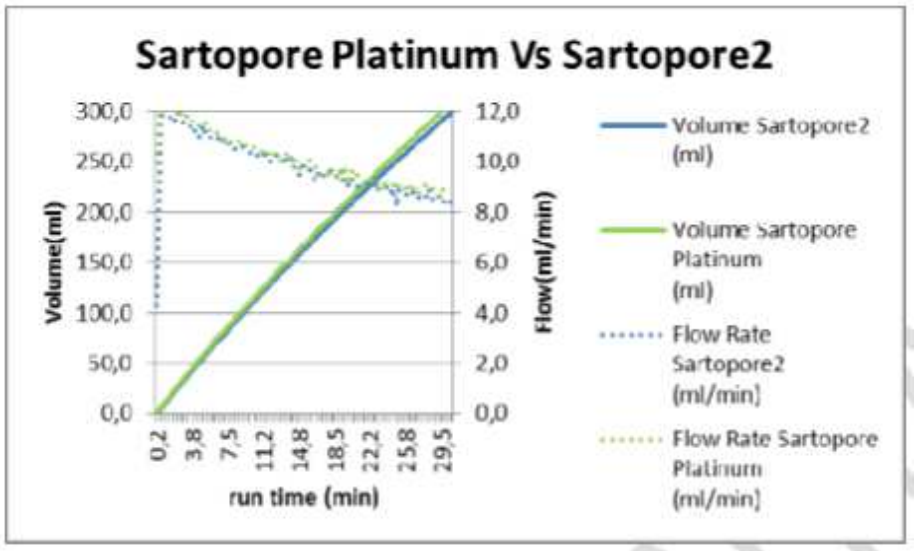

Figure 2. Filtration parameters measured with the two Sartorius filters.

Despite both filters showed the same results in terms of performance, Sartopore® Platinum was selected, due to its new pleating technology, which offered a greater effective filtration area (1 m^2) than Sartopore® 2 (0.6 m^2). In fact, a 10'' inch length element of Sartopore® Platinum proved suitable for filtration in 1 h of an industrial batch (300 L) of a HMW HA 0.4% w/v aqueous solution, which represents the "worst case" for sterile filtration [20].

2.3. Characterization of artificial tears formulations prepared on lab scale

2.3.1. Rheological characterization

Rheological properties of lab scale solutions were evaluated by means of the rotational rheometer (Modular Compact Rheometer MCR302, Anton Paar GmbH, Graz, Austria) equipped with a coaxial cylinders combination as measuring system. All samples were subjected to rheological measurements both at 25°C (storage temperature) and 37°C (*in vivo* temperature).

At first, viscosity measurements were carried out in a shear rate interval ranging from 1 (η_0) to 1000 (η_{1000}) s^{-1} in order to investigate whether a pseudoplastic non Newtonian behaviour occurred.

Besides flow measures, another test called Rot Rot Rot test was performed at 37° C to better mimic the shear conditions (and relevant viscosity) with open eyelid or during blinking. Rot Rot rot is a step test consisting in the application of three shear rate intervals during three subsequent time periods, each one lasting 15 s:

- Step 1: application of a low shear rate (1 s^{-1}) during the time period t_0 (0 s) - t_1 (15 s). The aim was to achieve a fairly constant η_0 value in the whole first period, to be considered as the "reference value of the viscosity-at-rest" and to be compared with the viscosity measured in the third step.
- Step 2: immediate increase (0.1 s) of shear rate to 1000 s^{-1} and maintenance of this high shear rate value during the time period t_1 (15 s) - t_2 (30 s), to mimic the lowering of the eyelid (during blinking).
- Step 3 of: immediate decrease (0.1 s) of shear rate to 1 s^{-1} and maintenance of this low shear value in the period between t_2 (30 s) - t_3 (45 s), to check the recovery of viscosity conditions "at rest" (open eye).

In order to evaluate the pseudoplastic, non-thixotropic, behavior of formulations, the percentage of η_0 recovery between the first and the third time period was calculated.

In detail the "percentage of recovery" taking place in the third time interval was determined at the beginning of this period (t_2= 30 s) to exclude a time-dependent behaviour of the samples.

The percentage of recovery was calculated by dividing the η_0 value measured at the beginning of step 3 by the one measured at the end of step 1.

2.3.2. Tribology measures

Tribology tests were effected using the rotational rheometer (Modular Compact Rheometer MCR302, Anton Paar GmbH, Graz, Austria) equipped with the "Pins on disc" system (Figure 3), which is suitable for tribology measurements of ophthalmic products. The measures were effected at 25°C.

Figure 3."Pins on disc" system configuration.

During the test, the sample was loaded on a glass disc and the probe, equipped with special silicone pins, was fixed to the rotating shaft and lowered to contact the sample. The probe was

thereby rotated over the sample at a sliding speed that was logarithmically increased from 10^{-9} to 1 m/s.

Stribeck curves relating the friction factor with the sliding velocity (Figure 4) were obtained. These curves enable to appreciate the transit of the tribosystem (i.e. probe plus sample) from a static to a kinetic state of motion. The value of the friction factor in the static regimen, before the onset of macroscopic motion, only represents the frictional resistance offered by the trybosystem to reach the set sliding velocity. In the static regimen, the sliding velocity is a result of deformation – elastic and plastic – mainly occurring at the interface between the probe and the sample [21].

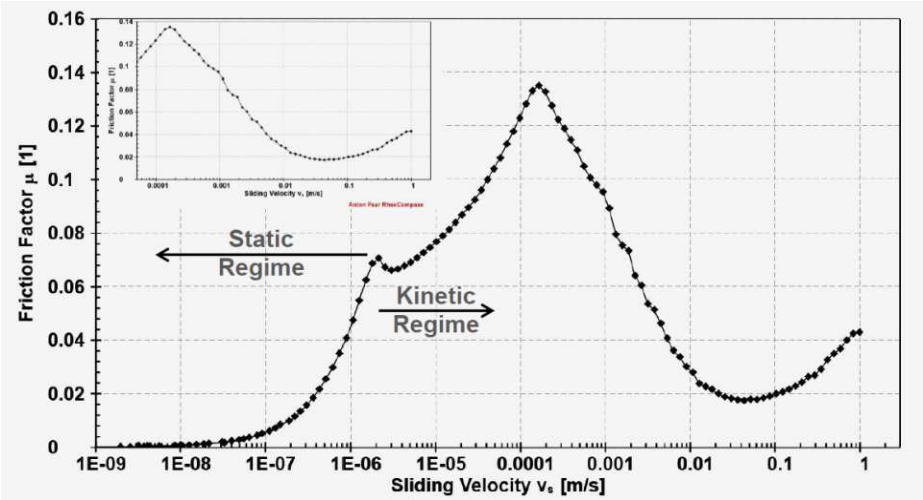

Figure 4. Example of Stribeck curve [21].

Tribology measures had to be effected on the lab scale formulation best simulating tear fluidity according to [19], on Octilia 0.3% w/v artificial tears and on water for injections used as control.

2.4. Pilot batch: preparation and characterization

The lab scale formulation characterized by the best rheological properties was scaled up on the industrial plant of a COC (Chemical Organic Compound) company; the pilot batch volume (150 L) corresponded to half a standard industrial production.

143 L of WFI were loaded into a preparation vessel for liquid products (Olsa, Milan, Itay) heated at 85°C (±5°C) under mixing at 200 rpm with an anchor type mixer. Then 1.125 kg of sodium chloride, 450 g of dibasic sodium phosphate dodecahydrate and 99 g of monobasic sodium phosphate monohydrate were added and mixed at 400 rpm up to complete salts dissolution. Subsequently 375 g of each HA grade were added to the saline solution. The polymeric solution obtained was mixed at 400 rpm for further 15 min at 85°C. Then heating was turned off and the temperature was settled down to 25°C (±3°C). After 1 h, the preparation reached 25°C; stirring was continued at 400 rpm for additional 30 min to obtain complete HA hydration. Subsequently pH and osmolality were measured to verify the neutrality and isotonicity of the solution. Additional WFI (4,58 L) was added to complete the preparation.

The final solution was sterilized by sterile filtration through a PES filter, consisting of a 0.45 μm pre-filter and by a 0.22 μm final filter (Sartopore® Platinum MidiCaps®, Sartorius Stedim Biotech GmbH, Gottingen, Germany).

Finally, artificial tears were divided by an automatic filler (Comas Srl, Firenze, Italy) into 10 mL low density polyethylene bottles (Purell PE 1810E, Lyondellbasell, Houston, Texas, USA). The bottles were closed by OSD (Ophthalmic Squeeze Dispenser) preservative free pump caps (Aptar Pharma GmbH, Eigeltingen, Germany) sterilized with 25.5 KGY gamma ray irradiation.

2.4.1. Pilot batch stability study

A stability study lasting 36 months was set up for the pilot batch according to ICH Q1A guidelines (Stability Testing Guidelines: stability testing of new drug substances and products, Rev. 2), to check the physical-chemical and microbiological stability in long term, intermediate and accelerated storage conditions.

The check points of the study are shown in Table 2.

Table 2. Check points of the stability study provided for the pilot batch.

Storage conditions	**Check points (months)**							
	0	**3**	**6**	**9**	**12**	**18**	**24**	**36**
25°C/60%RH	P + M	P	P	P	P + M	P	P + M	P + M
30°C/65%RH		P	P	P	P + M			
40°C/75%RH		P	P	P + M				

P= Physical-chemical tests M= Microbiological tests

The study in intermediate storage conditions (30°C/65%UR) is optional; tests would have been carried out on samples stored in these conditions only if significant changes in samples stored in accelerated conditions (40°C/75% UR) have occurred.

The number of samples was calculated considering the possibility to repeat the analysis for each test; for each check point the number of vials needed was:

- N° samples for each physical-chemical check point (C) : 10 vials
- N° samples for each microbiological check point (M) : 20 vials

Except samples used for the analysis at T zero, for each storage condition the number of stored samples were:

- 130 vials at 25°C/60% RH
- 60 vials at 30°C/65% RH
- 50 vials at 40°C/75% RH

At each check point, the physical-chemical and microbiological properties of stored samples had to be compared with the preliminary specifications reported in Table 3.

Table 3. Preliminary specifications of the parameters considered in the stability study.

PARAMETERS	PRELIMINARY SPECIFICATIONS
Solution aspect	Transparent and colorless solution, without visible particles
pH	6.5 – 7.5
Osmolality	250-350 mOsm/kg
HA HMW+LMW identification	Positive
HA content	0.45 - 0.55 %w/v
Dynamic viscosity	12 – 55 cP
Sterility	Sterile

pH

pH measurements were carried out according to Ph. Eur. 10th Ed., Par. 2.2.3 using a pH meter (Seven Compact S220, Mettler Toledo, Columbus, Ohio, USA).

Osmolality

Osmolality measurements were carried out according to Ph. Eur. 10th Ed., Par. 2.2.35 using the Cryoscopic Osmomat O30 (Gonotec, Berlin, Germany).

Viscosity

The dynamic viscosity was measured using a viscosity-rotating viscometer according to Ph. Eur. 10th Ed., Par. 2.2.10. In particular, a spindle viscometer (Brookfield), equipped with a TL5 spindle, was used and the viscosity was determined by rotating a spindle immersed in the liquid.

Measures were carried out at 25°C and at 20 rpm.

Sterility

The sterility test was carried out according to Ph. Eur. 10th Ed., Par. 2.6.1.

Identification of peaks of the two HA grades (HMW and LMW)

HPLC-GFC analysis was performed using an Agilent 1260 HPLC, equipped with a quaternary pump, an auto-sampler and a UV−DAD detector (Agilent, Santa Clara, CA, USA). A PL-aquagel-ON MIXED-H column (250×4.6 mm, 8 μm) from Agilent Technologies (Santa Clara, CA ,USA) was used. The mobile phase consisted of Milli-Q grade water buffered with 1.36% w/v dihydrogen potassium phosphate; a potassium hydroxide solution 32% w/v was added to adjust the pH to 7.0. The auto-sampler and column temperatures were maintained at 25°C and 32°C, respectively. The injection volume was set at 15 μL and the flow rate at 0.5 mL/min.

The run time was 8 min. The chromatograms were registered at 205 nm; the retention times were 3.9 min for HA HMW and 4.6 min for HA LMW.

The reconstituted standard solution was prepared in a 50 mL flask; 50 mg of each HA grade (HMW e LMW) were added in a flask to about 30 mL of mobile phase. The sample was heated to

about 50°C on a heating magnetic stirrer equipped with an electronic thermometer (IKA C-MAG HS 7 e ETS-D5, IKA®-Werke GmbH & Co. KG, Staufen, Germany) and stirred at 400 rpm for 60 min. Then heating was turned off and the sample reached 25°C after 30 min; stirring was continued at 200 rpm until complete hydration of HA. Mobile phase was then added to the flask up to 50 mL. 1 mL of this solution was withdrawn and with mobile phase up to 10 mL. The final solution was filtered on a 0.45 μm cellulose membrane filter (Sartorius Stedim Biotech GmbH, Gottingen, Germany).

The sample solution was prepared in a volumetric flask by diluting with mobile phase 2.5 g of formulation up to 50 mL volume, in order to reduce sample viscosity. The solution was then magnetically stirred at 200 rpm for 30 min (IKA C-MAG HS 7, IKA®-Werke GmbH & Co. KG, Staufen, Germany) and filtered on a 0.45 μm cellulose membrane filter (Sartorius Stedim Biotech GmbH, Gottingen, Germany).

The result of the identification test was considered positive only if the retention time and the UV-DAD spectrum of the two HA grades peaks of the sample solution were comparable with those of the reconstituted standard solution, which are reported in Figures 5 and 6, respectively.

The analytical method was validated according to ICH guideline Q2(R1): Validation of analytical Procedures: text and methodology.

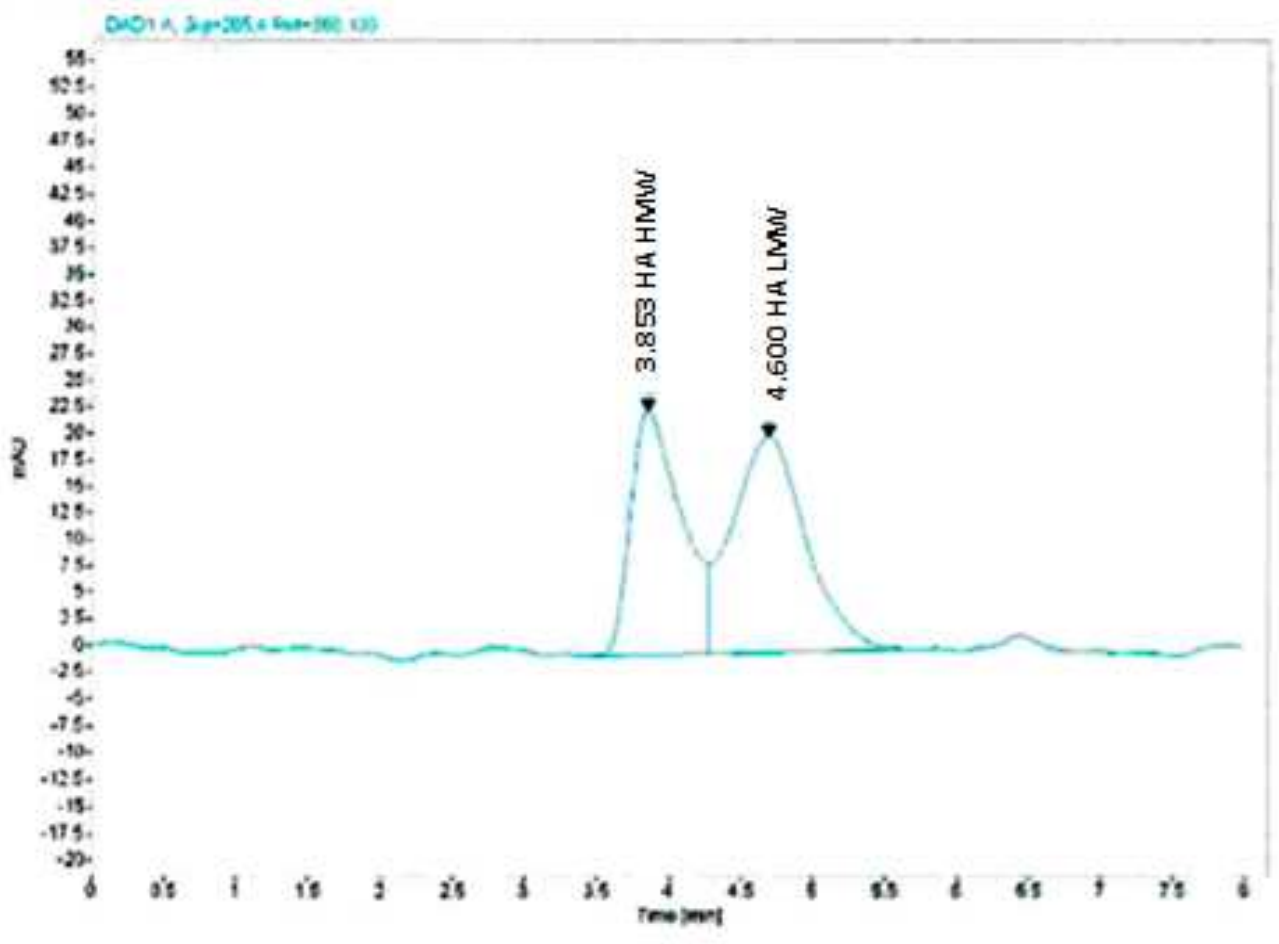

Figure 5. Typical chromatogram of the reconstituted standard solution.

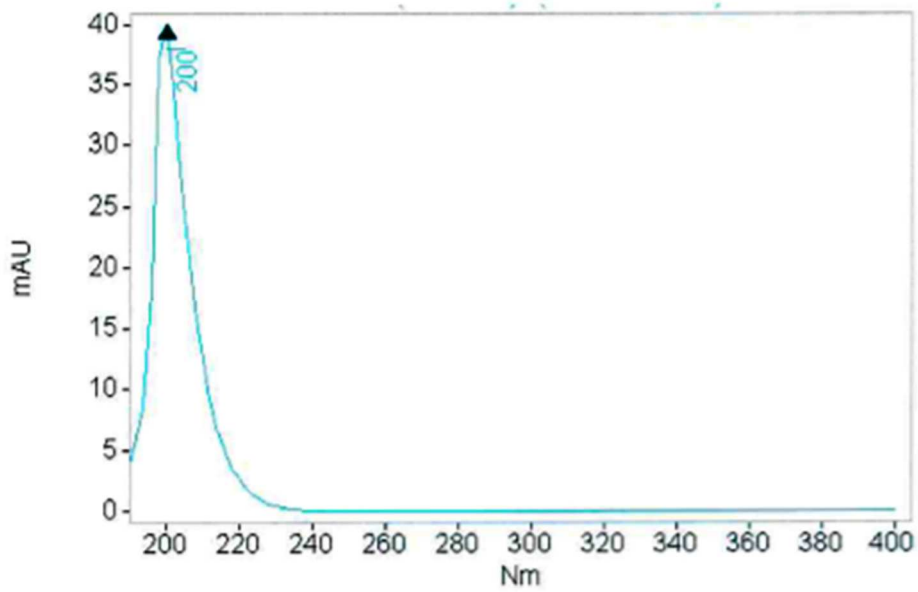

Figure 6. UV-DAD spectrum of the reconstituted standard solution.

Hyaluronic acid content

UV-Visible analysis was performed using a double-beam spectrophotometer Lambda 25 PerkinElmer (Waltham, MA, USA) controlled by a personal computer and equipped with a 1-cm path length quartz cell. Absorption was detected at 530 nm.

Two reagents were used in the test: reagent A was obtained by dissolving 1.9 g of sodium tetraborate dodecahydrate in 200 mL of concentrated sulphuric acid (95-97% w/w), reagent B was prepared by dissolving 125 mg of carbazole in 100 mL of absolute ethyl alcohol.

The standard solution was obtained by dissolving in a volumetric flask 60 mg of glucuronic acid in 250 mL of water; the solution was magnetically stirred at 300 rpm for 30 min. Then an aliquot of 5 mL was withdrawn and diluted with distilled water in a 50 mL volumetric flask.

The sample solution was prepared by diluting 2 g of artificial tears with water in a 100 mL volumetric flask; the solution was magnetically stirred at 200 rpm for 30 minutes. Then an aliquot of 10 mL was withdrawn and diluted with water in a 20 mL volumetric flask.

Standard and sample solutions were prepared in triplicate.

For HA assay 5 samples were analysed at a time: 1 sample was distilled water (blank), 2 samples were standard solutions and 3 were sample solutions.

Each sample for analysis was prepared in a glass test tube in which 1 mL of standard solution or sample solution or water (control) and 5 mL of reagent A were added. Each preparation was mixed for 3 s with a vortex (ZX4, VELP scientific, Monza Brianza, Italy) and then heated at 100°C for 15 minutes in a block heating system suitable for thermosetting glass test tube (Tecnovetro, Milan, Italy) and quickly cooled in ice. Subsequently, 0.2 mL of reagent B was added to each sample, which was then subjected to mixing, heating and cooling as previously described for reagent A. Finally, the samples were subjected to spectrophotometric analysis.

The % (w/v) HA content in the sample solution was calculated by applying the formula:

$$HA\%(w/v) = \frac{Ac * Fm * Vdc * 401.3}{Pc * 194.1} * 100$$

where:

Ac= average absorbance of the 3 sample solutions

Fm= average factor of 2 standard solutions = conc. (mg/mL) / average absorbance

Vdc= dilution volume of sample solution

Pc= sample weight (mg)

401.3= MW of D-glucuronic acid plus N-acetyl- D-glucosamine

194.1= MW of D-glucuronic acid

The acceptability range for HA assay was ± 5% of the theoretical content.

Specificity, linearity, accuracy and intermediate precision were assessed in order to validate the analytical method. The validation acceptance criteria and the experimental results obtained are reported in Table 4.

Table 4. Validation acceptance criteria and results of the UV-Vis method.

Parameters	Specifications	Results
Specificity		
Absorbance of the blank solution compared to that of the sample solution	≤ 2.0 %	1.0 %
Linearity		
Correlation coefficient	≥ 0.98	1.0
Intercepts	≤ ± 5.0 %	-0.80917
Total RDS%	≤ 5.0 %	1.7 %
Regression residues	Random and homogeneous arrangement around 0	Compliant
Accuracy		
Recovery	90.0 – 110.0 %	98.6 %
RDS%	≤ 5.0 %	4.9 %
Recovery confidence intervals	Must contain 100%	86.8 – 110.5 %
Precision		
System repeatability	≤ 1.0 % (check on 6 analysis)	Std: 0.02 % Sample: 0.1 %
Method repeatability	≤ 5.0 % (6 different preparations)	1 day: 3.3 % 2 days: 3.2 %
Intermediate precision	≤ 5.0 % (on 12 samples)	3.1 %
Difference % Analysis 1/Analysis 2	± 5.0 %	-0.1%

On the basis of the results reported in Table 4, the UV-Vis analytical method was considered validated in the assay range 70 – 130 % (w/v).

2.4.2. Pilot batch biocompatibility studies

Since artificial tear formulation is classified as IIb class medical device, the CE mark was required to reach the marketplace.

For this reason the pilot batch was subjected to biocompatibility studies according to the ISO guideline 10993:

- Cytotoxicity by indirect contact test – agar diffusion test
- Delayed hypersensitivity test (GMPT)
- Ocular irritation test

Biocompatibility tests were carried out on the pilot batch after checking its stability upon 3 month storage in accelerated conditions.

A compatibility test between artificial tears containing HA 0.25%+0.25% (w/v) and contact lenses was also performed in accordance to the ISO guideline 11981, to claim such a compatibility in the leaflet of the commercial product.

2.4.2.1 Citotoxicity by indirect contact test – agar diffusion test

Cytotoxicity by indirect contact test – agar diffusion test was performed according to the ISO guideline 10993-5: 2009 (Biological evaluation of medical devices – Part 5: Tests for *in vitro* cytotoxicity).

For this test, a sub-confluent NCTC clone L929 cell culture was used and a qualitative evaluation was performed by observing the cell culture by means of an inverted microscope.

50 µl of the sample were placed on at filter paper disc directly on a solid agar medium. After 24 and 48 h contact, the cells were observed under microscope (qualitative evaluation) to investigate the biological reaction.

2.4.2.2 Delayed hypersensitivity test

Delayed hypersensitivity test was carried out in accordance to the ISO guideline 10993-10: 2010 (Biological evaluation of medical devices – Part 10: Tests for irritation and skin sensitization).

For the Guinea pig maximization tests 15 Guinea pigs were used, 10 of which were treated with the pilot batch and 5 were used as a control group. Others 3 Guinea pigs were used for a preliminary test. The maximization test consisted of a preliminary test, an induction phase and a challenge phase. In details: the preliminary test aimed to determine the concentration of the test sample to be used in the main test, the induction phase intended to select the highest concentration that caused mild to moderate erythema with no adverse effects on animals, the challenge phase was carried out with the highest concentration that produced no erythema.

During the test the sample (a dressing loaded with 0.5 mL of pilot batch solution) was applied to the dorsum of guinea pigs and the dressing was left in place 24 h; 24 and 48 h after patch removal, all treated and control animals were evaluated for a skin reaction.

2.4.2.3 Ocular irritation test

Ocular irritation test was carried out in accordance to the ISO 10993-10:2010 guideline (Biological evaluation of medical devices – Part 10: Tests for irritation and skin sensitization) to evaluate any irritation effects at ocular level. For the ocular irritation test, the artificial tears (0.1 mL) were instilled in the conjunctive sac of the right eye of three albino male rabbits. The left eye was not treated and was used as control. Animals' eyes were examined after 1, 24, 48 and 72 h from the treatment by means of a binocular loupe. The ocular areas examined were cornea, iris and conjunctivae.

2.4.2.4 Compatibility between artificial tears and contact lenses

The pilot batch formulation was tested according to ISO 11981: 2009 (Ophthalmic optics – Contact lenses and contact lens care products – Determination of physical compatibility of contact lens care products with contact lenses). Physical properties of the lenses (aspect, surface and diameter) were evaluated according to ISO 18369-3: 2006 (Ophthalmic optics – Contact lenses – Part 3: Measurement methods) after contact with artificial tear formulation and compared with those of non-treated lenses. To simulate the worst-case exposure, the storage solution of 10 soft daily contact lenses was replaced at room temperature for five consecutive days with the test product.

2.5. Industrial batch: preparation and characterization

It was decided to proceed to industrial batch production in case the pilot batch proved to be stable after 6 month storage in accelerated conditions and the biocompatibility studies had shown that artificial tears were not irritating for the eye and well tolerated even in the presence of contact lenses.

The manufacturing process of industrial batch had to be the same used for the pilot batch, since the plant and equipment used were the same. The only difference would have regarded the volume of solution prepared, that would have been 300 L (doubled in comparison with pilot batch).

The industrial batch had to be subjected to the same characterization as the pilot batch.

3. Results and Discussion

3.1. Properties of lab scale artificial tears

The flow curves of the three lab scale artificial tear formulations measured at 25°C (storage condition temperature) and 37°C (*in vivo* temperature) are shown in Figures 7 and 8, respectively.

Since the HA concentration in artificial tears is very low, it was not possible to obtain reliable results at shear rates values equal to 0,001 s^{-1}; therefore the zero shear viscosity (η_0) was measured at shear rates of 1 s^{-1}.

As expected, all formulations, containing binary mixtures of the two HA grades, are characterized by a pseudoplastic behaviour, which is more evident on increasing polymer concentration. For a given formulation, the increase in temperature from 25°C to 37 °C determines a concomitant decrease of viscosity.

Similar considerations apply to the comparison of the viscosity data, measured at 25°C and 37°C, which are reported in Tables 5 and 6, respectively.

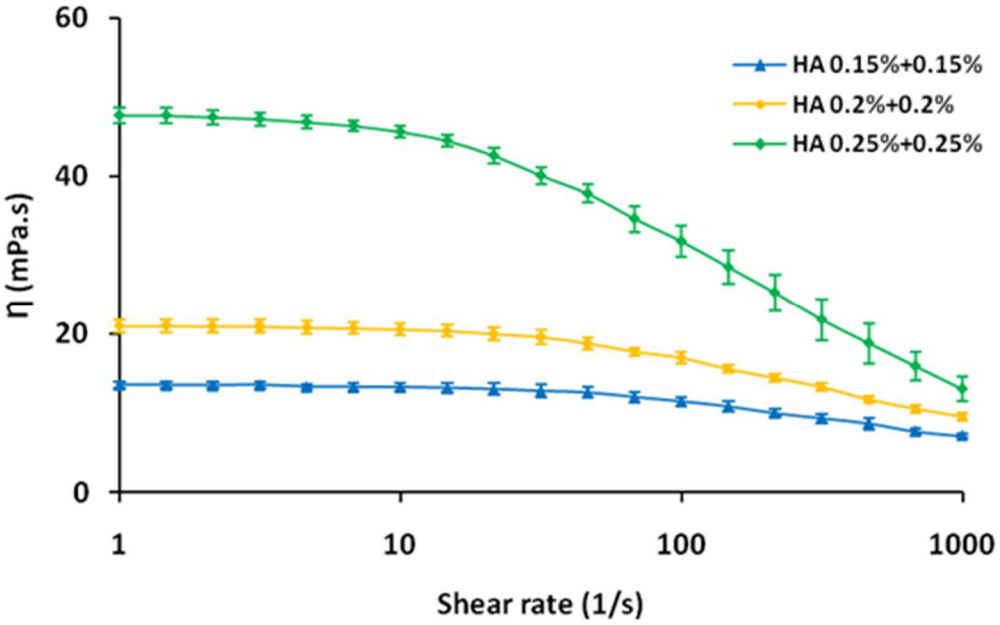

Figure 7. Flow curves of three lab scale artificial tear formulations, measured at 25°C (mean values ± s.d., n=3).

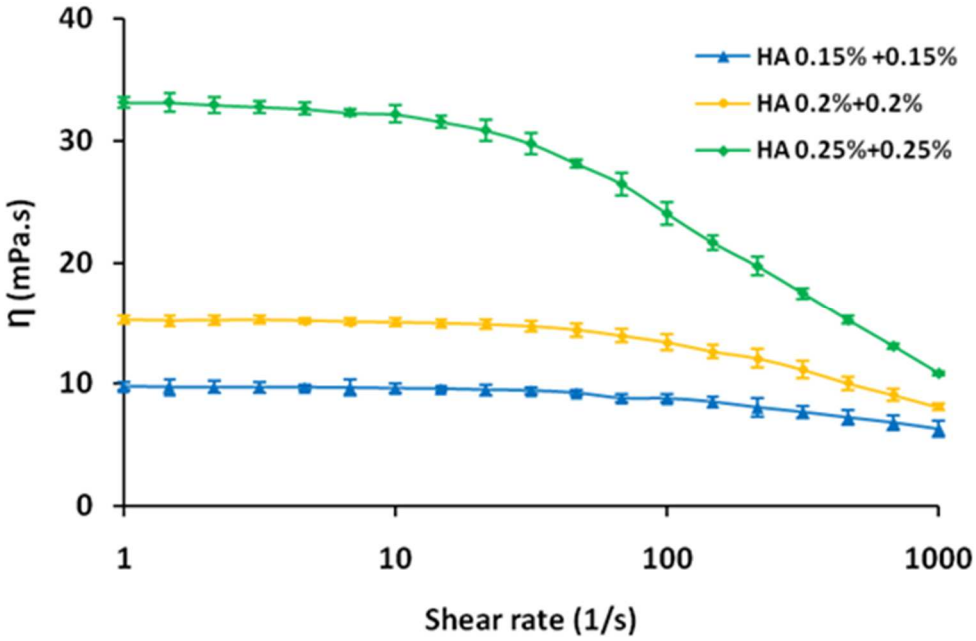

Figure 8. Flow curves of three lab scale artificial tear formulations, measured at 37°C (mean values ± s.d., n=3).

Table 5. Dynamic viscosity values of the three lab scale artificial tears measured at 25°C (mean values ± s.d., n=3).

Shear rate(1/s)	HA 0.15%+0.15%(w/v) η (mPa.s)	HA 0.2%+0.2%(w/v) η (mPa.s)	HA 0.25%+0.25%(w/v) η (mPa.s)
1	13.56 (±0.46)	21.04 (±0.79)	47.67 (±0.92)
1.47	13.54 (±0.39)	21.02 (±0.80)	47.67 (±0.92)
2.15	13.50 (±0.42)	20.99 (±0.83)	47.44 (±0.84)
3.16	13.55 (±0.45)	20.96 (±0.83)	47.22 (±0.84)
4.64	13.34 (±0.37)	20.80 (±0.78)	46.82 (±0.84)
6.81	13.30 (±0.30)	20.73 (±0.74)	46.36 (±0.73)
10	13.28 (±0.28)	20.57 (±0.77)	45.61 (±0.68)
14.7	13.17 (±0.32)	20.39 (±0.73)	44.49 (±0.76)
21.5	13.01 (±0.36)	20.01 (±0.78)	42.60 (±0.95)
31.6	12.77 (±0.40)	19.61 (±0.89)	40.1 (±1.09)
46.4	12.59 (±0.37)	18.83 (±0.72)	37.80 (±1.12)
68.1	12.02 (±0.64)	17.78 (±0.51)	34.64 (±1.63)
100	11.48 (±0.56)	16.99 (±0.73)	31.78 (±2.00)
147	10.85 (±0.72)	15.56 (±0.51)	28.51 (±2.17)
215	10.00 (±0.48)	14.46 (±0.50)	25.28 (±2.24)
316	9.37 (±0.57)	13.28 (±0.52)	21.81 (±2.69)
464	8.71 (±0.72)	11.70 (±0.43)	18.85 (±2.53)
681	7.70 (±0.39)	10.54 (±0.49)	14.91 (±1.82)
1000	7.14 (±0.27)	9.53 (±0.43)	11.58 (±1.53)

Table 6. Dynamic viscosity values of the three lab scale artificial tears measured at 37°C (mean values ± s.d., n=3).

Shear rate(1/s)	HA 0.15%+0.15%(w/v) η (mPa.s)	HA 0.2%+0.2%(w/v) η (mPa.s)	HA 0.25%+0.25%(w/v) η (mPa.s)
1	9.77 (±0.32)	17.23 (±0.30)	33.14 (±0.43)
1.47	9.72 (±0.36)	16.67 (±0.42)	33.15 (±0.78)
2.15	9.70 (±0.33)	16.19 (±0.43)	32.94 (±0.65)
3.16	9.69 (±0.31)	15.22 (±0.35)	32.78 (±0.50)
4.64	9.70 (±0.26)	15.16 (±0.24)	32.62 (±0.52)
6.81	9.67 (±0.23)	15.08 (±0.27)	32.29 (±0.28)
10	9.62 (±0.27)	15.01 (±0.31)	32.17 (±0.70)
14.7	9.58 (±0.23)	14.95 (±0.31)	31.56 (±0.53)
21.5	9.50 (±0.24)	14.85 (±0.38)	30.86 (±0.90)
31.6	9.43 (±0.27)	14.69 (±0.46)	29.76 (±0.89)
46.4	9.24 (±0.26)	14.40 (±0.55)	28.12 (±0.33)
68.1	9.01 (±0.31)	13.91 (±0.56)	26.45 (±0.94)
100	8.78 (±0.35)	13.38 (±0.62)	24.02 (±0.95)
147	8.51 (±0.43)	12.62 (±0.55)	21.65 (±0.60)
215	8.06 (±0.43)	12.07 (±0.79)	19.70 (±0.79)
316	7.68 (±0.49)	11.15 (±0.72)	17.47 (±0.44)
464	7.23 (±0.56)	10.02 (±0.54)	15.22 (±0.34)
681	6.82 (±0.59)	9.09 (±0.46)	13.07 (±0.24)
1000	6.29 (±0.62)	8.08 (±0.28)	10.85 (±0.14)

In Table 7 the dynamic viscosity values of the lab scale artificial tear formulations measured at 37°C in a three step Rot Rot Rot test are reported. In detail:

- Step 1: shear rate 1 s^{-1} from 0 to 15 s (reference value of viscosity at rest – open eye)
- Step 2: shear rate 1000 s^{-1} from 16 to 30 s (to mimic the lowering of the eyelid- blinking)
- Step 3: shear rate 1 s^{-1} from 31 to 45 s (to check the recovery at rest – open eye)

Table 7. Dynamic viscosity values of the three lab scale artificial tears measured at 37°C in a Rot Rot Rot test (mean values ± s.d., n=3).

Time (s)	HA 0.15%+0.15% (w/v) η (mPa.s)	HA 0.2%+0.2%(w/v) η (mPa.s)	HA 0.25%+0.25% (w/v) η (mPa.s)
1	9.80 (±0.16)	17.45 (±1.05)	33.16 (±2.73)
2	9.80 (±0.16)	17.37 (±1.00)	33.97 (±2.64)
3	9.73 (±0.21)	17.44 (±0.89)	33.06 (±2.72)
4	9.69 (±0.21)	17.48 (±0.97)	32.91 (±3.04)
5	9.71 (±0.26)	17.39 (±0.90)	33.24 (±2.51)
6	9.72 (±0.19)	17.68 (±1.22)	33.09 (±2.98)
7	9.72 (±0.18)	17.43 (±0.83)	32.95 (±3.19)
8	9.73 (±0.18)	17.50 (±0.95)	32.74 (±3.10)
9	9.69 (±0.24)	17.42 (±0.96)	33.00 (±2.53)
10	9.75 (±0.21)	17.47 (±0.97)	32.91 (±2.76)
11	9.75 (±0.20)	17.43 (±0.95)	32.55 (±3.24)
12	9.74 (±0.22)	17.51 (±0.83)	32.79 (±2.86)
13	9.75 (±0.25)	17.50 (±0.93)	32.85 (±2.73)
14	9.73 (±0.24)	17.45 (±0.91)	32.73 (±2.60)
15	9.70 (±0.21)	17.37 (±0.95)	32.97 (±3.06)
16	6.27 (±0.25)	7.74 (±0.27)	10.57 (±0.42)
17	6.27 (±0.23)	7.67 (±0.19)	10.59 (±0.45)
18	6.26 (±0.23)	7.63 (±0.17)	10.58 (±0.41)
19	6.24 (±0.17)	7.67 (±0.22)	10.45 (±0.32)
20	6.29 (±0.18)	7.56 (±0.12)	10.54 (±0.40)
21	6.25 (±0.21)	7.56 (±0.09)	10.56 (±0.32)
22	6.31 (±0.20)	7.53 (±0.18)	10.56 (±0.36)
23	6.24 (±0.19)	7.56 (±0.29)	10.56 (±0.30)
24	6.29 (±0.18)	7.51 (±0.13)	10.58 (±0.33)
25	6.27 (±0.18)	7.59 (±0.07)	10.51 (±0.30)
26	6.22 (±0.22)	7.49 (±0.24)	10.42 (±0.40)
27	6.26 (±0.18)	7.42 (±0.07)	10.42 (±0.28)
28	6.21 (±0.17)	7.53 (±0.17)	10.39 (±0.34)
29	6.26 (±0.20)	7.43 (±0.19)	10.46 (±0.33)
30	6.26 (±0.19)	7.50 (±0.07)	10.32 (±0.40)
31	9.66 (±0.09)	17.37 (±1.16)	33.09 (±2.32)
32	9.71 (±0.15)	17.52 (±1.17)	33.09 (±2.05)
33	9.71 (±0.17)	17.38 (±0.99)	33.47 (±2.21)
34	9.67 (±0.23)	17.49 (±0.97)	33.39 (±1.81)
35	9.70 (±0.19)	17.37 (±0.97)	33.70 (±1.99)
36	9.71 (±0.18)	17.43 (±1.07)	33.78 (±1.89)
37	9.71 (±0.20)	17.47 (±0.87)	33.73 (±1.78)
38	9.71 (±0.22)	17.52 (±0.96)	33.90 (±1.79)
39	9.71 (±0.24)	17.43 (±0.96)	33.39 (±2.18)
40	9.75 (±0.19)	17.47 (±0.99)	33.41 (±2.07)
41	9.74 (±0.21)	17.44 (±0.95)	33.61 (±1.70)
42	9.73 (±0.21)	17.51 (±0.83)	33.49 (±1.92)
43	9.74 (±0.23)	17.49 (±0.95)	33.53 (±1.72)
44	9.73 (±0.22)	17.47 (±0.93)	33.65 (±1.53)
45	9.72 (±0.21)	17.44 (±0.99)	33.74 (±1.75)

For ease of comparison the raw data listed in Table 7 are reported in Figure 9. As expected, the rank order of viscosity is the same observed in Figure 8: that is, viscosity increases on increasing HA concentration in the binary mixture. For a given formulation viscosity decreases on increasing shear rate (step 2- blinking).

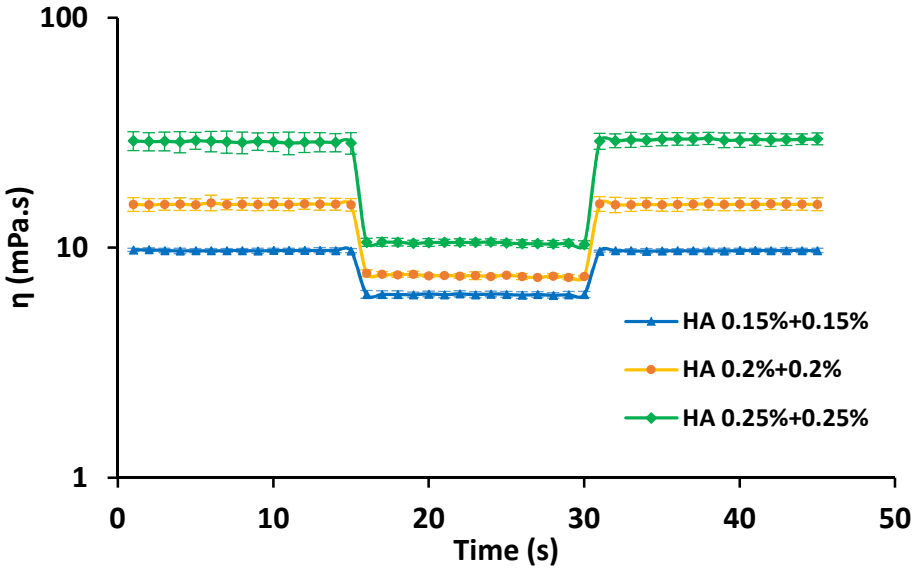

Figure 9.Viscosity *vs* time profiles of the three lab scale artificial tear formulations measured at 37°C in a Rot Rot Rot test (mean values ± s.d., n=3).

The % recovery values of the three formulations, calculated by dividing the η_0 value measured at the beginning of step 3 by the one measured at the end of step 1 are reported in Table 8.

Table 8. % recovery values of three lab scale artificial tear formulations.

PARAMETERS	HA 0.15%+0.15%(w/v) (mPa.s)	HA 0.2%+0.2%(w/v) (mPa.s)	HA 0.25%+0.25%(w/v) (mPa.s)
η_0 at the end of the 1st step (15 s)	9.70	17.37	32.97
η_0 at the beginning of the 3rd step (31 s)	9.66	17.37	33.09
% recovery	99.6	100	100.4

As shown in Table 8, each formulation is characterized by % recovery values around 100%, indicating a pseudoplastic non-thixotropic behaviour.

In Table 9 the three lab scale artificial tear formulations are compared on the basis of the values of η_0 and η_{1000} measured at 37°C (see Table 7) and are classified in accordance to Muller-Lierheim's paper [19].

Table 9. Classification of the three artificial tear formulations on the basis of η_0 and η_{1000} values [19].

FORMULATION	η_0 (1 s^{-1}) (mPa.s)	η_{1000} (1000 s^{-1}) (mPa.s)	Classification
HA 0.15% + 0.15%(w/v)	9.70	6.31	η_0 <16 mPa.s: HA eye drops with low effectiveness and without "prolonged effect"
HA 0.2% + 0.2%(w/v)	17.37	7.53	16<η_0<32mPa.s: HA eye drops with good effectiveness
HA 0.25% + 0.25%(w/v)	33.09	10.56	η_0 >32 mPa.s and η_{1000}<12 mPa.s: **HA eye drops simulating tear fluidity**

On the basis of the classification reported in Table 9, formulations HA 0.15% + 0.15% (w/v) and HA 0.2% + 0.2% (w/v) were excluded from the further steps of characterization.

On the contrary, formulation HA 0.25% + 0.25% (w/v), thanks to its η_0 and η_{1000} values perfectly mimics tear fluidity and was therefore selected for scale up. A low η_{1000} is very important because if it were too high the artificial tears could cause difficulty in eyelid movement and blurred vision phenomena.

The flow curve of the new lab scale HA 0.25% + 0.25% (w/v) artificial tears and the one of the commercial product Octilia 0.3% (w/v) measured at 25°C and 37°C are compared in Figure 10 and 11, respectively.

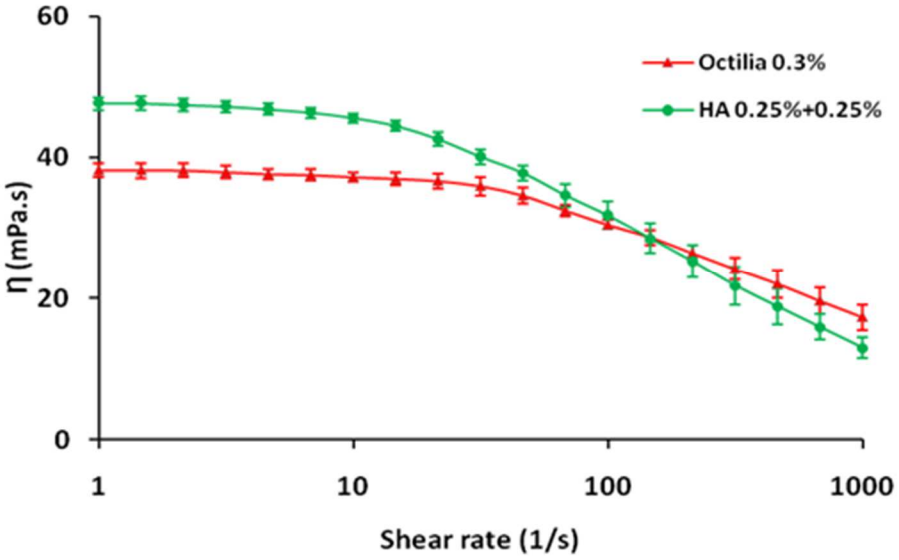

Figure 10. Flow curves of the lab scale HA 0.25% + 0.25% (w/v) artificial tears and of the commercial product Octilia 0.3 % (w/v), measured at 25°C (mean values ± s.d., n.3).

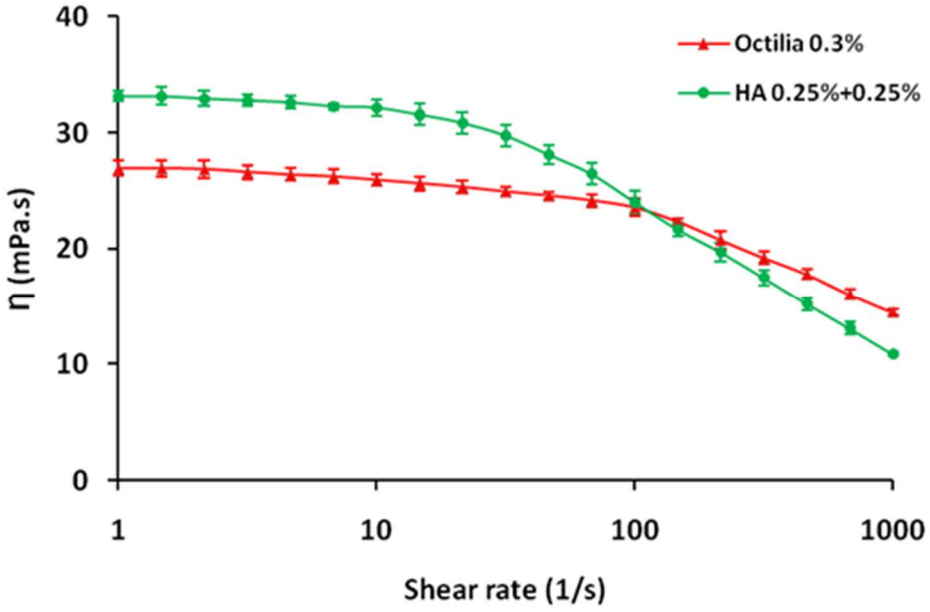

Figure 11. Flow curves of the lab scale HA 0.25% + 0.25% (w/v) and of the commercial product Octilia 0.3% (w/v), measured at 37°C (mean values ± s.d., n=3)

At 37°C (temperature mimicking the *in vivo* conditions) the lab scale HA 0.25% + 0.25% (w/v) formulation perfectly matches with the specifications established by Tiffany [12] for human tears and by Muller-Lierheim [19] for HA eye drops belonging to type 4, best simulating tear fluidity and indicated not only for universal application, but also for patients with recurrent corneal erosions. The commercial product Octilia 0.3% (w/v), although characterized by good efficacy and belonging to type 3 artificial tears, indicated for universal application, doesn't satisfy both criteria required to best simulate tear fluidity, being characterized at 37° C by η_0 lower than 32 mPa.s and η_{1000} higher than 12 mPa.s.

It must moreover be underlined that the new HA 0.25% + 0.25% (w/v) formulation, showing higher viscosity values at low shear rates than the commercial product, should be more effective because it should guarantee a longer contact of HA with the eye, thus promoting a greater moisturizing, protective and lubricating action.

The lubricating properties, determined by means of tribology measurements, of the new HA 0.25% + 0.25% (w/v) and of Octilia 0.3% (w/v) artificial tears are compared in Figure 12, where the Stribeck curves of the two samples and of water for injections (WFI), used as control, are reported.

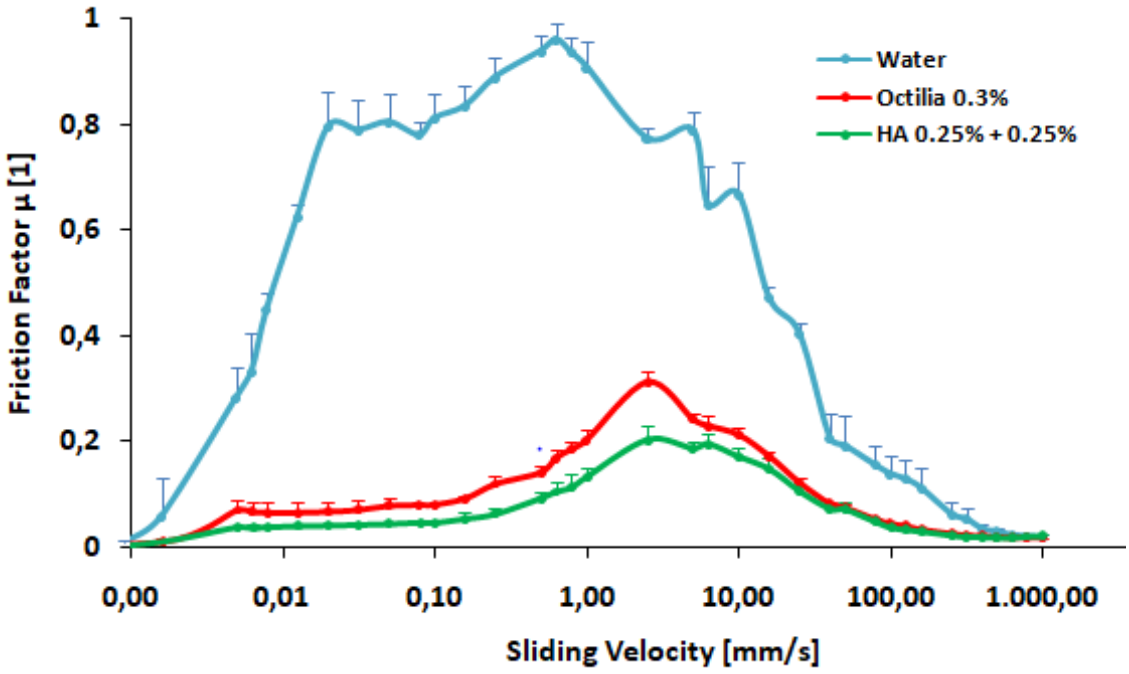

Figure 12. Stribeck curves of : HA 0.25% + 0.25% (w/v) artificial tears, Octilia 0.3% (w/v) artificial tears, and WFI (control) (mean values ± s.d., n.3).

Both artificial tear formulations possess good lubricating properties, since they oppose much lower resistance to motion than water. Between the two products, the Stribeck curve of the new HA 0.25% + 0.25% (w/v) artificial tears shows an even lower resistance to motion than the commercial product Octilia 0.3% (w/v), thus evidencing a greater lubricating power and, consequently, a better effectiveness.

3.2. Pilot batch stability study

The results of the stability studies carried out on the pilot batch in long term and accelerated ICH conditions are reported in Tables 10 and 11, respectively. The HA 0.25% + 0.25% (w/v) artificial tears fulfilled the specifications at each and every check point.

Given the results obtained in accelerated conditions (40°C/60% RH), that proved the stability of the pilot batch at high temperature and % relative humidity (see Table 11), it was not necessary to test the stability of the sample in intermediate (30°C/65% RH) accelerated conditions.

Table 10. Results of the stability study carried out on the pilot batch in long term ICH conditions.

Parameters	Specification	T = 0	3 months	6 months	9 months	12 months	18 months	24 months
Solution aspect	**Transparent and colorless solution, without visible particles**	Compliant	Compliant	Compliant	Compliant	Compliant	Compliant	Compliant
pH	**6.5 – 7.5**	7.05	7.03	7.04	7.05	7.10	7.02	7.03
Osmolality (mOsm/Kg)	**250-350**	279	279	281	280	286	282	285
HA HMW+LMW identification	**Positive**	Positive	Positive	Positive	Positive	Positive	Positive	Positive
HA content (% w/v)	**0.45 – 0.55**	0.52	0.50	0.50	0.51	0.47	0.49	0.49
Dynamic viscosity (cP)	**12 -55**	48.2	32	30.5	26.2	21.6	15.5	14.2
Sterility	**Sterile**	Sterile	Sterile	Sterile	Sterile	Sterile	Sterile	Sterile

Table 11. Results of the stability study carried out on the pilot batch in accelerated ICH conditions.

Parameters	Specification	T = 0	3 months	6 months	9 months
Solution aspect	**Transparent and colorless solution, without visible particles**	Compliant	Compliant	Compliant	Compliant
pH	**6.5 – 7.5**	7.05	7.05	7.03	7.02
Osmolality (mOsm/Kg)	**250-350**	279	279	285	285
HA HMW+LMW identification	**Positive**	Positive	Positive	Positive	Positive
HA content (% w/v)	**0.45 – 0.55**	0.52	0.51	0.49	0.50
Dynamic viscosity (cP)	**12 -55**	48.2	18.9	19.1	15.3
Sterility	**Sterile**	Sterile	Sterile	Sterile	Sterile

The chromatogram and the UV-DAD spectrum of the HA 0.25% + 0.25% (w/v) artificial tears, measured at time zero are reported in Figures 13 and 14, respectively.

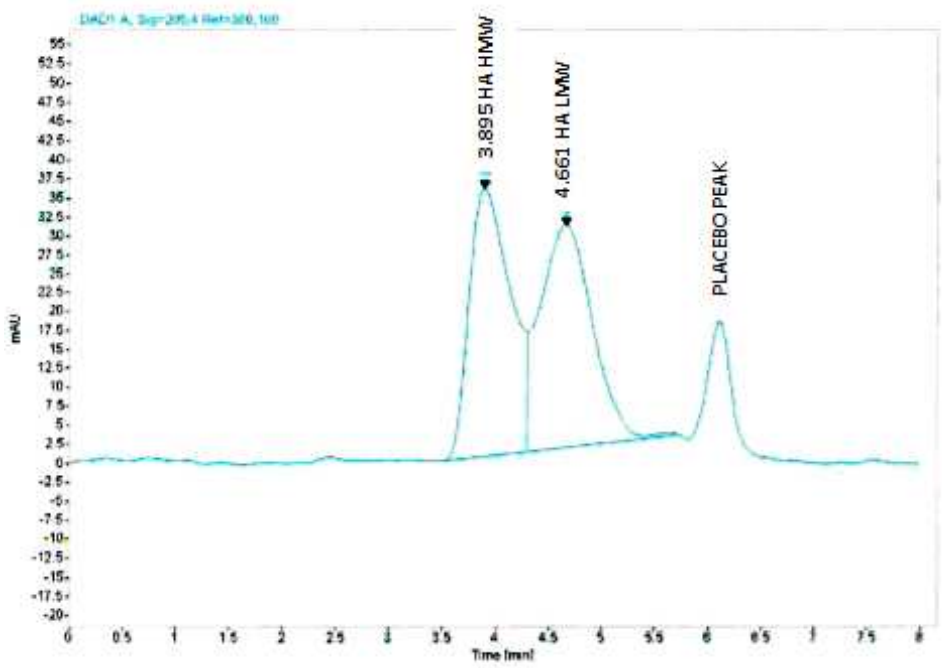

Figure 13. Chromatogram of the HA 0.25% + 0.25% (w/v) artificial tears, measured at time zero.

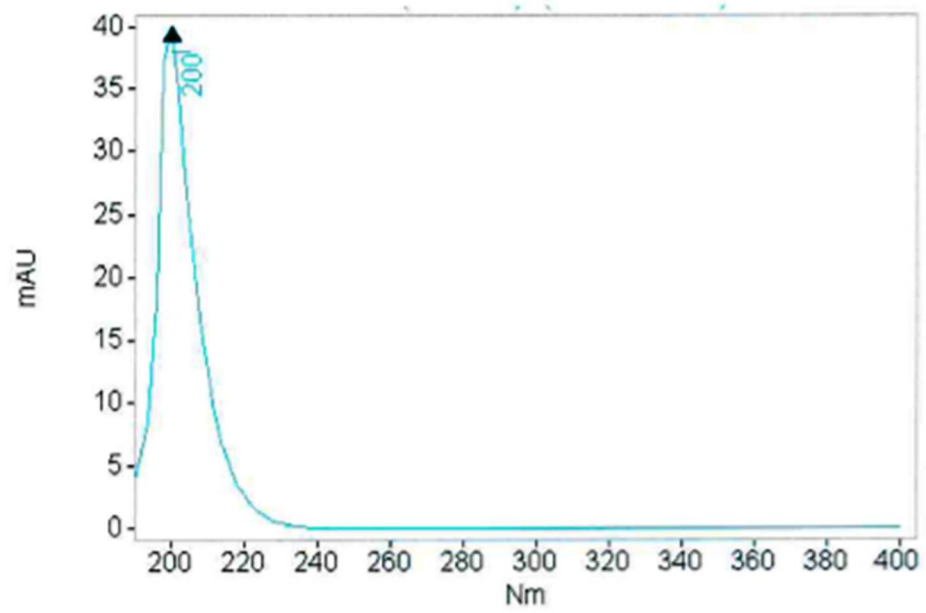

Figure 14. UV-DAD spectrum of the HA 0.25% + 0.25%(w/v) artificial tears, measured at time zero.

The retention time and the UV-DAD spectrum of the two HA grades peaks of the HA 0.25% + 0.25% (w/v) artificial tears are comparable with those of the reconstituted standard solution (see Figures 5 and 6).

As in all formulations based on HA, the dynamic viscosity measured at 25 °C decreases over time but, as shown in Figure 15 and in Table 12, after 24 months storage at 25°C/60% RH, the pilot batch still satisfies the parameters η_0 >32 mPa.s and η_{1000}< 12 mPa.s.

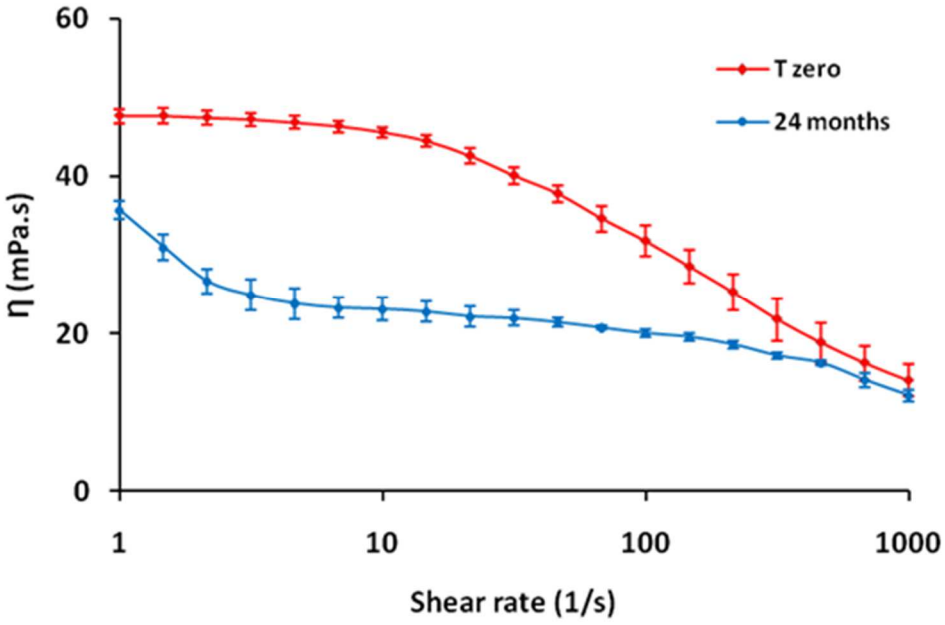

Figure 15. Flow curves measured for pilot batch at time zero and after 24 month storage at 25°C/60% RH (mean values± s.d., n.3).

Table 12. Dynamic viscosity values measured at 25°C for pilot batch at time zero and after 24 month storage at 25°C/60% RH (mean values± s.d., n.3).

Shear rate(1/s)	Time zero η (mPa.s)	24 months η (mPa.s)
1	47,67 (±0.919)	35.69 (±1.12)
1.47	47,67 (±0.92)	31.02 (±1.64)
2.15	47.44 (±0.84)	26.68 (±1.51)
3.16	47.22 (±0.84)	24.89 (±1.94)
4.64	46.82 (±0.84)	23.82 (±1.98)
6.81	46.36 (±0.73)	23.29 (±1.26)
10	45.61 (±0.68)	23.11 (±1.47)
14.7	44.49 (±0.76)	22.78 (±1.35)
21.5	42.60 (±0.95)	22.18 (±1.26)
31.6	40.1 (±1.09)	21.94 (±0.99)
46.4	37.80 (±1.12)	21.43 (±0.63)
68.1	34.64 (±1.63)	20.73 (±0.29)
100	31.78 (±2.00)	20.03 (±0.50)
147	28.51 (±2.17)	19.56 (±0.51)
215	25.28 (±2.24)	18.61 (±0.48)
316	21.81 (±2.69)	17.20 (±0.44)
464	18.85 (±2.53)	16.27 (0.36)
681	14.91 (±1.82)	14.10 (±0.92)
1000	11.58 (±1.53)	11,02 (±0.74)

Given the maintenance of all the chemical and physical-chemical properties upon storage in long term conditions it was decided to assign a storage time of 24 months at the new artificial tear formulation. The stability study in long term condition is in progress and it will go on up to 36 months. If after this time all the specifications will be satisfied as well, the shelf life of the product will be extended to 36 months.

3.3. Pilot batch biocompatibility studies

3.3.1. Citotoxicity by indirect contact test – agar diffusion test

The biological reactivity (cell degeneration and malformations) was evaluated after 24 and 48 h of incubation: no detectable zone around or under the specimen was observed. On the basis of the results, interpreted according to the ISO guideline 10993-5: 2009, the HA 0.25% + 0.25% (w/v) artificial tears had to be considered not cytotoxic after 24 and 48 h.

3.3.2. Delayed hypersensitivity test

24 and 48 h after removal of the patches, all treated and control animals showed no visible skin irritation. On the basis of the results, interpreted according to the ISO guideline 10993-10: 2010, the HA 0.25% + 0.25% (w/v) artificial tears had to be considered not sensitizing.

3.3.3. Ocular irritation test

After 1, 24, 48 and 72 h from treatment, the ocular areas (cornea, iris and conjunctivae) of each animals were examined; no abnormalities were observed. On the basis of the results, interpreted according to the ISO guideline 10993-10: 2010, the HA 0.25% + 0.25% (w/v) artificial tears had to be considered not irritant at ocular level.

3.3.4. Compatibility between pilot batch artificial tears and contact lenses

The soft daily contact lenses used for this test were Dailies AquaComfort Plus (batch N0633408). The lenses were completely dipped (worst case) into the test sample. The analysed parameters had to meet the ISO guideline 18369-2: 2012 (Ophthalmic optics – Contact lenses – Part 2: Tolerances) requirements. The results are reported in Table 13.

Table 13. Results of compatibility test between HA 0.25% + 0.25% (w/v) artificial tears and contact lenses.

Parameters	Before treatment	After treatment	Result
Aspect	Pale blue soft lenses	Pale blue soft lenses	No changes
Surface properties	No defect or surface inclusion	No defect or surface inclusion	No changes
Mean diameter	13.98 mm	13.98 mm	No diameter variation

All the analyses were effected on 10 lenses; the mean diameter was calculated as the arithmetic mean of 10 measurements and the tolerance was ± 0.20 mm.

The aspect, surface properties and mean diameter of contact lenses determined before and after treatment meet the tolerance required by the ISO guideline 18369-2: 2012. In the adopted experimental conditions, the HA 0.25% + 0.25% (w/v) artificial tears proved to be physically compatible with soft contact lenses for all the tested parameters according to the ISO guideline 11981: 2009.

3.4. Industrial batch properties

The industrial batch was characterized for the parameters listed in Table 14 and it proved to be compliant to all the specifications reported in the same table.

Table 14 - Analytical specifications and results found for the industrial batch.

PARAMETERS	SPECIFICATIONS	RESULTS
Solution aspect	Transparent and colorless solution, without visible particles	Compliant
pH	6.5 – 7.5	7.0
Osmolality	250-350 mOsm/kg	280 mOsm/kg
HA HMW+LMW identification	Positive	Positive
HA content	0.45 - 0.55 % w/v	0.51 %w/v
Dynamic viscosity	40-60 cP	49.1 cP
Sterility	Sterile	Sterile

4. Conclusion

The choice of two different HA grades (HMW in association with LMW) and their mixture in aqueous solution according to the thermal cycle described in the IBSA patent WO 2012032151 proved fruitful for the attainment of artificial tears containing a HA amount higher than that of similar products already available on the market without an excessive increase in viscosity, thanks to the formation of hybrid cooperative complexes between the two grades.

The new artificial tears developed in this study are characterized by rheological and lubrication properties better than those of the existing commercial product Octilia 0.3% (w/v) artificial tears by Ibsa Farmaceutici, and simulate at best tear fluidity.

The scale up to pilot and industrial batch size didn't point out any critical aspect: in particular, despite the high HA concentration, no challenge occurred in sterile filtration. The stability studies

carried out on pilot batch proved that the new product is stable for 24 months in long term storage conditions.

To commercialize the new artificial tear as a class IIb medical device (in accordance with the 93/42/CEE Directive), it was necessary to obtain the CE mark from a certification body. The selected certification agency was IMQ, that evaluated the technical file containing all the information given in this study and certified this medical device with the certification number 2068/MDD.

The product is now on the Italian market with the trade name "Octilia Lacrime artificiali" (Figure 16).

Figure 16 - Octilia artificial tears packaging.

5. References

1. Mengi, S.A; Deshpande, S.G. *Ocular Drug Delivery*. In: Controlled and Novel Drug Delivery, CBS Publishers and Distributors, New Delhi, India, 1997; pp. 82-90.
2. Murube, J.; Paterson, A.; Murube, E. *Classification of artificial tears*. In: Lacrimal Gland, Tear Film, and Dry Eye Syndromes 2, D.A Sullivan ed.; Plenum Press, New York, USA, 1998; Chapter 99, pp. 693-704.
3. Lemp, M.; Foulks, G. The definition and classification of Dry Eye Disease, *Ocul. Surf.*. **2007**, 75-92.
4. Delaleu, N.; Jonsson, R.; Koller, M.M. Sjogren's syndrome. *Eur. J. Oral Sci.* **2005**, *113*, 101-113.
5. Schaumberg, D.A.; Dana, R.; Buring, J.; Sullivan, D. Prevalence of dry eye disease among US men: estimates from the physicians' health studies. *Arch. Ophthalmol.* **2009**, *127*, 763-768.
6. Fujiita, M.; Igarashi, T.;Kurai, T.; Sakane, M.; Yoshino, S.; Takahashi, H. Correlation between dry eye and rheumatoid arthritis activity. *Am. J. Ophtalmol.* **2005**, *140*, 808-813.
7. Blehm, C.; Vishnu, S.; Khattak, A.; Mitra, S.; Yee, R. Computer vision syndrome: a review. *Survey Ophthalmol.* **2005**, *50*, 253-262.

8. Takashi, K. Contact lens-associated dry eye disease: recent advances worldwide and in Japan. *Invest. Ophthalmol. Visual Sci.* **2018**, *59*, DES 102-DES 108.
9. Savini, G.; Prabhawasat, P.; Koijima, T.; Grueterich, M.; Espana, E.; Goto, E. The challenge of dry eye diagnosis. *Clin. Ophthalmol.* **2008**, *2*, 31-55.
10. Zhou, X.Q.; Wei, R.L. Topical cyclosporine A in the treatment of dry eye: a systematic review and meta-analysis. *Cornea* **2014**, *33*, 760-767.
11. Tiffany, J.M. The viscosity of human tears. *Int. Ophtalmol.* **1991**, *15*, 371-376.
12. Tiffany,J.M. *Viscoelastic properties of human tears and polymer solutions.* In: Lacrimal gland, tear film, and dry eye syndromes, D.A. Sullivan ed.; Plenum Press, New York, USA, 1998; Chapter 33, 267-270.
13. Moshirfar, M.;, Kasey, P.; Hanamaikai, K.; Santiago-Caban, L.; Muthappan, V.; Passi, S.F. Artificial tears potpourri: a literature review. *Clin. Ophthalmol.* **2014**, *8*, 1419-1433.
14. Muller-Lierheim, W.G.K. Tear substitutes. *Current Contactology* **2015**, *11*, 17-19.
15. Aragona, P.; Papa, V.; Micali, A.; Santocono, M.; Milazzo, G. Long term treatment with sodium hyaluronate-containing artificial tears reduces ocular surface damage in patients with dry eye. *Br. J. Ophthalmol.* **2002**, *86*, 181-184.
16. Brignole, F.; Pisella, P.; Dupas, B.; Baeyens, V.; Baudouin, C. Efficacy and safety of 0.18% sodium hyaluronate in patients with moderate dry eye syndrome and superficial keratitis. *Graefes Arch..Clin. Exp. Ophtalmol.* **2005**, *243*, 531-538.
17. Prabhasawat, P.; Tesakibul, N.; Kasetsuwan, N. Performance profile of sodium hyaluronate in patients with lipid tear deficiency randomised, double-blind, controlled, exploratory study. *Br. J. Ophthalmol*. **2007**, *91*, 47-50.
18. De Rosa, M.; D'Agostino, A.; La Gatta, A.; Schiraldi, C. Hybrid cooperative complexes of hyaluronic acid, WO2012032151.
19. Muller-Lierheim, W.G.K. Hyaluronic acid eye drops. *Current Contactology* **2015**, *11*, 1-3.
20. Sartorius Stedim Biotech Italy - Test Report on Filterability trials of "TF15G01E" by using the Filtration technologies INCREASE® - Personal communication to IBSA.
21. Pondicherry, K.; Rummel, F.; Laeuger, J. Extended Stribeck curves for food samples. *Biosurf. Biotribol.* **2018**, *4*, 34-37.

Chapter 3

Development of an NMR method for the release and stability assessment of medical devices based on binary mixtures of HA in aqueous solutions

1. Introduction

NMR spectroscopy represents a useful analytical technique since simple measures such as single pulse experiments give reliable signal area integrals that are directly related to compound ratios [1].

In particular NMR spectroscopy represents an important tool for the analysis of structure, conformation and dynamics of carbohydrates. The structural differences between carbohydrates are often small, sometimes only the orientation of one bond differentiate two carbohydrates from each other; NMR spectroscopy is one of the few analytical techniques that enables differentiation between these isomers [2]. Information about ring connectivities, anomeric configuration and sites of modifications on sugars can also be obtained by NMR spectroscopy [3].

The nucleus most commonly used for analysis of carbohydrates with NMR spectroscopy is proton (^{1}H). Since the intensity of the NMR signal is directly proportional to the number of nuclei contributing to the signal, one-dimensional (1D) ^{1}H NMR is widely used for quantification purposes. Specific signals representative of a particular molecule or of part of it, which are located in a well resolved part of the NMR spectrum can be used for identification or quantification and are referred to as "structural-reporter-resonances" [4].

One limitation of ^{1}H NMR as a tool for quantification is overlapping signals. For carbohydrates, proton signals in the anomeric region (4.4-5.5 ppm) are generally well resolved, while the other ring protons are located in a narrow region (3-4.2 ppm) and usually suffer from signal overlap [5].

When signals overlap in the ^{1}H NMR spectra, quantitative ^{13}C NMR which has significantly higher signal dispersion can be used [6]. The use of ^{13}C NMR spectroscopy as a quantitative tool requires the elimination of the nuclear Overhauser effect by inverse-gated decoupling sequence and sufficiently long recycle delays [7].

Hydroxyl, amide and amine protons are referred to as exchangeable protons since they easily exchange with protons from the solvent. To be able to analyze these protons, either aprotic solvents (solvents with no exchangeable protons e.g. DMSO, acetone-d6) or non-deuterated protic solvents are required. When non-deuterated protic solvents (e.g. H_2O) are used, the signal from the solvent will dominate and needs to be suppressed. The pH and temperature should be adjusted to reduce the chemical exchange between exchangeable protons of the sample and of the solvent [8]. If the exchange is too fast the signal of the hydroxyl protons will coalesce with the water proton signal.

The measure of the chemical shift difference between the hydroxyl protons of an oligo- or polysaccharide in comparison with the corresponding monosaccharide can provide information about hydration and hydrogen bonding. An upfield shift indicates hydrogen bonding to a neighbor ring oxygen or steric hindrance from bulk water while a downfield shift has been attributed to hydrogen bonding with another hydroxyl group [9].

Structural analysis of carbohydrates is usually effected using a combination of ^{1}H-^{1}H homonuclear (COSY, TOCSY, NOESY) and ^{1}H-^{13}C heteronuclear (HSQC, HMBC) 2D NMR experiments [10,11].

The COSY (correlation spectroscopy) spectrum shows correlation through scalar coupling between adjacent protons, whereas the TOCSY (total correlation spectroscopy) spectrum shows correlations between all of the coupled protons in a spin system. This experiment is useful in carbohydrate analysis because each monosaccharide unit will be one separate spin system.
The NOESY (nuclear Overhauser effect spectroscopy) experiment shows correlations through space. The heteronuclear single quantum correlation (HSQC) experiment provides correlations between proton and carbon linked by one covalent bond (i.e. H-C).
Quaternary carbons are not put in evidence by HSQC because they do not connect directly to protons. Long-range couplings (2-3 bonds) between protons and carbons can be observed using a heteronuclear multiple bond correlation (HMBC) experiment. In carbohydrate chemistry, this experiment is important for determination of ring connectivities.

In the pharmaceutical field, the NMR analysis of carbohydrate polymer solutions can be very informative about polymer configurations, secondary structure and intermolecular interactions, and thus, in principle, about situations of physiological interest [12].

As for the case of hyaluronic acid (HA), the use ^{13}C NMR to study polymer configuration in solution and in the solid state revealed significant differences indicating loss of inter- and/or intra-molecular hydrogen bonds and a change in chain conformation [13,14].

In this perspective, this technique could be particularly informative of *in vivo* conformation of HA, which is likely to be affected by the local environment (e.g. ionic strength, interactions with ions and macromolecules, excluded volume), giving information on how different conformations can contribute to the different biological functions of HA together with its size [15,16].

NMR characterization of pharmaceutical products based on HA is not always easy: for instance, NMR analysis of high molecular weight (HMW) HA hydrogels proved to be difficult or even not feasible due to the high product viscosity, which led to poor sensitivity and severe line broadening of resonances, resulting in inaccurate area of proton signals [1].

Given these premises, the aim of this work was the development of a NMR analytical method suitable as a control test for the release of medical devices based on aqueous solutions containing binary mixtures of HA characterized by different MW.

In addition, the developed method should be able to detect the presence of hyaluronic acid-like structure contaminants present in low concentrations (5% w/v) and degradation products in view of its use as a stability indicator method.

An aqueous 3.2% w/v HA solution was chosen as a model formulation, which was based on the mixture of two different HA grades in a 1:1 weight ratio: 1.6 % w/v LMW HA + 1.6 % w/v HMW HA .

In order to achieve a short (up to 30 min) time for NMR analysis, the ^{1}H NMR technique was selected. This choice represents an analytical challenge because the sample is an aqueous solution and the hydrogens of water can influence the spectrum. To overcome this problem, it was necessary not only to develop a new, easy and reliable method for sample preparation but also to choose the suitable pulse program, which enable the suppression of the water signal and the attainment of well resolved spectra.

To evaluate the method ability to detect the presence in HA solutions of hyaluronic acid-like structures, non-sulfated chondroitin (NSC), also called sodium chondroitin, was selected as contaminant. This glycosaminoglycan represents the optimal candidate to evaluate the discriminating power of NMR analysis of HA-based aqueous solutions, since NSC is not only an endogenous polymer like HA, but it is characterized by a chemical structure close to that of HA, differing only for a chiral center.

NSC, in fact, is a linear copolymer of glucuronic acid and N-acetylgalactosamine, with an average molecular weight between 50 and 100 kDa. NSC is a precursor of chondroitin sulfate (CS), a GAG present in human extracellular matrix (ECM). Sulfation of NSC by specific sulfotransferases usually occurs during polymer formations, before release of proteoglycans in the extracellular medium ECM [17, 18]. Sulfation not always occurs, therefore some NSC is also present in ECM of several tissues and organs (e.g. prostate), even if in lower quantity in comparison with CS and other sulfated GAGs [18, 19].

The NSC grade used in this work is a biotechnological product obtained from *E. coli* according to the IBSA patent WO 2010/136435 [20], based on the optimization of a three-phases fermentation process (batch-fed, batch-in and microfiltration regimen).

IBSA is also the owner of the patent WO2012032151 "Hybrid cooperative complexes of hyaluronic acid" [21], which protects the use of HMW HA in association with NSC for the formation of low viscosity hybrid complexes.

For this reason the company has recently developed an innovative and patented formulation containing a hybrid cooperative complex of HA HMW 2.4% w/v + NSC 1.6% w/v enables the employment of a high HA concentration without a significant increase in viscosity and the use of the same HMW HA loaded in other IBSA products containing HA.

The rationale for the addition of NSC is to modulate the viscosity of high concentration, high MW HA solutions. In fact, the short chains of NSC intercalate between the long chains of HA, making the three-dimensional network of HA in solution less rigid, thanks to a reduction of inter–chain interactions. By acting on the short chain properties (in terms of chemical structure, MW and concentration) a fine-tuning of HA viscosity is possible.

The safety and efficacy of the new association HA HMW 2.4% w/v + NSC 1.6% w/v were evaluated in a clinical study. The new product proved to be well tolerated, safe, and effective in the treatment of symptomatic hip osteoarthritis [22].

Since ^{1}H NMR spectra of NSC are not reported in the literature, the NSC spectrum was obtained and characterized by a thorough peak assignment, in view of the use of NMR measures also for the stability assessment of the new product containing HA and NSC and, more generally, of formulations based on aqueous solutions containing mixtures of different glycosaminoglycans. More precisely, a 5% w/v solution of LMW HA was added with decreasing NSC concentrations (in the range 5-0.16% w/v) to check not only the discriminating power of NMR analysis between HA and NSC but also the sensitivity towards NSC detection in aqueous mixtures. The sensitivity of the method was further assessed by adding the lowest NSC concentration (0.16% w/v) to the 3.2 % w/v HA solution (model formulation).

Finally, the 3.2 % w/v HA formulation was subjected to acid, alkaline and hydrogen peroxide degradation. The samples were then characterized by gel permeation (GPC)/ size exclusion (SEC) chromatography to assess the possible influence of degradation procedure on HA MW. The same

samples were also subjected to NMR analysis with the aim to evaluate if NMR results could help the understanding of possible HA MW changes pointed out by GPC/SEC chromatography: namely if changes were due to depolymerization or to the formation of degradation products.

2. Materials and Methods

2.1. Materials

The following materials were used: injectable grade sodium hyaluronate low MW (LMW): 100000 Da (HTL Sas, Javene, France); injectable grade sodium hyaluronate high MW (HMW): 1.4-2.1 $x10^6$ Da (HTL Sas, Javene, France); injectable grade sodium hyaluronate very high MW (VHMW HA): 3.5 $x10^6$ Da (HTL Sas, Javene, France); non-sulfated chondroitin (Altergon Italia srl, AV, Italy); water for injections (WFI) (Ph. Eur. 10th Ed., Monograph 0169); sodium chloride (Merck & Co., Frankfurt, Germany); dibasic sodium phosphate anhydrous (Chemische Fabrik Budenheim KG, Budenheim, Germany); monobasic sodium phosphate dehydrate (Chemische Fabrik Budenheim KG, Budenheim, Germany); hydrochloric acid 37% (w/v) ACS grade (Merck KGaA, Darmstadt, Germany); sodium hydroxide pellets ACS grade (Merck KGaA, Darmstadt, Germany); hydrogen peroxide 30% (w/v) (Merck KGaA, Darmstadt, Germany); deuterated water for NMR spectroscopy (Merck KGaA, Darmstadt, Germany); sodium nitrate ACS grade (Merck KGaA, Darmstadt, Germany); sodium azide ACS grade (Merck KGaA, Darmstadt, Germany)

2.2. Preparation of HA solutions in deuterated water for ^{1}H NMR analysis

Three different solutions having 1% w/v HA concentration were prepared by hydrating for 12 h at 50°C the polymer in deuterated water. The three preparations differed in the HA molecular weight used: LMW, HMW and VHMW.

A polymer solution, having total HA concentration equal to 3.2% w/v, was also prepared by hydrating for 12 h at 50°C in pH 7.0 buffered deuterated water solution two HA grades (HMW and LMW) in a 1:1 weight ratio. The pH 7.0 buffer solution was obtained by adding a fixed NaCl amount (0.75% w/w) to a pH 7.4 phosphate buffer solution (0.05% dibasic sodium phosphate anhydrous, monobasic sodium phosphate dihydrate in 100 mL of deuterated water).

Then a half of the four solutions was divided into syringes formed by a luer lock syringe barrel 2.25 mL (BD Hypack™SCF™, Becton Dickinson, Le Point de Claix, France) and a plunger (West Pharmaceutical Services Inc., Exton, *Penn*, USA).

Pre-filled syringes were steam sterilized in autoclave (mod. FOB2-TS, Fedegari, Pavia, Italy) at 121°C for 15 min.

The spectra of HA HMW and HA LMW 1% w/v were compared with those of the non-sterilized solutions to verify that the eventual depolymerization caused by sterilization doesn't determine the formation of degradation products.

The spectra of solutions containing only one HA grade were compared with that of the mixture of the two HA grades, in order to check whether such a mixture and the presence of salts could eventually determine changes in the peaks of the spectrum.

2.3. Preparation of HA 3.2 % w/v aqueous solution for ^{1}H NMR analysis

The HA 3.2% w/v aqueous solution (mixture of two HA grades) was prepared by hydrating for 12 h at 50°C the two HA grades (HA HMW 1.6% w/v + HA LMW 1.6% w/v) in pH 7.0 buffered aqueous solution, which was prepared as described in section 2.2 by substituting water for injections with deuterated water .

The bulk solution was then divided into syringes and was sterilized as described in section 2.2.

In order to obtain a ^{1}H NMR spectrum, it was necessary to mix the sample with deuterated water. The sample solution was added with deuterated water in a 9:1 volume ratio. The two phases were mixed for 30 min at 50°C under magnetic stirring (C-MAG HS 7, IKA®-Werke GmbH & Co. KG, Staufen, Germany) at 200 rpm, to obtain a new and homogeneous liquid phase, suitable for ^{1}H NMR analysis.

2.4. Preparation of NSC solution for ^{1}H NMR analysis

NSC was solubilized under magnetic stirring at 200 rpm for 10 min in deuterated water in a concentration equal to 1% w/v.

2.5. Preparation of HA solutions added with NSC for ^{1}H NMR analysis

A 5% w/v LMW HA aqueous solution was prepared by hydrating for 12 h at 50°C the polymer in pH 7.0 buffered aqueous solution. In order to check the sensitivity of NMR analysis, the HA solution was divided into aliquots and added under magnetic stirring for 1 h at 200 rpm with decreasing NSC amounts to obtain NSC concentrations equal to 1%, 0.5%, 0.25% and 0.16% w/v.

NSC was also added in 0.16% w/v concentration to the HA 3.2% w/v formulation.

Then, all bulk solutions were divided into syringes and sterilized as described in section 2.2.

In order to detect the ^{1}H NMR spectrum, each sample was mixed with deuterated water, as described in section 2.3.

2.6. Degradation procedure and characterization of degraded HA solutions

In order to induce degradation of the 3.2% w/v HA formulation (HA HMW 1.6% + HA LMW 1.6% w/v solution), three stress reagents were selected: NaOH 2N, HCl 2N and H_2O_2 15% v/v.

4 g of HA HMW 1.6% + HA LMW 1.6% solution were weighed in three beaker to which either 1 g of NaOH 2N or 1g of HCl 2N or 1 g of H_2O_2 15% v/v was added. Each sample was magnetically stirred at 300 rpm for 3 h at 60°C. Then the sample treated in alkaline conditions was neutralized with 1 g of HCl 2N, the sample treated in acidic conditions was neutralized with 1 g of NaOH 2N, whereas 1 g of water for injections was added to the sample treated with hydrogen peroxide. Each solution was then magnetically stirred at 200 rpm for 15 min and the pH was determined (pH meter Seven Compact S220, Mettler Toledo, Columbus, Ohio, USA).

The same samples were subjected to gel permeation (GPC)/ size exclusion (SEC chromatography to assess HA MW after degradation (see section 2.6.1) as well as to NMR analysis carried out at 700 MHz (see section 2.7), to verify the formation of degradation products.

For NMR analysis, each sample subjected to degradation was mixed with deuterated water, as described in section 2.3.

2.6.1 Gel Permeation (GPC)/Size Exclusion (SEC) Chromatography

A Gel Permeation Chromatography (GPC)/ Size Exclusion Chromatography (SEC) system (OmniSEC Resolve, Malvern Panalytical LTD, Cambridge, UK), a multi-detector module (OmniSEC Reveal, Malvern Panalytical LTD, Cambridge, UK) that include refractive index, viscometer and light scattering and a software (OmniSEC software (version 10.41), Malvern Panalytical LTD, Cambridge, UK) were used for the measurement of molecular weight.

Two TSKGMPWXL columns (7.8 mm ID X 30 cm) from Tosoh Bioscience (Griesheim, Germany) were employed. The mobile phase consisted of 0.1M sodium nitrate and 0.05% (w/v) of sodium azide.

The auto-sampler and column temperatures were maintained at 25°C and 40°C, respectively. The multi-detector measured at angles equal to 90° and 8°. The injection volume was set to 100 μL and the flow rate to 0.6 mL/min. The run time was 60 minutes.

Data were recorded and processed with the OmniSEC software with a dn/dc (increase in the refractive index of the sample) equal to 0.155.

1.14 g of each sample subjected to degradation procedure was accurately weighted and diluted with mobile phase in a 25 mL flask in order to obtain a 1 mg/mL HA (HMW+LMW) concentration. Each sample was magnetically stirred (IKA C-MAG HS 7, IKA®-Werke GmbH & Co. KG, Staufen, Germany) at 300 rpm for 15 min.

2.7 NMR analysis

NMR spectra were recorded on a Bruker Avance III 400 MHz spectrometer and on a Bruker AV-NEO 700MHz equipped with cryo-probe (Bruker Corporation, Billerica, MA, USA), both available at the CGS of the University of Pavia.

All 1D and 2D NMR spectra were acquired at 298 K in D_2O or H_2O:D_2O 9:1 v:v mixture, using the standard pulse sequences available with the Bruker Topspin software package. Chemical shifts are given in ppm and were referred to the solvent signals.

Structure assignment was performed by means of 2D-COSY, TOXY and HSQC, HMBC.

3. Results and Discussion

3.1. Chemical shift assignment to HA

The signal assignment to hyaluronic acid (Figure 1) was possible thanks to the combination of ^{1}H and ^{13}C NMR spectra with 2D-COSY, TOCSY and HSQC, HMBC and are reported in Table 1.

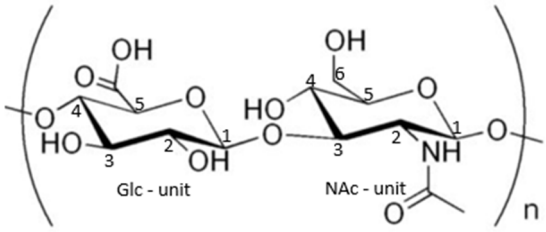

Figure 1. Chemical structure of hyaluronic acid.

Table 1. Chemical shifts of ^{1}H and ^{13}C NMR spectra of Hyaluronic acid.

1H	Frequency (ppm)	13C	Frequency (ppm)
Glc-H1	4.38	Glc-C1	103.3
Glc-H2	3.27	Glc-C2	72.5
Glc-H3	3.50	Glc-C3	73.7
Glc-H4	3.66	Glc-C4	80.0
Glc-H5	3.63	Glc-C5	82.7
NAc-H1	4.47	NAc-C1	100.4
NAc-H2	3.76	NAc-C2	54.0
NAc-H3	3.62	NAc-C3	76.4
NAc-H4	3.44	NAc-C4	68.6
NAc-H5	3.41	NAc-C5	75.3
NAc-H6	3.83, 3.69	NAc-C6	60.3
CH3-CO	1.94	NAc-**CH3**-CONH	22.5
		NAc-CH3-**CONH**	175.0
		Glc-COOH	174.1

3.2. Spectra of HA solutions containing different HA grades

Figure 2 shows the 400 MHz ^{1}H NMR spectra of the three HA grade solutions in deuterated water. All signals appear at the same chemical shift (δ).

It can be observed that the spectra resolution decreases as molecular weight increases: the signals broadening is attributable to the viscosity of the solution, which increases on increasing HA molecular weight, as well as to the T2 (transverse (or spin-spin) relaxation time) effect that decreases on increasing polymer dimensions. Relaxation is, in fact, the process by which spins return to equilibrium after applying radiofrequency pulses; in particular, T2 is used to quantify the

decay rate of the magnetization within the xy plane: such a rate is inversely proportional to the polymer size.

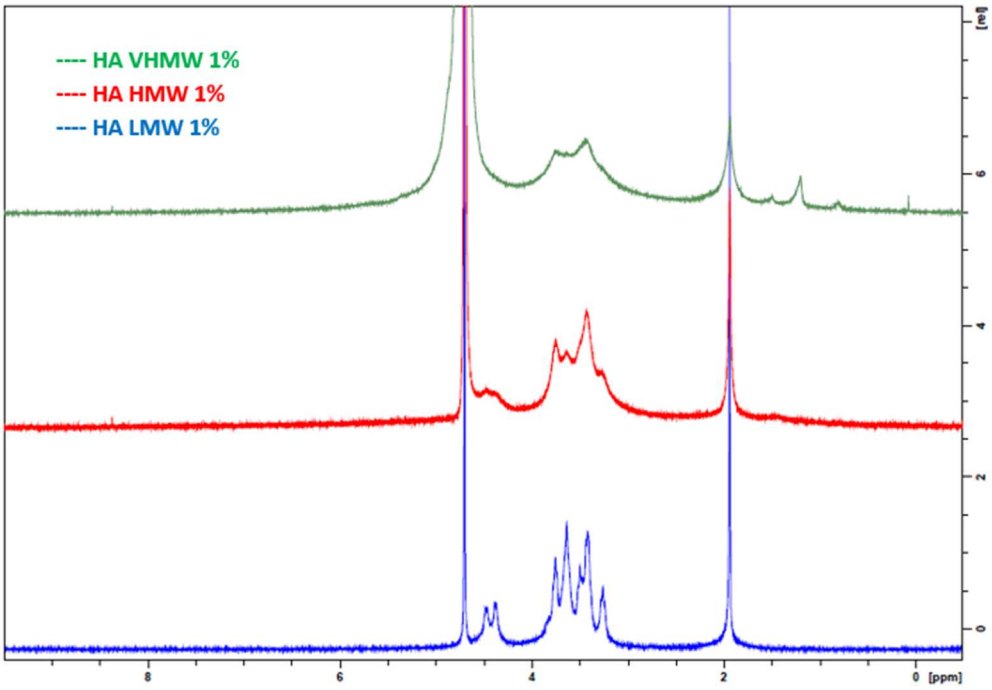

Figure 2. ^{1}H NMR spectra at 400 MHz of the three HA solutions in deuterated water.

The comparison of ^{1}H NMR spectra measured at 400 MHz for the non-sterilized and sterilized HA LMW 1% w/v and HA HMW 1% w/v solutions in deuterated water is reported in Figures 3 and 4, respectively.

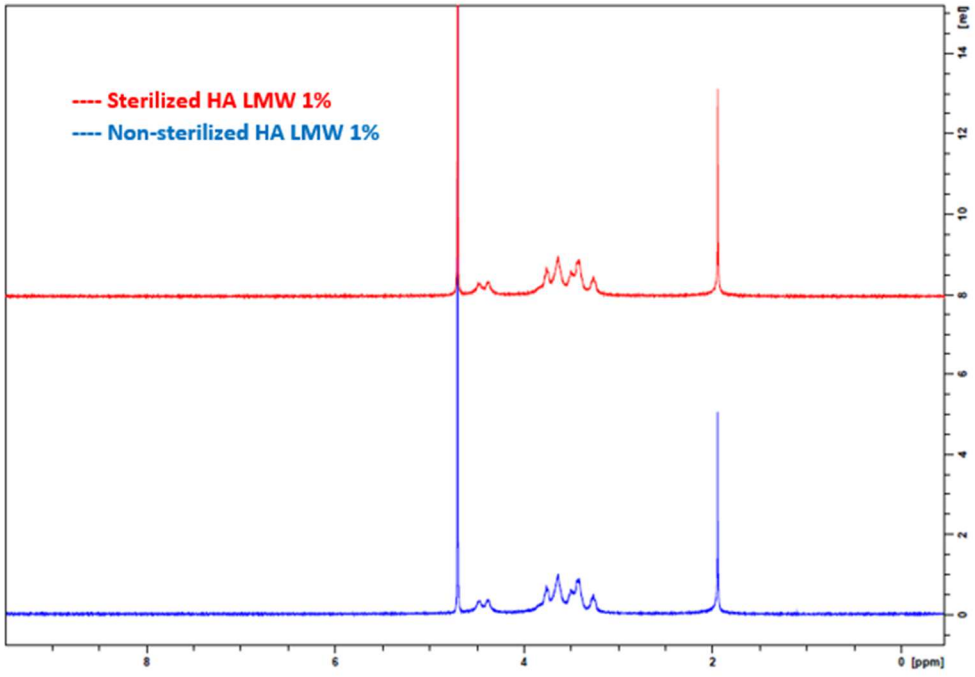

Figure 3. ^{1}H NMR spectra at 400 MHz of the non-sterilized and sterilized HA LMW 1% w/v solution in deuterated water.

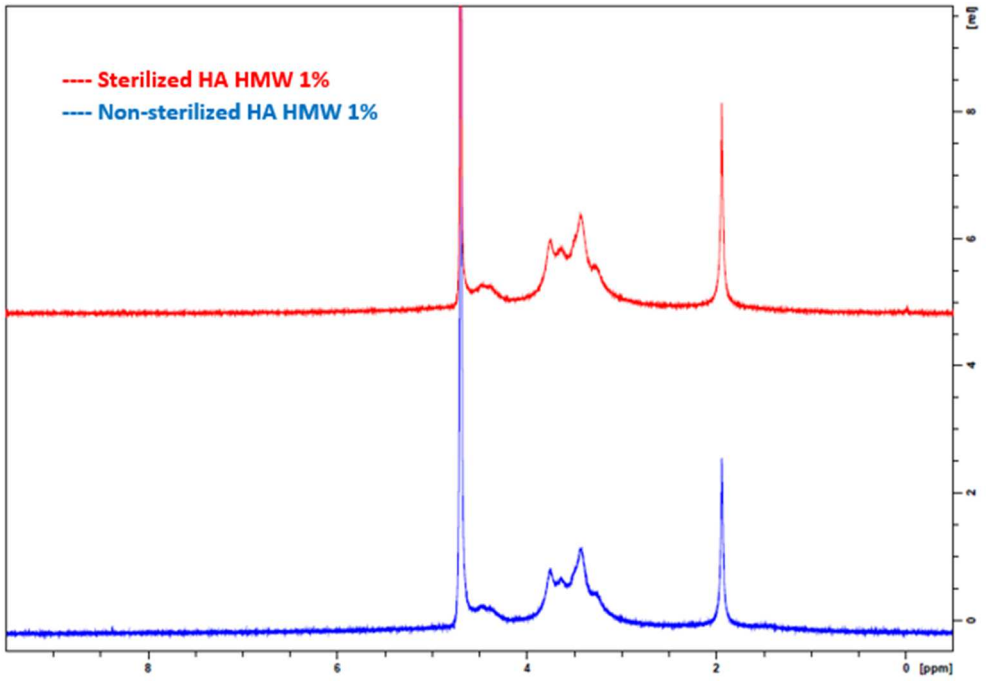

Figure 4. ^{1}H NMR spectra at 400 MHz of the non-sterilized and sterilized HA HMW 1% w/v solution in deuterated water.

The spectra recorded before and after sterilization are similar for both HA solutions. As reported in Chapter 1, sterilization determines a lowering of viscosity due to the cleavage of the long polymer chains. As no new peak appears in the spectra of the sterilized solutions, depolymerization doesn't lead to the formation of degradation products in detectable amounts.

Figure 5 shows the comparison of ^{1}H NMR spectra measured at 400 MHz for the sterilized HA LMW 1% w/v, HA HMW 1% w/v and HA 3.2% w/v (mixture) solutions in deuterated water.

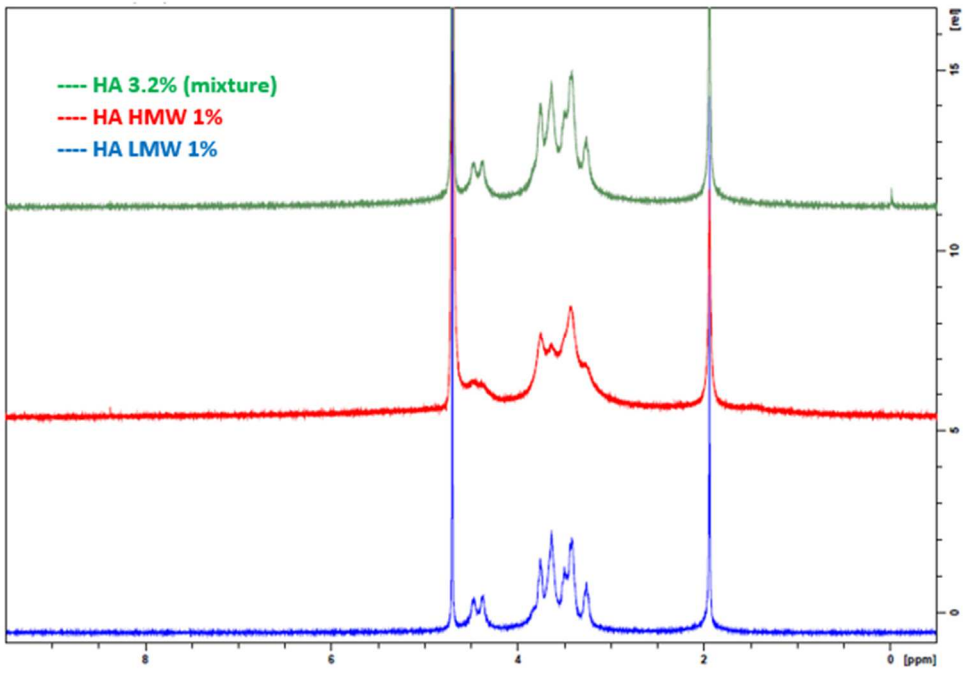

Figure 5. ^{1}H NMR spectra at 400 MHz of the sterilized HA LMW 1% w/v, HA HMW 1% w/v and HA 3.2% w/v (mixture) solutions in deuterated water.

The spectra of the two solutions based on a single HA grade present peaks at the same δ although the signals are less resolved for the HMW HA solution.

The peaks of the 3.2% w/v solution in deuterated water, mixture of the two HA grades, appear at the same δ of the two solutions containing a single HA grade. The signals are more resolved than those of the HA HMW 1% w/v solution but less resolved than those of the HA LMW 1% w/v solution.

This result, prompted us to use the 700 MHz NMR spectrometer for the further analysis of the 3.2% w/v formulation (binary mixture of HA HMW 1.6% w/v + HA LMW 1.6% w/v aqueous solutions) since this instrument allows a higher sensitivity and better signal resolution, accompanied by faster analysis than the 400 MHz one.

3.2.1. Influence of medium composition on NMR spectra

In Figure 6 the 1D ^{1}H NMR spectra measured at 400 MHz for the HA LMW 1% w/v aqueous solution mixed with deuterated water (H_2O:D_2O 90:10 v:v) as described in section 2.3 and in pure deuterated water (D_2O 100%) are compared.

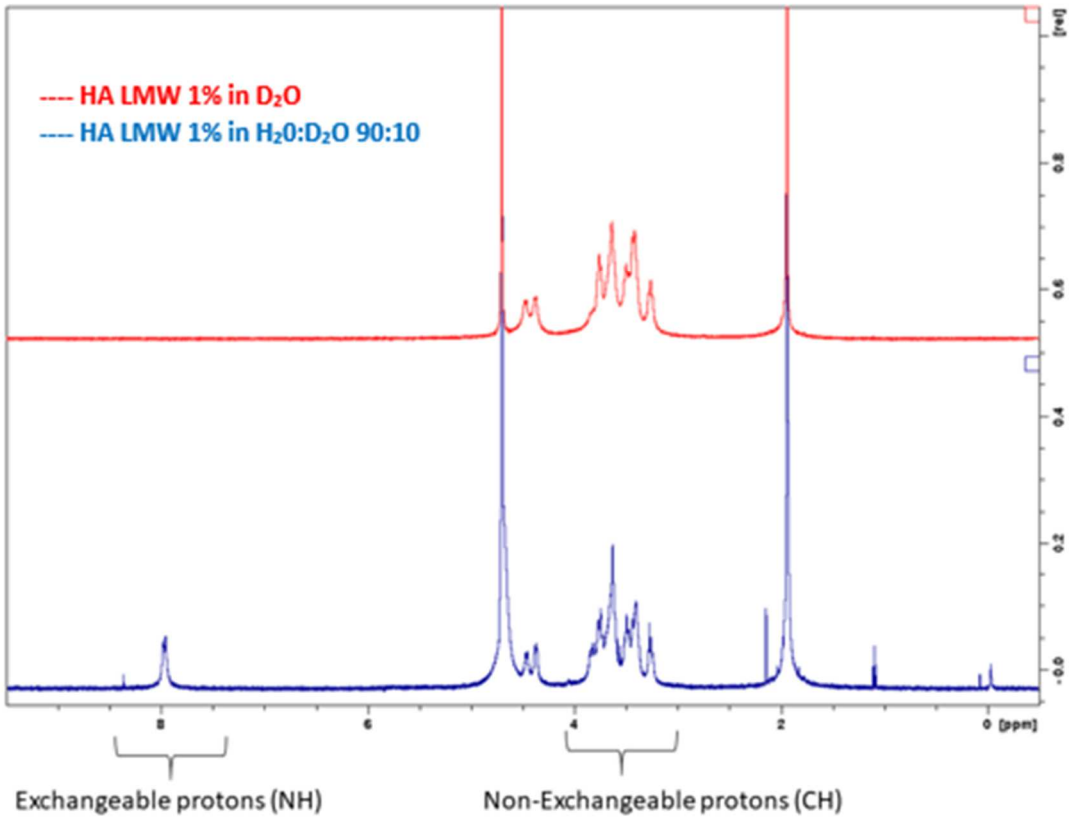

Figure 6. ^{1}H NMR spectra of HA LMW 1% w/v solution in H_2O:D_2O (90:10 v:v ratio) and in D_2O.

The spectrum measured in pure D_2O shows that all the exchangeable protons have exchanged with the deuterium of the solvent.

On the contrary, in the spectrum measured in the H_2O:D_2O (90:10 v:v) mixture the exchange between exchangeable protons was too fast: the signal of the hydroxyl protons coalesced with the water proton signal, as indicated by the peak measured at 8 ppm.

3.3. Spectra of HA 3.2% w/v formulation

The ^{1}H NMR spectra measured at 700 MHz on two different samples of the 3.2% w/v HA formulation (binary mixture of HA HMW 1.6% w/v + HA LMW 1.6% w/v aqueous solution), added with deuterated water in a 9:1 volume ratio, are compared in Figure 7. Both spectra are well resolved and show all peaks at the same δ, thus indicating reproducibility of the results.

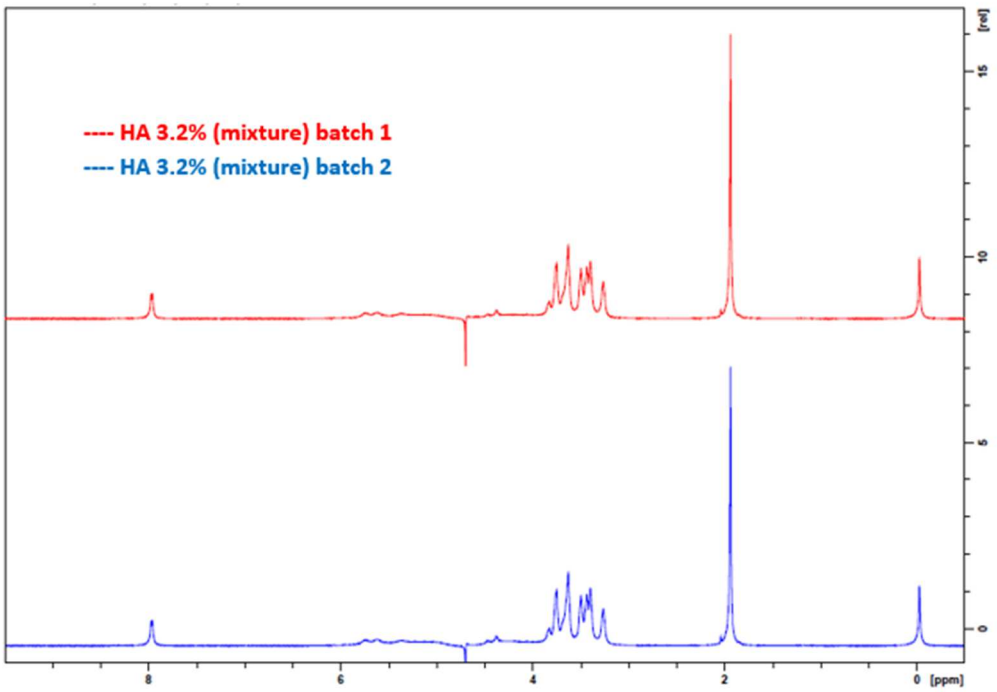

Figure 7. ^{1}H NMR spectra at 700 MHz of two different samples of 3.2 % w/v HA formulation (HA HMW 1.6% w/v + HA LMW 1.6% w/v aqueous solution) added with deuterated water in 9:1 volume ratio.

3.4. Chemical shift assignment to NSC

The ^{1}H NMR spectrum at 400 MHz of non-sulfated chondroitin 1% w/v solution in deuterated water, reported in Figure 8, is similar to that of HA 1% w/v solutions in the same medium but shows two characteristic peaks at 4.03 ppm (for GalNAc-H_4) and 3.91 ppm (for GalNAc-H_2).

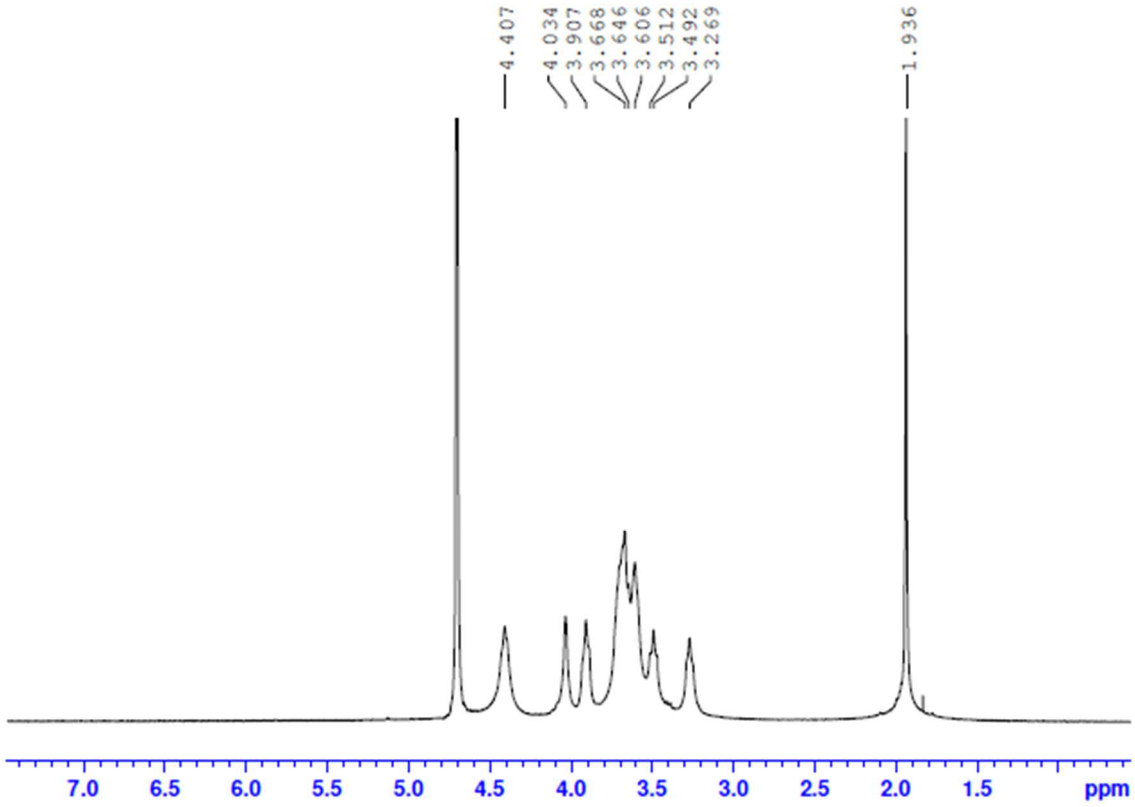

Figure 8. ^{1}H NMR spectrum at 400 MHz of non-sulfated chondroitin 1% w/v in deuterated water.

As described in Section 3.1 for HA, the signal assignment to non-sulfated chondroitin (Figure 9) was possible thanks to the combination of ^{1}H and ^{13}C NMR spectra with 2D-COSY, TOCSY and HSQC, HMBC. The results are reported in Table 2.

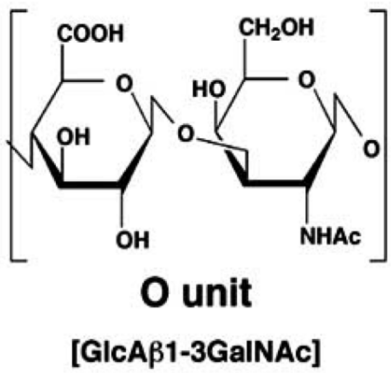

Figure 9. Chemical structure of non-sulfated chondroitin.

Table 2. Chemical shifts of ^{1}H and ^{13}C NMR spectra of non-sulfated chondroitin

1H	Frequency (ppm)	13C	Frequency (ppm)
Glc-H1	4.40	Glc-C1	104.3
Glc-H2	3.27	Glc-C2	72.5
Glc-H3	3.49	Glc-C3	73.6
Glc-H4	3.73	Glc-C4	80.3
Glc-H5	3.67	Glc-C5	79.6
GalNAc-H1	4.42	GalNAc-C1	100.7
GalNAc-H2	**3.91**	GalNAc-C2	51.2
GalNAc-H3	3.71	GalNAc-C3	76.3
GalNAc-H4	**4.03**	GalNAc-C4	67.6
GalNAc-H5	3.65	GalNAc-C5	74.9
GalNAc-H6	3.70	GalNAc-C6	61.2
CH3-CO	1.94	GalNAc-**CH3**-CONH	22.4
		GalNAc-CH3-**CONH**	175.0
		Glc-COOH	174.6

3.5. Spectra of HA solutions added with NSC

Figure 10 shows the ^{1}H NMR spectra measured at 700 MHz for HA LMW 5% w/v solution as such and after addition of NSC at decreasing concentrations in the range 1% - 0.16% w/v, and of the HA 3.2% w/v formulation added with NSC at 0.16% w/v concentration.

The two characteristic peaks of NSC have chemical shift values slightly different than those assigned in Table 2: 3.96 instead of 4.03 and 3.84 instead of 3.91 ppm. This difference is due to the solvent used to prepare the samples: deuterated water for NSC 1% w/v solution, whose results are discussed in section 3.4, and water for injections for all the samples reported in Figure 10. Even when NSC concentration decreases in the mixture with HA LMW 5% w/v solution, these two characteristic signals are well resolved.

This result indicates that the NMR method allows to detect the presence of hyaluronic acid-like structure contaminants, even at low concentrations (0.16% w/v).

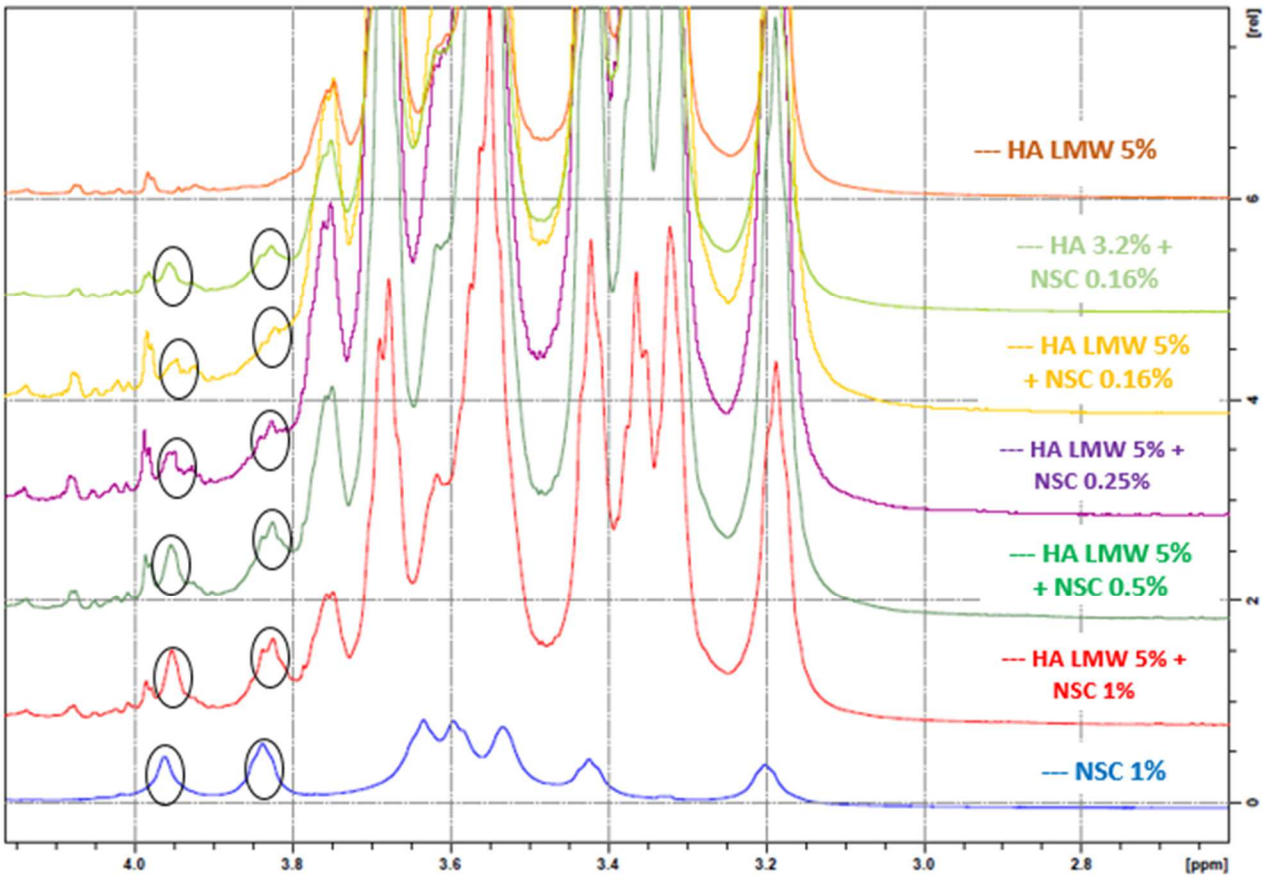

Figure 10. ^{1}H NMR spectra at 700 MHz of non-sulfated chondroitin (NSC), HA LMW 5% w/v solution, HA LMW solutions added with NSC in various % w/v and HA 3.2% w/v formulation added with 0.16% w/v NSC.

All the spectra reported in Figure 10 were acquired with the zgesgp pulse sequence, which is graphically described in Figure 11.

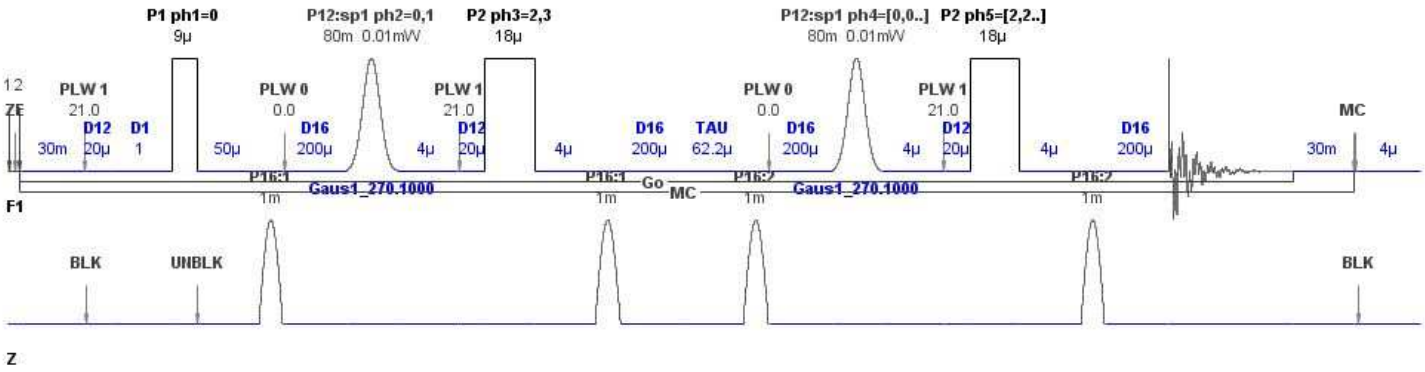

Figure 11. Graphical description of the zgesgp pulse sequence.

This pulse program uses excitation sculpting with gradients to suppress water signals. The advantage of this sequence is that it is fast to be set and the residual water signal is very small. On

the other side, the region near to the residual signal usually appears distorted and doesn't ensure an exact quantification of the peak area.

To obtain a better quantitative result, the noesygppr1d pulse sequence can be employed, that pre-saturates the water signal with relaxation delay and mixing time. In Figure 12 the D8 mixing time used to pre-saturate the water signal is reported.

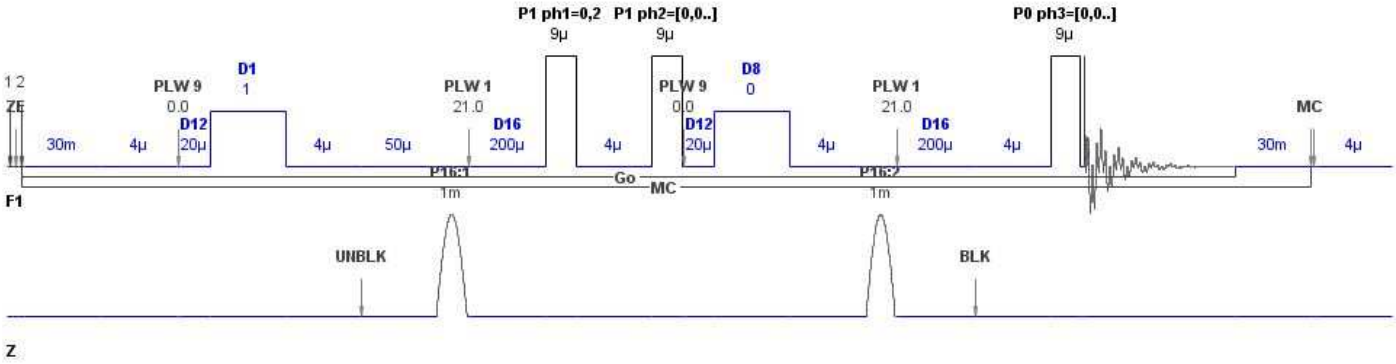

Figure 12. Graphical description of the noesygppr1d pulse sequence.

In Figure 13 the ^{1}H NMR spectra measured at 700 MHz for the HA 3.2% w/v formulation are reported: the two spectra are obtained by applying the two different pulse sequences (noesygppr1d and zgesgp, respectively) to suppress water signal.

The spectrum obtained using the noesygppr1d pulse sequence shows both a greater noise and a greater water signal than the spectrum measured with the zgesgp pulse sequence, but the baseline is less distorted and allows for precise integration of the signals.

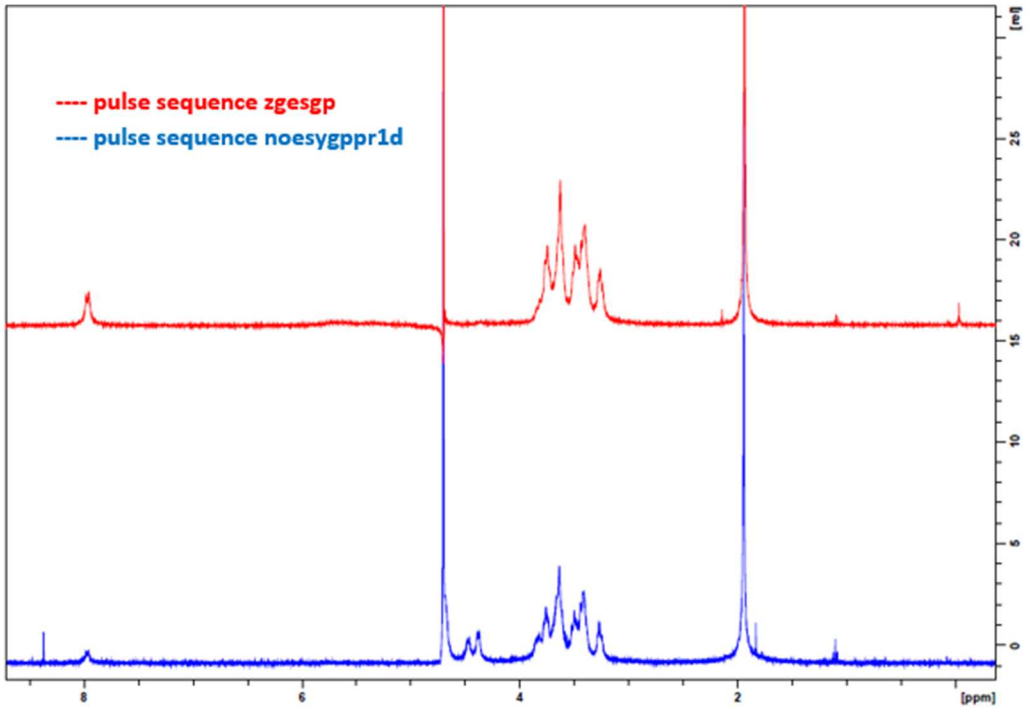

Figure 13. Comparison of ^{1}H NMR spectra measured at 700 MHz for the 3.2% w/v HA formulation by applying two different pulse sequences.

Given the better results obtained with noesygppr1d pulse sequence, it is conceivable that using a proper calibration line, it could be possible to quantify the A% of an impurity present in a HA solution.

3.6. Influence of degradation procedure on physical-chemical properties of 3.2% w/v HA formulation

The pH values of 3.2% w/v HA formulation (HA HMW 1.6% + HA LMW 1.6% w/v aqueous solution) subjected to degradation procedure are reported in Table 3.

Table 3. pH values of HA solutions.

SAMPLE	*pH*
Untreated *	6.7
Subjected to acid degradation	3.0
Subjected to alkaline degradation	3.5
Subjected to H_2O_2 degradation	5.0

*Untreated sample: 3.2% w/v HA formulation (HA HMW 1.6% + HA LMW 1.6% w/v aqueous solution)

HP-SEC-TDA double injections mean results of 3.2% w/v HA formulation undergone to degradation protocol are reported in Table 4, where the MWs (as sum of HA HMW+LMW) and the % fraction under 10000 Da are listed. The CV% was < 5% for all the results reported in the table.

Table 4. MWs and % fraction under 10000 Da of degraded samples.

SAMPLE	Mw (kDa)	Fraction (%) > 10000 Da	Fraction(%) < 10000 Da
Untreated Sample *	484.3	99.98	0.02
Subjected to acid degradation	29.4	86.6	13.4
Subjected to alkaline degradation	53.7	96.9	3.1
Subjected to H_2O_2 degradation	29.7	88.0	12.0

*Untreated sample: 3.2% w/v HA formulation (HA HMW 1.6% + HA LMW 1.6% w/v aqueous solution)

The MW reduction, observed in all stress conditions, indicates that HA undergoes depolymerization, which determines a lowering of HA molecular weight accompanied by an increase of the MW fraction < 10000 Da; this effect is less marked in the case of alkaline degradation.

In Figure 14 the ^{1}H NMR spectra measured at 700 MHz for the 3.2% w/v HA formulation (HA HMW 1.6% + HA LMW 1.6% w/v aqueous solution) before and after degradation in different experimental conditions are reported.

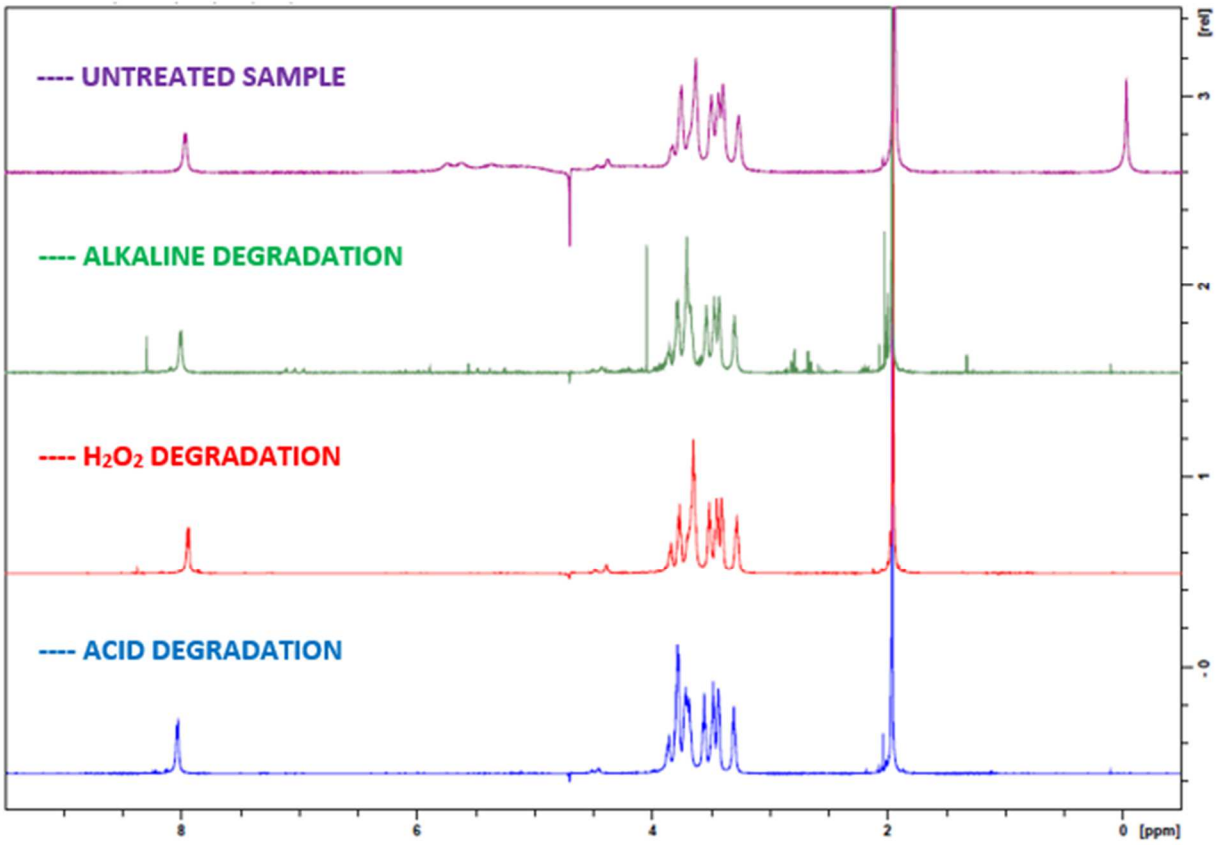

Figure 14. ^{1}H NMR spectra at 700 MHz of 3.2% w/v HA formulation (HA HMW 1.6% + HA LMW 1.6% w/v aqueous solution) before and after degradation in three different stress conditions.

The ^1H NMR spectrum of the sample treated with H_2O_2 is similar to the one of the untreated sample.

On the contrary, the spectrum of the sample treated in alkaline conditions shows additional peaks; in particular in Figure 15 the region 6.4 - 5.0 ppm of the ^1H NMR spectrum measured at 700 MHz for this sample is considered.

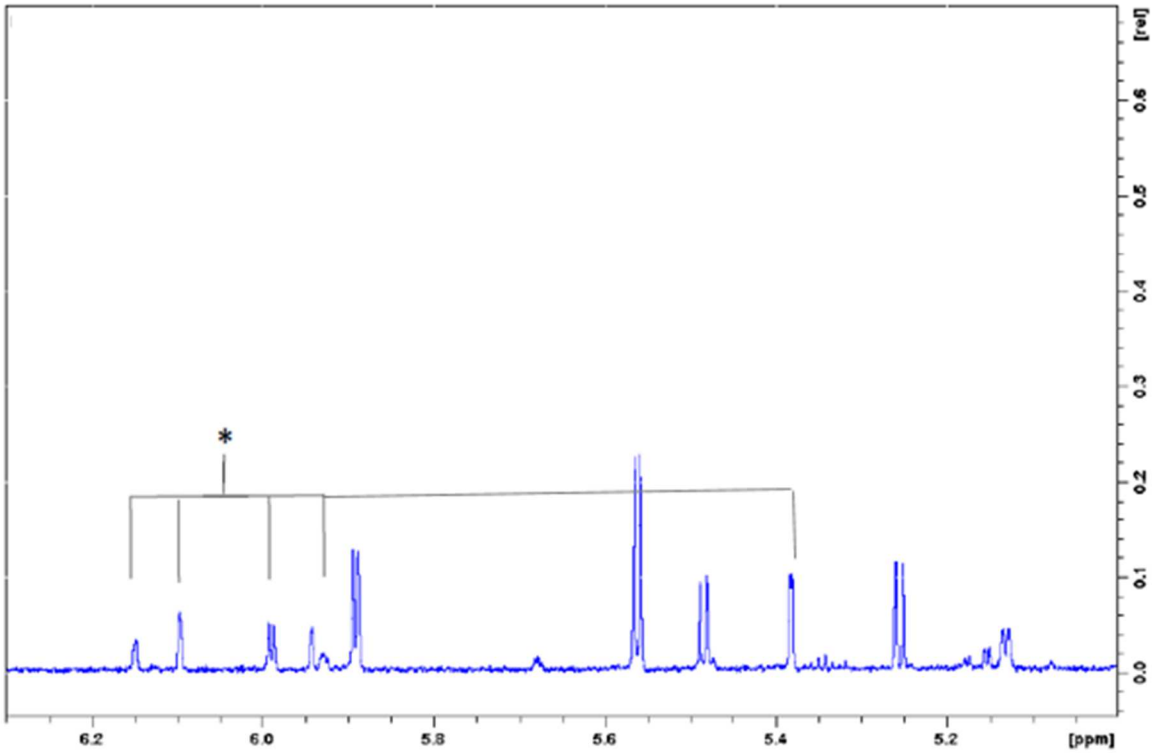

Figure 15. 6.4 -5.0 ppm region of the ^1H NMR spectrum measured at 700 MHz for the sample subjected to alkaline degradation.

The asterisk (*) highlights signals visible, upon scale magnification, only in the spectrum of the sample subjected to degradation procedure; these signals are attributable to protons of glucuronic units, formed after alkaline treatment, that cause the breaking of cross-link bonds and polymer fragmentation.

Similar signals between 5.0 e 6.0 ppm are present and visible, upon scale magnification, in the spectrum of the product treated in acidic conditions.

This means that both alkaline and acid degradation not only induce sample depolymerization causing the HA MW decrease, but also lead to the formation of degradation products.

These results suggest that NMR analysis coupled with (GPC)/(SEC) chromatography can be regarded as a stability indicating method for formulations based on HA water solutions.

4. Conclusion

An easy and quick preparation method was developed to analyze binary mixtures of HA in aqueous solution by means of the ^1H NMR technique.

This approach proved suitable as a routine analytical method to guarantee the quality of a finished product to be released.

The analyses carried out on samples subjected to stress conditions demonstrated that ^{1}H NMR measures can be used as a stability indicating method.

The tests carried out using NSC as a contaminant of HA solutions demonstrated that NMR technique was capable of detecting the occurrence of hyaluronic acid like structures, even when present in low concentration. NMR analysis should therefore be employed to investigate the stability of formulations containing mixtures of different glycosaminoglycans, like the one under development, consisting of a HA + NSC mixture in aqueous solution.

5. References

1. Wende, F.; Gohil, S.; Mojarradi, H.; Gerfaud, T.; Nord, L.; Karlsson, A.; Boiteau, J.; Kenne, A.; Sandstrom, C. Determination of substitution positions in hyaluronic acid hydrogels using NMR and MS based methods. *Carbohydr. Polym.* **2016**, *136*, 1348–1357.
2. Simpson, A.; Simpson, M.; Soong, R. Environmental nuclear resonance spectroscopy: an overview and a primer. *Anal. Chem*. **2018,** *90*, 628-639.
3. Bubb, W.A. NMR spectroscopy in the study of carbohydrates: Characterizing the structural complexity. *Concepts Magn. Reson. Part A*, **2003**, *19*, 1-19.
4. Vilegenthart, F.G; Introduction of NMR spectroscopy of carbohydrates. In: *NMR Spectroscopy and Computer Modeling of Carbohydrates.* American Chemical Society, Washington DC, USA, 2006; pp.1-19.
5. Duus, J.Ø.; Gotfredsen, C.H.; Bock, K. Carbohydrate structural determination by NMR spectroscopy: Modern methods and limitations. *Chem. Rev.* **2000**, *100*, 4589-4614.
6. Zhang, Q;, Wang, A;, Meng, Y.; Ning, T.; Yang, H.; Ding, L. NMR method for accurate quantification of polysorbate 80 copolymer composition. *Anal. Chem.* **2015**, *87*, 9810–9816.
7. Freeman, R.; Hill, D.; Kaptein, R. Proton-decoupled MNR spectra ofcarbon-13 with the nuclear Overhauser effect suppressed. *J. Magn. Reson.***1972**, *7*, 327–329.
8. Liepinsh, E.; Otting, G.; Wuthrich, K. NMR spectroscopy of hydroxyl protons in aqueous solutions of peptides and proteins. *J. Biomol. NMR* **1992**, *2*, 447-465.
9. Bekiroglu, S.; Kenne, L.; Sandstrom, C. NMR study on the hydroxyl protons of the Lewis X and Lewis Y oligosaccharides. *Carbohydr. Res.* **2004**, *339*, 2465-2468.
10. Balakshin, M.; Capanema, E.; Gracz, H.; Chang, H.; Jameel, H. Quantification of lignin-carbohydrate linkages with high-resolution NMR spectroscopy. *Planta* **2011**, *233*, 1097-1110.
11. Ronnols, J.; Engstrom, O.; Schnupf, U.; Sawen, E.; Brady, J.; Wildmalm, G. Inter-residual hydrogen bonding in carbohydrates unraveled by NMR spectroscopy and molecular dynamics simulations. *Chembiochem.* **2019**, *20*, 2519-2528.
12. Scott, J.; Heatley, F.; Hull, W.E. Secondary strucure of hyaluronate in solution. A ^{1}N-NMR investigation at 300 and 500 MHz in [$^{2}H_6$]dimethyl sulphoxide solution. *Biochem. J.* **1984**, *220*, 197-205.
13. Feder-Davis, J.; Hittner, D.M.; Cowman, M.K. Comparison of solution and solid-state structures of sodium hyaluronan by ^{13}C NMR Spectroscopy. In: *Water-Soluble Polymers.* American Chemical Society, Washington D.C., USA, 1991; pp. 493-501.
14. Matsubara, C.; Kajiwara, M.; Akasaka, H.; Haze, S. Carbon-13 Nuclear Magnetic Resonance studies of the biosynthesis of hyaluronic acid. *Chem. Pharm. Bull.* **1991**, *39*, 2446-2448.
15. Gargiulo, V.; Morando, M.A.; Silipo, A.; Nurisso, A.; Pérez, S.; Imberty, A.; Cañada, F.J.; Parrilli, M.; Jiménez- J.; De Castro, C. Insights on the conformational properties of hyaluronic acid by using NMR residual dipolar couplings and MD simulations. *Glycobiology* **2010**, *20*, 1208-1216.

16. Yang, L.; Zhang, L. Chemical structural and chain conformational characterization of some bioactive polysaccharides isolated from natural sources. *Carbohydr. Polym.* **2009**, *76*, 349-361.
17. Silbert, J.E.; Geeth, S. Biosynthesis of chondroitin/dermatan sulfate. *IUBMB life* **2002**, *54*, 177-186.
18. Prydz, K.; Knut, T.D. Synthesis and sorting of proteoglycans. *J. Cell Sci.* **2000**, *113*, 193-205.
19. Sugahara, K.; Mikami, T.; Uyama, T.; Mizuguchi, S.; Nomura, K.; Kitagawa, H. Recent advances in the structural biology of chondroitin sulfate and dermatan sulfate. *Curr. Opin. Struct. Biol.*, **2003**, *13*, 612-620.
20. De Rosa, M.; Schiraldi, C.; Cimini, D. Biotechnological production of chondroitin *Patent No. WO 2010/136435 A1.*
21. De Rosa M., D'Agostino A., La Gatta A.,Schiraldi C. Hybrid cooperative complexes of hyaluronic acid *Patent No. WO2012/032151.*
22. Papalia, R.; Salini, V.; Voglino, N.; Fortina, M.; Carta, S.; Sadile, F.; Costantino, C. Single-dose intra-articular administration of a hybrid cooperative complex of sodium hyaluronate and sodium chondroitin in the treatment of symptomatic hip osteoarthritis: a single-arm, open-label, pilot study. *Rheumatol. Ther.* **2020**, *https://doi.org/10.1007//s40744-020-00255-y.*